Cosmetic glove stiffness compensation for body-powered hand prostheses

Design of a novel negative stiffness element

Ronald A. Bos

Master of Science thesis

TU Delft Delft University of Technology

Challenge the future

Cosmetic glove stiffness compensation for body-powered hand prostheses

Design of a novel negative stiffness element

Thesis submitted in partial fulfilment
of the requirements for the degree of

MASTER OF SCIENCE

in

BIOMEDICAL ENGINEERING

with specialisation in

BIOMECHATRONICS

at

Delft University of Technology

December 18, 2013

Author:
R.A. Bos
#1518089

Examining Committee:
Dr.ir. D.H. Plettenburg
Prof.dr. F.C.T. van der Helm
Ir. J.W. Spronck

Department of Biomechanical Engineering

DON'T PANIC

-Douglas Adams

Contents

Preface **iii**

Introduction **v**

I Scientific Paper **1**

1 Introduction **3**

2 Methods & Materials **4**

3 Results **9**

4 Discussion **11**

II Literature Study **17**

1 Cosmetic gloves **19**

2 Compensation mechanisms **27**

3 Energy storage **35**

4 Mechanical linkage **47**

5 Conclusions **51**

III Appendices **55**

A Cosmetic glove measurements **57**

B Concept synthesis **63**

C Manufacturing & assembling **81**

D Prototype performance **87**

E Future work **95**

F Technical drawings **109**

Preface

This thesis contains an accumulation of results I have obtained during my graduation project, but also represents the long path towards this milestone and withcoming knowledge, frustration and inspiration. This project has haunted my mind for an extended period of 15 months and has never stopped poking my interest. It has given me an interesting relationship with my computer, revealing insights in practicalities and a great deal of relief and confidence when the final product actually turned out to work quite all right.

During this process, many people have helped me to make this project as it is. First of all, many thanks to my supervisor, Dick Plettenburg, for his guidance, readiness and fun weekly talks. Thanks to everyone at DIPO who has shared interests and helped me improve along the way. Thank you to Jan van Frankenhuyzen, for his always helpful advice on practical prototype design, and to those at the 3ME Workshop who helped me manufacture and assemble it. Another thank you goes to Peter Kyberd and everyone else at the Institute of Biomedical Engineering in Fredericton, Canada, for the knowledge and fun times they have given me during my internship, which have certainly proven to be useful in this thesis. I would also like to thank my parents, who eventually made it all possible and supported me through every step. Thank you to my brother, René, for always being ready to discuss hair-splitting matters. Thank you to my girlfriend, Esmé, for making the pictures, for her endless support and for having to cope with the many hours I had my attention glued to papers, models (the numerical kind), CAD drawings and thesis chapters. Last but not least, a special thanks to you, the reader, for coming this far and actually reading my report. Well, at least this page.

Introduction

Despite continuous research in prosthetics, modern-day upper limb prostheses still show high rejection rates—reaching an average of 26% among adults (Biddiss and Chau, 2007)—and seem to lack in significant improvement (Smit et al., 2012). In body-powered prostheses, high activation forces can cause pain in the back and neck, or overuse injuries occur in the remaining limb due to resulting disuse (Datta et al., 2004; Biddiss and Chau, 2007). The addition of a cosmetic glove bares a share of responsibility in this situation, as the stiff glove material degrades the mechanical properties of the prosthesis and the overall usability. In this thesis, an attempt at solving this problem is performed with the addition of a novel mechanical device designed to compensate this added glove stiffness.

Background

Field of upper limb prosthetics The missing of a limb can be due to several reasons. Be it congenital or because of a disease or trauma, it will always strongly affect ones life. People with acquired limb loss will often cope with strong emotions, one of them being the concerns of losing mobility, functionality or the ability to work (Yong et al., 2011). Especially with the loss of an upper limb, the loss of hand functionality severely affects ones ability to perform his/her activities of daily living. Consequently, it has dramatic consequences on ones physical abilities and mental health (Darnall et al., 2005; Desmond, 2007; Stevens, 2011). The field of upper limb prosthetics offers artificial replacements for the missing limb, which may help in improving those factors.

Upper limb prostheses can be roughly divided into passive, externally powered and body-powered prostheses. Passive prostheses are not equipped with an active hand, they only provide for passive hand functionality and are often worn for cosmetic purposes. Externally powered prostheses can use external energy sources such as electricity to power the prosthesis, whereas body-powered prostheses harvest body movements with a shoulder harness or use elbow control. Control theory shows that one of the most important aspects for controlling an external device is the provision of feedback. Externally powered prostheses are limited to providing such feedback via sensors and additional actuators. Body-powered prostheses, on the other hand, have the substantial advantage of providing direct feedback to the user in the form of phys-

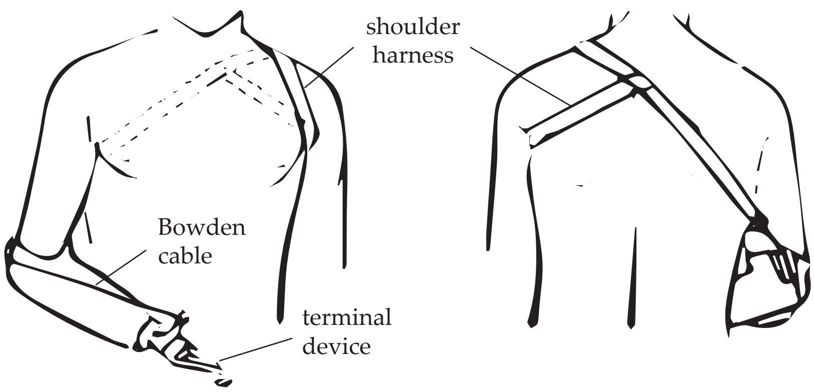

Figure 1: *Example of a figure nine shoulder harness, also showing the Bowden cable and terminal device (adapted from Hess (n.d.)).*

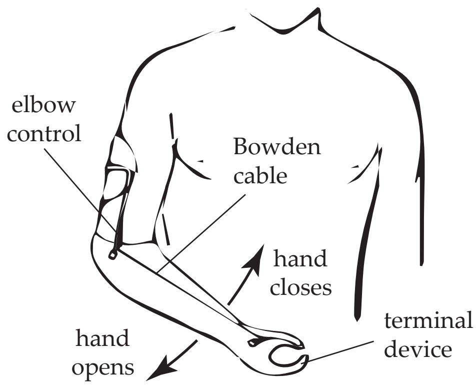

Figure 2: *Example of elbow control, also showing the Bowden cable and terminal device (adapted from Hess (n.d.); Delft Prosthetics BV (n.d.)).*

iological proprioception. This presence of direct physiological feedback shows clear advantages for the body-powered alternative (Plettenburg and Herder, 2003).

Body-powered prostheses A body-powered prosthesis uses, as the name suggests, the movement of the user's own body in order to operate the prosthesis. This is done by using a shoulder harness (Figure 1) or with elbow control (Figure 2), where a Bowden cable can be operated by moving the ipsilateral shoulder or elbow, respectively. This Bowden cable then connects to and operates the active part of the prosthesis, also called the terminal device. As both force and displacement in the Bowden cable directly relates to the force and displacement the user is exerting, it is able to provide for direct physiological feedback.

Because only one cable can be operated with this system, body-powered terminal devices often show only one controllable degree of freedom that is directly connected to the grasping function. As a result, different body-powered prostheses have emerged that can either open or close upon pulling this cable, where a passive stiffness inside the mechanism is able to return the device back to resting position. Hence, these terminal devices are then called voluntary opening or voluntary closing prostheses, respectively.

Voluntary opening vs. voluntary closing The working principle of a voluntary opening device is much like a washcloth pin, one can grasp objects by using its passive stiffness, thus not having to exert force in order to keep grasping. The force at which the prosthesis is opened is fed back to the user via the Bowden cable. Furthermore, it provides for a closed resting state, which is ought to look more natural in a prosthesis. A voluntary closing device *does* require continuous force from the user when grasping an object, much like a pair of tweezers. However, the closing force—or grasping force—is fed back through the user via the Bowden cable. This is considered to be more intuitive as it allows the user to estimate the exact amount of grasping force. For example: imagine picking up a contact lens with a washcloth pin (~voluntary opening) or with a pair of tweezers (~voluntary closing). One will find that the voluntary closing mechanism is more capable of performing such precision tasks.

Prosthesis rejection Unfortunately, high rejection rates are still reported on all types of prostheses and range from 20%–40% (Biddiss and Chau, 2007). A modern upper limb prosthesis is still not able to provide for the same functionality as a normal hand, resulting in the remaining limb to fill in the void. More specifically, awkward compensatory movements of the trunk and limbs can result in a range of overuse injuries and high activation forces may give back and neck pains (Datta et al., 2004; Biddiss and Chau, 2007; Carey et al., 2008; Metzger et al., 2012). These factors often account for reported cases of rejection, but can also result in an active prosthesis ending up to be used for cosmesis only (Plettenburg, 2006a). Clearly, current prosthesis are subject to improvement.

The cosmetic glove

In order to protect the mechanism of the terminal device and improve its appearance, a cosmetic glove is used, being a synthetic layer of skin-like material. Furthermore—and perhaps more importantly—it also provides for psychological advantages for the limb absent person. As the study of Dembo and Tane-Baskin (1955) shows, the mere presence of a cosmetic glove already allows users to walk around and interact in public places, without being recognised as an amputee. In fact, the realism of a cosmetic glove can be expressed in a combination of meters and intensity of social contact (Dembo and Tane-Baskin, 1955; Schweitzer, 2011).

When designing prostheses, the three main aspects in prosthesis design should be considered: cosmesis, comfort and control (Plettenburg, 2006b). Here, the cosmetic glove is an essential part in enhancing the overall cosmesis. The material of which the cosmetic glove is made, however, shows viscoelastic properties. Consequently, it adds

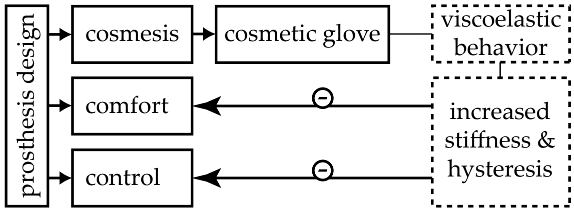

Figure 3: *Schematic showing the three main aspects in prosthesis design. The mechanical properties of the cosmetic glove have a negative influence on comfort and control.*

a passive stiffness to the combined mechanism and introduces energy losses due to hysteresis. This increases the required operating forces and can reach up to 250 N (Wijsman, 2010; Tolou et al., 2012), well exceeding the comfortable limit of 40 N (Hichert, 2010). As a result, the cosmetic glove exerts a negative influence on the comfort and control of the prosthesis (Figure 3).

A more elaborate analysis on the cosmetic glove's material and mechanical properties, can be found in Chapter 1 of Part II: Literature Study.

Problem statement

Clearly, the mechanical properties of the cosmetic glove pose a problem, leading to the following problem statement:

> The addition of a cosmetic glove increases the stiffness and hysteresis of the prosthesis dramatically, reducing overall usability of the prosthesis.

The added stiffness and hysteresis of the cosmetic glove interferes with the intended functioning of the prosthesis and has been an on-going issue for years. This has already lead to a series of mechanisms and methods (Kuntz, 1995; Herder et al., 1998; de Visser and Herder, 2000; Plettenburg, 2002; Wijsman, 2010; Tolou et al., 2012), but have not provided a single best solution due to challenges that lie in non-linearities, high forces and small working volumes. These different methods of approaching the problem can be categorised according to:

- Cosmetic glove omission: avoid the use of a cosmetic glove.
- Cosmetic glove modification: modify the cosmetic glove.
- Prosthesis modification: modify the prosthesis.
- Cosmetic glove compensation: compensate the cosmetic glove's stiffness with an additional mechanism.

Glove omission involves avoiding the cosmetic glove completely. In the previous section, however, the importance of a cosmetic glove is already briefly discussed, where especially the social impacts make it an indispensable component. Glove and prosthesis modification are able to provide for partial solutions, as they are able to reduce the experienced stiffness & hysteresis. Cosmetic glove compensation, on the other hand, is able to fully address the glove stiffness and substantially reduce necessary operating forces.

Objective

Given the possibilities to reduce the experienced stiffness from the cosmetic glove, the main objective of this thesis is:

> To design and create a working glove stiffness compensation mechanism for body-powered prostheses that reduces activation forces to below the comfortable limit of 40 N.

This main objective is pursued by first providing an impartial view on the problem by the means of a literature study. Using this information, an ideal working principle for a glove stiffness compensation mechanism is chosen and translated into a working concept. As a result, a prototype is manufactured and tested to show its potential in practice.

Reader's guide

This thesis report is divided into three different parts. Their purpose is to clearly mark different stages during the performed study and to separate the superficial from the more in-depth information. In general, Part I describes the study in a familiar, scientific format. Parts II and III, on the other hand, form a complete and detailed description of the work done. More precisely:

Part I shows the scientific paper that has emerged from the performed study and symbolises the final product. It summarises the most important results and is probably most time-efficient to read if you do not want to know every single detail.

Part II is meant to provide background information as well as to provide a summary of the performed literature study, explaining several often-used terms along the way. Chapter 1 discusses cosmetic gloves in general, how they affect the prosthesis' mechanical properties and whether there is room for improvement. Chapter 2 provides for an overview of existing compensation mechanisms from a multidisciplinary perspective. Chapters 3 and 4 then discuss the necessary components that make a compensation mechanism, eventually making an objective choice for the best options in the case of a cosmetic glove stiffness compensation mechanism. Chapter 5 summarises all conclusions that are made based on the information found and calculations performed.

Part III describes the different crucial parts that succeed the literature study and are divided into separate appendices. Appendix A describes the performed measurements made on different types of cosmetic gloves. In Appendix B the concept's design process is described, along with an elaborate description on its working principle, characteristics and how its behaviour is modelled. Appendix C describes the choices related to the manufacturing and assembling of the prototype. In Appendix D, the prototype's performance is tested by measuring its characteristic and compare it to the predicted behaviour from the model. Consequently, Appendix E lists several recommendations for future work in order to further improve the design. Lastly, Appendix F shows the collection of 2D technical drawings that are used to manufacture the prototype.

PART I

Scientific Paper

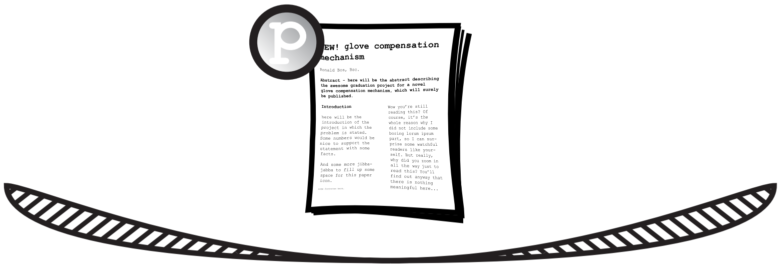

Design of a cosmetic glove stiffness compensation mechanism for toddler-sized hand prostheses

Ronald A. Bos

Delft Institute of Prosthetics and Orthotics, Department of Biomechanical Engineering
Delft University of Technology
r.a.bos@student.tudelft.nl

Abstract

The addition of a cosmetic glove to an upper limb prosthesis has an indispensable effect on the cosmetic value, but its viscoelastic behaviour adds a substantial amount of stiffness and hysteresis to the system. Consequently, the overall usability of the prosthesis is degraded. A novel negative stiffness element is designed to compensate for the cosmetic glove's stiffness. A combination of using linear helical springs and the concept of rolling link mechanisms has resulted in a Rolling Stiffness Compensation Mechanism (RSCM). Results show that the RSCM is capable of exerting a progressive negative stiffness characteristic and fits into a 33 mm diameter wrist. Consequently, an otherwise voluntary opening toddler-sized prosthesis is converted into a voluntary closing device, reducing maximum operation forces down to 40 N with a combined effieny of 52%. Further adjustments to the design are able to further improve the efficiency of the mechanism. Moreover, changes in geometric relations of the mechanism offers possibilities for a wide range of prostheses and other applications.

1 Introduction

The missing of an upper limb has dramatic consequences on ones physical abilities and mental health (Darnall et al., 2005; Desmond, 2007; Stevens, 2011). An upper limb prosthesis is designed to improve those factors and can do so with a perfect fulfilment of the three main requirements in prosthesis design: cosmesis, comfort and control (Plettenburg, 2006b). However, reports show that a lot of users are dissatisfied with their prosthesis and rejection rates range from 20%–40% (Biddiss and Chau, 2007). Overuse injuries to the remaining limb, as well as back- and neckpain often account for rejection. If not rejected, active prostheses sometimes end up being used only for cosmesis (Datta et al., 2004; Plettenburg, 2006b; Biddiss and Chau, 2007). Clearly, current prostheses do not meet all requirements.

Among body-powered hand prostheses the mechanical efficiency is low, whereas hooks often show much better performances (Corin et al., 1987; LeBlanc et al., 1992; Smit and Plettenburg, 2010; Smit et al., 2012). The activation forces for hands are high and range from 60–130 N for a small 15 N pinch force (Smit et al., 2012), while the comfortable limit is at 40 N and therefore disturb the proprioceptive feedback (Plettenburg et al., 2011). The addition of a cosmetic glove is the most prominent cause of these high forces. The viscoelastic behaviour of the material adds a large amount of stiffness and energy losses due to hysteresis (Herder et al., 1998; Wijsman, 2010; Tolou et al., 2012; Smit and Plettenburg, 2013). Moreover, it limits the usability of voluntary closing devices (a prosthesis that closes upon activation by the user), which are advantageous due to their increased mechanical efficiency and proprioceptive feedback compared to their voluntary opening counterparts (LeBlanc et al., 1992; Plettenburg and Herder, 2003). This problem increases in severity for toddler-sized prostheses, as the relative thickness of the glove increases and children are less capable of producing such forces (Shaperman et al., 1995). It appears that the desire for a natural looking hand, i.e. improved cosmesis, counteracts the comfort and control of the prosthesis – being the main advantages of a body-powered prosthesis.

Several solutions are possible in order to address this problem, namely:

- cosmetic glove omission;
- cosmetic glove modification;
- prosthesis modification; or,
- cosmetic glove stiffness compensation.

However, the cosmetic glove is indispensable (Dembo and Tane-Baskin, 1955), alternative materials are very hard to find (Klopsteg and Wilson, 1954; Davies et al., 1977; Fillauer and Quigley, 1979; Krouskop et al., 1974; Bilotto, 1986) and glove and prosthesis modification can only provide for partial solutions (Herder et al., 1998). Consequently, compensating the glove stiffness is left as solution. This ideology has already lead to a series of mechanisms and methods (Kuntz, 1995; Herder et al., 1998; de Visser and Herder, 2000; Plettenburg, 2002; Wijsman, 2010; Tolou et al., 2012), but none of them have resulted in a working concept due to challenges that lie in the non-linear behaviour of the glove stiffness, high occurring forces and small working volume.

This study aims to design a new glove stiffness compensation mechanism for a toddler-sized hand prosthesis. Its goal is to reduce activation forces to a minimum and fit into the wrist of the prosthesis. Consequently, emphasis is put on reducing energy dissipation within the mechanism and maximising energy density. This is done by completely omitting the use of bearings and any sliding contact by using the concept of rolling link mechanisms (Kuntz, 1995) to reduce friction losses to a minimum, leading to the development of a Rolling Stiffness Compensation Mechanism (RSCM). As a result, the apparent presence of the cosmetic glove stiffness can be decreased.

2 Methods & Materials

2.1 Design criteria

The main objective for the compensation mechanism was to reduce activation forces down to the comfortable limit of 40 N (Plettenburg et al., 2011). Furthermore, it should passively open the prosthesis and create a voluntary closing device, due to the advantages in enhanced feedback. A toddler-sized WILMER WHD-4 prosthesis, with a mass of 69 g, was used as a reference point. Consequently, the compensation mechanism needed to be lightweight and fit into a compatible wrist, which may range from 30–38 mm in diameter (Plettenburg, n.d.). At such small scale, the use of hinged and sliding joints becomes impractical and can introduce coefficients of friction of up to $f = 0.02$. For this reason, the concept of rolling link mechanisms was used, which is a method that uses only rolling friction and is able to reduce the friction coefficient down to $f < 0.001$ (Kuntz, 1995). The prosthesis operated by using a central pushrod, which allowed for a voluntary opening or voluntary closing device by adding or omitting an extra lever, respectively.

2.2 Design approach

The cosmetic glove's stiffness can be compensated by adding a negative stiffness element in parallel to the glove's stiffness, such that the addition of the two gives a reduced, resultant stiffness. A cosmetic glove generally possesses a progressive stiffness characteristic (Herder et al., 1998; Wijsman, 2010; Tolou et al., 2012). By mimicking the shape of this glove stiffness characteristic, but acting in opposite direction, the resultant stiffness can be reduced to a minimum. Moreover, by overcompensating the glove characteristic, a voluntary closing device can be acquired (Figure 1).

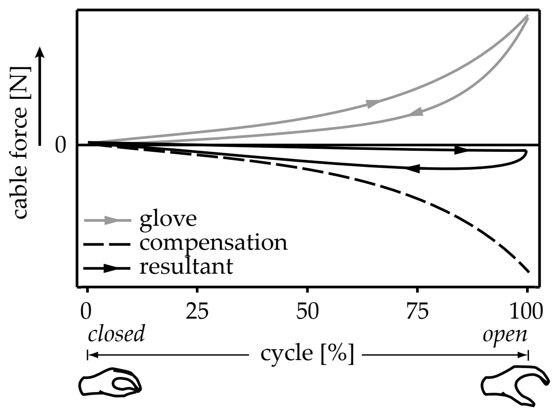

Figure 1: *An ideal case of overcompensation of the glove characteristic. The operation of the resultant characteristic is reversed and turns an otherwise voluntary opening device into a voluntary closing device.*

Merely using a pretensed spring as a negative stiffness element does not suffice, because the compensation force would decrease as the spring releases energy. The opposite is necessary: the compensation force should increase as energy is released from the compensation mechanism. As a result, the design of the mechanism was dependent on three key components: the glove stiffness characteristic, method of energy storage and the used mechanical linkage.

2.2.1 *Glove stiffness characteristic*

The glove's stiffness characteristic defined the desired outcome of the compensation mechanism and was dependent on both the prosthesis and glove that was used. Consequently, a total of ten different pediatric gloves were fitted on the WILMER WHD-4 prosthesis and the resulting glove stiffness was measured. Six gloves were made of PVC (Otto Bock, size 8S6=142x50, thickness of 0.8–1.3 mm), two were made of silicone (Otto Bock, size 8S6=142x50, thickness of 2.2–2.5 mm) and two were made of silicone with applied smooth-coating (Regal, size CS, thickness of 2.8–3.0 mm). All gloves caused the prosthesis to close in rest. The combination that resulted in the lowest energy requirement was used for further dimensioning of the energy storage.

2.2.2 *Energy storage*

Because weight and volume needed to be minimised, energy density was the foremost factor in determining the ideal form of energy storage. Also, the working principle needed to be passive to conserve the body-powered ideology. Among applicable sources of potential energy, i.e. mechanical springs, gas springs and magnetic forces, linear helical springs were the best option with high energy density (1.21 MJm^{-3} (Cool, 2006)) and were most practical due to many variations in off-the-shelf products.

2.2.3 Mechanical linkage

The main purpose of the mechanical linkage was to reverse the operation of the linear springs as energy storage and create the desired compensation characteristic. This is possible with an asymptotic mechanical enhancement curve, which suppresses force when springs are fully tensed and enhances force when they are almost fully relaxed. This asymptote results in high reaction forces from the energy storage, causing energy dissipation due to friction. In order to minimise these losses, the concept of rolling link mechanisms was used. This increases the mechanism's efficiency and reduces the chance for it to fail. It does, however, introduce difficulties in stabilisation and alignment of the different parts.

2.3 Conceptual design

The combination of using linear helical springs as energy storage and a rolling link mechanism as mechanical linkage, led to the design of a Rolling Stiffness Compensation Mechanism (RSCM). The RSCM's overall shape and how the parts connect through stabilisation bands is shown in Figure 2a. Its working principle is shown in Figure 2b in three steps:

(1) The force from the glove stiffness (F_{glove}) has the tendency to close the hand, whereas the compensation force from the RSCM (F_{comp}) counteracts this force. Because $F_{comp} > F_{glove}$, the hand passively opens.

(2) As the user pulls on the RSCM (F_{user}), F_{comp} decreases and the remaining glove stiffness will cause the hand to close ($F_{user} + F_{glove} > F_{comp}$). As the hand closes, elastic energy from the cosmetic glove is transferred to the springs in the RSCM.

(3) The hand is closed and the glove is relaxed ($F_{glove} \rightarrow 0$). The springs in the RSCM are fully loaded while F_{comp} is minimal. Increase in F_{user} will now only increase grip strength. Because $F_{comp} > F_{glove}$, the hand will passively open again if F_{user} is zero, returning the system to step (1).

2.3.1 Compensation characteristic

The rolling link mechanism is shown in Figure 3a, which consists of four rollers with radius r that are pulled towards each other by linear tensile springs, and two opposing intermediate bodies whose widths are determined by parameter b and a contour radius R. Due to the horizontal and vertical symmetry of the mechanism, each roller makes the same contact angle α with the intermediate bodies. The distance between the rollers' centres is denoted by x_r and determines the spring length, while the vertical distance between the intermediate bodies is denoted by y and is directly related to the cable displacement from the prosthesis. They can be calculated as a function of α according to:

$$x_r(\alpha) = 2\left((R + r)\cos\alpha + b\right) \tag{1a}$$

$$y(\alpha) = 2\left((R + r)\sin\alpha - R + r\right) \tag{1b}$$

In Figure 3b, a free body diagram of one of the rollers is shown. It can be seen that the force from the springs on each roller (F_s) induces a reaction force from the adjacent roller (F_r) and intermediate body (F_R). The magnitude of these reaction forces are dependent on α, but the occurrence of free rolling resistance introduces friction angles (ψ_r, ψ_R) and change the direction and magnitude. In order for all forces to be in balance, the relations as shown in the force triangle need to hold, which can be expressed in the sine rule:

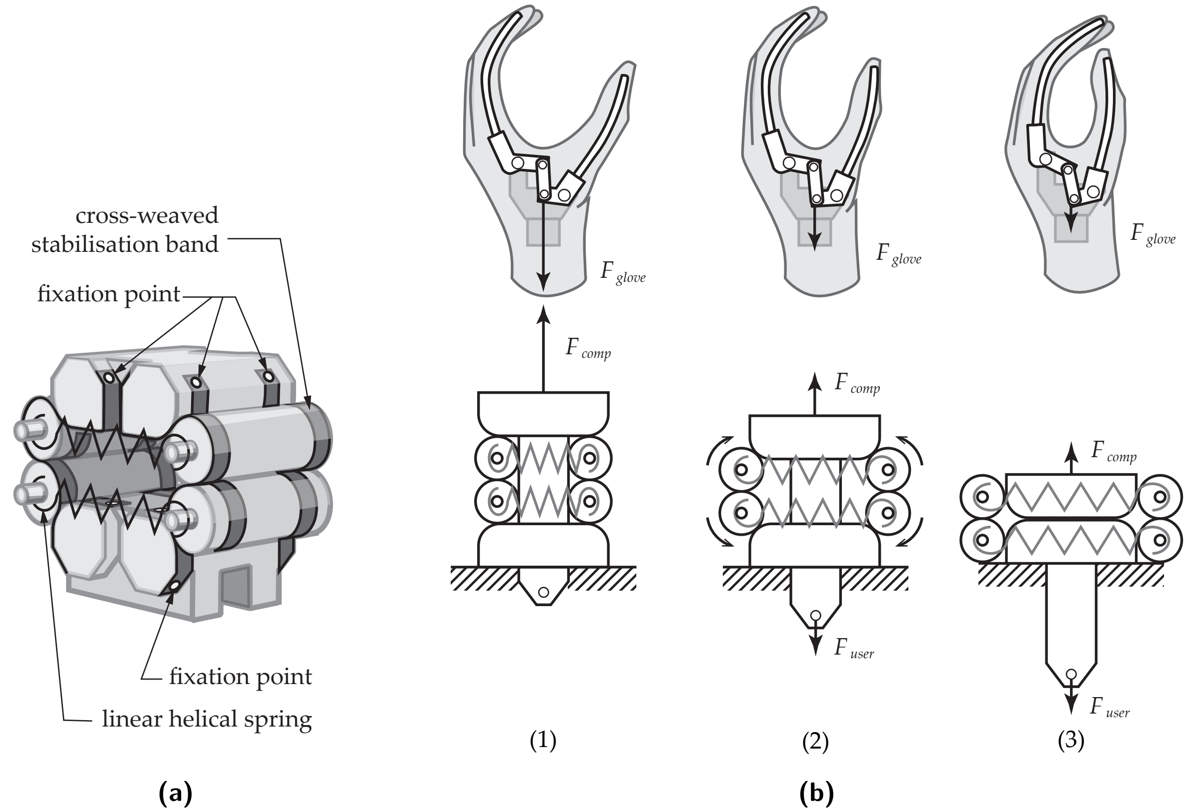

Figure 2: *Conceptual design of the Rolling Stiffness Compensation Mechanism (RSCM) with (a) its overall shape and how the parts connect through cross-weaved stabilisation bands, indicating the visible fixation points, and (b) its working principle in combination with the WILMER WHD-4 mechanism.*

$$\frac{F_r}{\sin(\alpha - \psi_R)} = \frac{F_R}{\sin(\pi/2 + \psi_r)} = \frac{F_s}{\sin(\pi - (\alpha - \psi_R) - (\pi/2 + \psi_r))} \tag{2}$$

Resultingly, F_r and F_R can be calculated:

$$F_r(\alpha) = \frac{\sin(\alpha - \psi_R)}{\cos(\alpha - \psi_R + \psi_r)} F_s \tag{3a}$$

$$F_R(\alpha) = \frac{\cos(\psi_r)}{\cos(\alpha - \psi_R + \psi_r)} F_s \tag{3b}$$

Additionally, F_s can be expressed in x_r (Equation (1a)) and the spring's stiffness (k), initial length (L_0) and pretension (F_0). Each roller is connected with two springs, it can therefore be calculated according to:

$$F_s(\alpha) = 2\left(k(x_r(\alpha) - L_0) + F_0\right) \tag{4}$$

The compensation force F_{comp} is dependent on the normal component of F_R ($= F_R\cos(\psi_R)$), of which the vertical component directly contributes to F_{comp}. Because four rollers contribute to the total compensation force, F_{comp} can now be calculated according to:

$$F_{comp}(\alpha) = 4\frac{\cos(\psi_r)\cos(\psi_R)\sin(\alpha)}{\cos(\alpha - \psi_R + \psi_r)} F_s \tag{5}$$

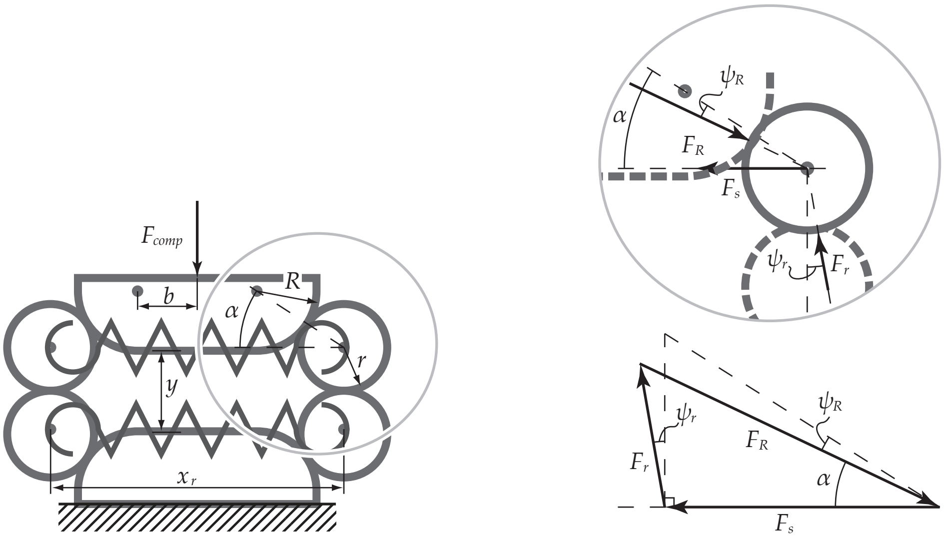

(a) **(b)**

Figure 3: *Figures showing (a) the used rolling link mechanism and used geometric annotations. In (b), the free body diagram is shown of the roller inside the encircled area, together with the accompanying force triangle in which the forces are in balance. The vertical component of force F_R directly contributes to the total compensation force F_{comp}.*

By combining Equations (1), (4) and (5) it can be observed that, when $\alpha = 0$, the spring force is at its maximum but the compensation force is zero. When $\alpha \to \pi/2$, the spring force is minimal but the compensation force reaches its maximum. In the absolute case of $\alpha = \pi/2$, the mechanism will approach a theoretical asymptote. Because of this asymptote, the mechanism expresses a negative progressive stiffness characteristic, making it suitable for a glove stiffness compensation mechanism.

2.3.2 Stabilisation

Although rolling link mechanisms show very low values for energy dissipation, they need to be stabilised by a stabilisation band (Kuntz, 1995). This is done by cross-weaving steel bands through the rolling elements and fixating their ends under tension with micro spot welds (see Figure 2a).

In order to prevent misalignment and asymmetry during operation, the part on which F_{user} operates (see Figure 2b) is guided between two axes. These axes are fixed on the lower intermediate body and fitted with plain bearings. This same part also prevents the rollers from rolling inwards too much, which can put the mechanism in a form-lock.

2.3.3 Materials

All main parts were made of AISI 314 stainless steel. The rollers' radius r was taken at 1.9 mm such that a vertical gap of at least 7.5 mm could be obtained – a necessity for the WILMER WHD-4. The contour radius R was set to 2.3 mm and width b to 7 mm in order to be able to fit the springs.

Two different types of springs were used in order to test the effect of spring stiffness and validity of the model. They were identical in dimensions but varied in material, one stainless steel (T40840) and one spring steel (T30840) from (Tevema Technical Springs, 2008). Both types of springs were able to overcompensate the measured glove stiffness characteristic, having a rated stiffness of 1.35 and 1.57 $\mathrm{N\,mm^{-1}}$ and pretension of 1.8 and 2.13 N, respectively. The stiffness and pretension were also measured for all springs in order to find their actual mechanical properties.

The stabilisation bands were made out of stainless steel. Moreover, they were varied in thickness between 20 and 50 µm to test their effect on the compensation characteristic.

2.4 Data acquisition

Stiffness characteristics were measured of the gloved prosthesis, the prototype and the combination of the two. A custom-built test bench was used to obtain the stiffness characteristics by measuring force and displacement (Smit and Plettenburg, 2013; Tolou et al., 2012; Smit et al., 2012; Wijsman, 2010; Smit and Plettenburg, 2010). In the test bench, the measurand was fixed into position and connected to a cable which inflicted displacement. The force at the end of the cable was measured by a load cell (model: B3G-C3-50kg-6B, Zemic, Etten-Leur, The Netherlands) and the position by a linear position transducer (model: LCIT 2000, S/N: J 0069, Schaevitz, Hampton, VA). Both force and position measurements were fed to a data acquisition (DAQ) device (model: NI USB-6008, 12-bit, 10 kS/s, National Instruments, Austin, TX) and into the computer, using LabView version 10.0.1 (National Instruments, Austin, TX) for visualisation and storing of the measured values.

All measurements were repeated five times. Before each series of measurements, the stiffness of connective elements (e.g. cable) was measured separately and eventually corrected for during data processing.

2.5 Data processing

The desired compensation characteristic needed to be based on a generalised shape of the used glove. As a result, each repetition from the glove stiffness measurements was fitted with polynomial and exponential functions. The best fit was chosen based on the adjusted R^2 and Root Mean Square Error (RMSE). The fits for every repetition were then averaged to obtain a generalised fit.

The measurements involving the prototype were first divided into discrete bins of 0.5 mm. Within these bins, an average force level was determined by calculating the mean over all repetitions.

For all tests, the amount of input energy was determined by calculating the surface area beneath the loading curve. Hysteresis was determined by calculating the surface area enclosed by the loading and unloading curve. The efficiency of the RSCM combined with prosthesis was determined by calculating the ratio between the loading and unloading curve.

All data processing was performed in Matlab 2010b (Mathworks, Natick, MA).

3 Results

3.1 Cosmetic gloves

A fifth-order polynomial proved to provide for the best fit for each separate glove (adjusted $R^2 > 0.99$, $RMSE < 5$ N). The fitted characteristics for all types of gloves are shown in Figure 4, where distinctive loading and unloading curves can be seen. The required input energy (E_{in}) to open the gloved device ranged between 277–833 N mm. The hysteresis (E_{hyst}) ranged between 105–259 N mm. The ungloved WILMER WHD-4 never showed forces higher than 10 N, confirming that the addition of the cosmetic glove has a dramatic effect.

The shapes and outcome measures are comparable to those of previous studies (Herder et al., 1998; Wijsman, 2010; Tolou et al., 2012). Here, the pure silicone gloves from Otto Bock show the lowest stiffness characteristic, requiring a maximum activation force of approximately 120 N. Resultingly, these were used as a reference point as they provide for the lowest energy requirement.

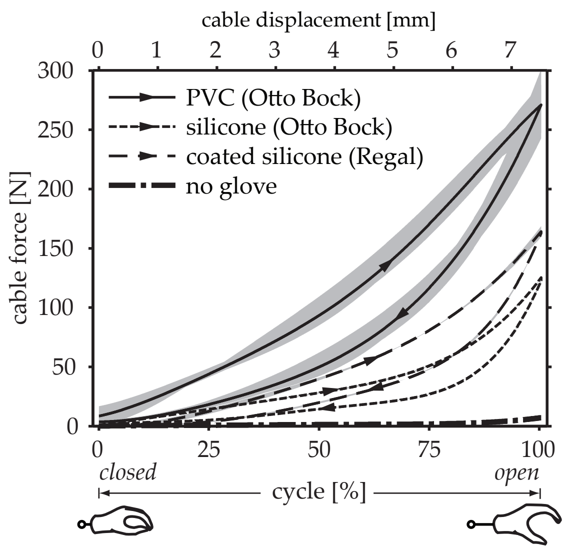

Figure 4: *Glove stiffness characteristics, showing the average fit (black) compared to the range of different fits (grey) for all types of glove material, as well as for the ungloved prosthesis. The surface area beneath the loading curve is equal to required input energy (E_{in}), surface area enclosed by both curves is equal to the hysteresis (E_{hyst}). Average energy values are for PVC (Otto Bock): E_{in} = 833 N mm, E_{hyst} = 259 N mm, for silicone (Otto Bock): E_{in} = 277 N mm, E_{hyst} = 105 N mm, for coated silicone (Regal): E_{in} = 388 N mm, E_{hyst} = 133 N mm*

3.2 Prototype

The resulting prototype is shown in Figure 5, where additional protrusions were added to the overall shape to guide the stabilisation bands. The outer dimensions (length$\times$width$\times$depth) are equal to 33 $\times$ 18.6 $\times$ 19 mm when the springs are relaxed (see Figure 5) and 33 $\times$ 26.2 $\times$ 19 mm when the springs are fully tensed. The total mass of the mechanism is equal to 26 g.

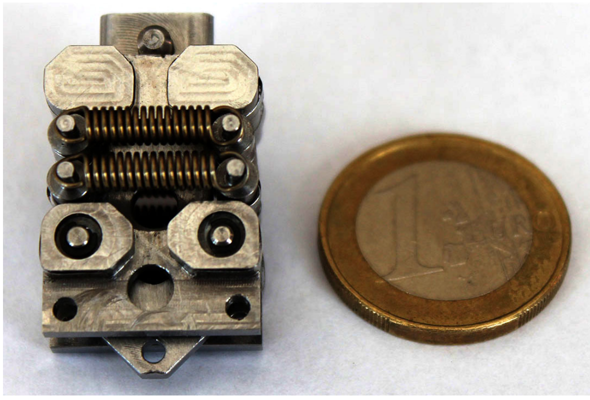

Figure 5: *The manufactured RSCM prototype, alongside a Euro coin for scale.*

The used springs appeared to have different mechanical properties than reported by manufacturer. Stainless steel springs showed an average stiffness of 1.05 N mm^{-1} and pretension of 0.63 N (versus rated 1.35 N mm^{-1} and 1.8 N), spring steel springs showed a stiffness of 1.18 N mm^{-1} and pretension of 0.86 N (versus rated 1.57 N mm^{-1} and 2.13 N).

The results for the RSCM's absolute compensation characteristic compared with the model output are presented in Figures 6. The resultant forces of the RSCM combined with the gloved prosthesis are presented in Figure 7, where a model prediction is established by subtracting the modelled compensation characteristic from the glove measurements. All graphs show that the model is largely comparable to the measured values.

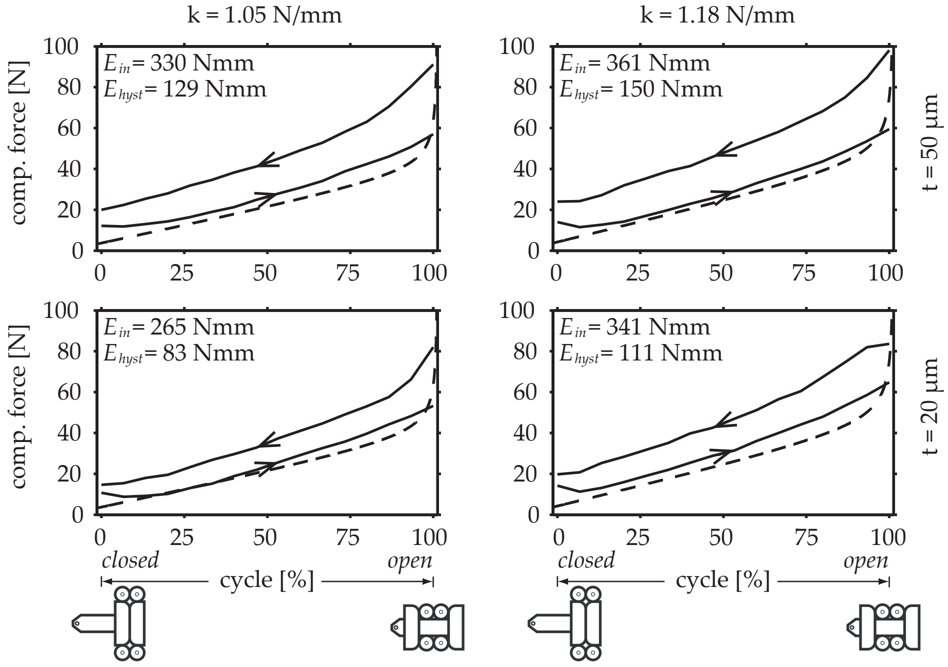

Figure 6: *Figures showing the measured absolute compensation force (solid) and as predicted by the model (dashed). Both spring stiffness (k) and stabilisation band thickness (t) were varied. Arrows indicate the direction of the curves, distinguishing loading and unloading curves.*

However, there is a clear difference in offset and a large hysteresis loop is present.

The slight differences due to variation in spring rate can be seen in both model and measurements. An increase in spring rate results in increased overall stiffness and higher reaction forces, causing the input energy and hysteresis to increase.

The stabilisation band thickness was not included in the model and therefore only affects the measured values. Clearly, the bands are large contributors to the mechanism's hysteresis, which is added to the glove's hysteresis in the resultant curve. Thinner bands bring the characteristic closer to the model—both in shape and in absolute values—by greatly reducing input energy and hysteresis. Stabilisation bands of 50 µm reduce maximum resultant forces down to 55 N with an average efficiency of 45%, whereas 20 µm bands are able to reduce them down to 40 N with an average efficiency of 52%.

4 Discussion

The RSCM is successful in having a progressive negative stiffness characteristic and is therefore suitable as a novel compensation mechanism. Resultingly, it is able to reduce operation forces of a gloved prosthesis and even reverse its working principle with overcompensation, making it possible to turn a voluntary opening device into a voluntary closing device. In the latter case, it is shown to be possible to reduce the maximum operating force from 120 N down to the comfortable limit of 40 N (Plettenburg et al., 2011).

The small dimensions of the RSCM allow it to be used inside the wrist of a toddler-sized

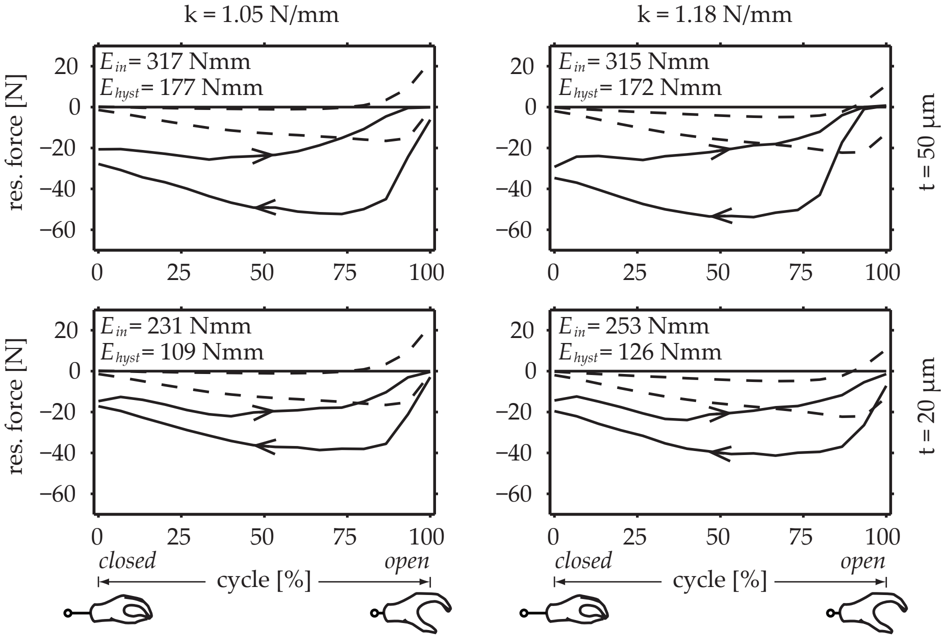

Figure 7: *Figures showing the measured resultant force of the prosthesis with compensation mechanism (solid) and as predicted by the model (dashed). Both spring stiffness (k) and stabilisation band thickness (t) were varied. Arrows indicate the direction of the curves, distinguishing loading and unloading curves. Notice how the sign of the force and direction of the curves have been reversed, creating a voluntary closing prosthesis.*

prosthesis. It requires a minimum inner diameter of 33 mm, which may fit into a 38 mm diameter wrist. The RSCM can also be integrated with the prosthesis mechanism as part of a pushrod, further reducing the length of the mechanism. The low mass minimally affects the overall mass of the prosthesis, bringing it to a total of 95 g. In conclusion, the compensation mechanism satisfies the design criteria. Its efficiency, however, is quite low and should be closer the model.

The performance of the mechanism is mostly influenced by the stabilisation bands and misalignment of parts. These effects were not included in the model and are therefore considered to be the main contributors to the higher forces and hysteresis.

Thicker stabilisation bands add more rigidity to the system, introducing a higher stiffness due to elastic deformation and energy dissipation due to plastic deformation. Consequently, they need to be as thin as possible. Thinner bands, however, are increasingly difficult to assemble. Their fixations (spot welds) become weaker and less pretension can be added to the bands. This causes parts to become misaligned, resulting in nonparallel axes of the rolling elements – one of the larger sources of rolling friction (Kuntz, 1995). Improved assembly strategies are possible that can reduce these issues, e.g. firm temporary fixations of the rolling elements while the stabilisation bands are being placed.

Misalignment of parts is not only caused by quality of assembly of stabilisation bands. It was also observed that the direction of pulling force (F_{user}) was not perfectly in line with the mechanism, which caused the rolling elements to become misaligned. This effect was much lower when the RSCM was tested in combination with the prosthesis, as operation forces are then substantially lower. This is confirmed by the fact that the resultant hysteresis is not equal to the glove hysteresis added with the RSCM's hysteresis, because it is dependent on the magnitude of the operation force. By adding an intrinsic alignment of the parts, for example by rolling in grooves, this effect can be reduced.

An additional practical improvement to the design would be to increase the rollers radius r, which further prevents a form-lock of the mechanism when $\alpha \to \pi/2$. Moreover, this increases the working space of the RSCM and even becomes larger than required. This allows the relative position of the RSCM to be tweaked on-the-spot, increasing its range of applicability and tolerance towards inaccuracies.

Apart from the presented configuration, i.e. the used geometry and springs, other configurations are also possible. In general, the springs' mechanical properties are the determining factor, as they are limited in their possible combinations of properties. From there on, several optimal geometric solutions can be calculated, depending on weight and volume criteria. This makes the RSCM suitable to be designed for other types of gloves and even other applications, making it a novel negative stiffness element with a large area of application.

References

Biddiss, E. and T. Chau (2007). "Upper limb prosthesis use and abandonment: A survey of the last 25 years." In: *Prosthetics and Orthotics International* 31.3, pp. 236–257. DOI: 10.1080/03093640600994581.

Bilotto, S. (1986). "Upper Extremity Cosmetic Gloves." In: *Clinical Prosthetics & Orthotics* 10.2, pp. 87–89.

Cool, J.C. (2006). *Werktuigkundige systemen*. 3rd ed. VSSD.

Corin, J.D. et al. (1987). "Mechanical Comparison of Terminal Devices." In: *Clinical Prosthetics & Orthotics* 11.4, pp. 235–244.

Darnall, B.D. et al. (2005). "Depressive symptoms and mental health service utilization among persons with limb loss: Results of a national survey." In: *Archives of Physical Medicine and Rehabilitation* 86.4, pp. 650–658. DOI: 10.1016/j.apmr.2004.10.028.

Datta, D., K. Selvarajah, and N. Davey (2004). "Functional outcome of patients with proximal upper limb deficiency - acquired and congenital." In: *Clinical Rehabilitation* 18.2, pp. 172–177. DOI: 10.1191/0269215504cr716oa.

Davies, E.W., W.B. Douglas, and A.D. Small (1977). "A cosmetic functional hand incorporating a silicone rubber cosmetic glove." In: *Prosthetics and Orthotics Internationa* 1.2, pp. 89–93.

Dembo, T. and E. Tane-Baskin (1955). "The Noticeability of the Cosmetic Glove." In: *Artificial Limbs* 2.2, pp. 47–56.

Desmond, D.M. (2007). "Coping, affective distress and psychosocial adjustment among people with traumatic upper limb amputations." In: *Journal of Psychosomatic Research* 62.1, pp. 15–21. DOI: 10.1016/j.jpsychores.2006.07.027.

Fillauer, C. and M.J. Quigley (1979). "Clinical Evaluation of an Acrylic Latex Material Used as a Prosthetic Skin on Limb Prostheses." In: *Orthotics and Prosthetics* 33.4, pp. 30–38.

Herder, J.L., J.C. Cool, and D.H. Plettenburg (1998). "Methods for reducing energy dissipation in cosmetic gloves." In: *Journal of Rehabilitation Research and Development* 35.2, pp. 201–209. PMID: 9651892.

Klopsteg, P.E. and P.D. Wilson (1954). "Human limbs and their substitutes." In: McGraw-Hill Book Company Inc., pp. 239–269.

Krouskop, T.A., P.H. Newell Jr., and L.A. Leavitt (1974). "Cosmetic Covers for Lower-limb Prostheses." In: *Bulletin of prosthetics research*, pp. 411–414.

Kuntz, J.P. (1995). "Rolling Link Mechanisms." PhD thesis. Delft University of Technology.

LeBlanc, M. et al. (1992). "Mechanical Work Efficiencies of Body-Powered Prehensors for Young Children." In: *Journal of the Association of Children's Prosthetic-Orthotic Clinics* 27.3, pp. 70–75.

Plettenburg, D.H. (2002). "A sizzling hand prosthesis." PhD thesis. Delft University of Technology.

Plettenburg, D.H. (2006b). *Upper extremity prosthetics: current status & evaluation*. 1st ed. VSSD.

Plettenburg, D.H. (n.d.). *WILMER Friction Wrist*.

Plettenburg, D.H. and J.L. Herder (2003). "Voluntary closing: A promising opening in hand prosthetics." In: *Technology and Disability* 15.2, pp. 85–94.

Plettenburg, D.H., M. Hichert, and G. Smit (2011). "Feedback in voluntary closing arm prostheses." In: *Proceedings of the MEC'11 conference*.

Shaperman, J. et al. (1995). "Is body powered operation of upper limb prostheses feasible for young limb deficient children?" In: *Prosthetics and Orthotics International* 19.3, pp. 165–175. DOI: 10.3109/03093649509168000.

Smit, G. and D.H. Plettenburg (2010). "Efficiency of voluntary closing hand and hook prostheses." In: *Prosthetics and Orthotics International* 34.4, 411—427. DOI: 10.3109/03093646.2010.486390.

Smit, G. and D.H. Plettenburg (2013). "Comparison of mechanical properties of silicone and PVC (polyvinylchloride) cosmetic gloves for articulating hand prostheses." In: *Journal of Rehabilitation Research & Development* 50.3, pp. 723–732. DOI: 10.1682/JRRD.2011.12.0238.

Smit, G. et al. (2012). "Efficiency of voluntary opening hand and hook prosthetic devices: 24 years of development?" In: *Journal of Rehabilitation Research & Development* 49.4, pp. 523–534. DOI: 10.1682/JRRD.2011.07.0125.

Stevens, P. (Dec. 2011). "Losses Beyond the Limb." In: *The O&P Edge*. URL: http://www.oandp.com/articles/2011-12_01.asp.

Tevema Technical Springs (2008). *Product Module*. Accessed at March 15, 2013. URL: http://www.tevema.com/.

Tolou, N. et al. (2012). "Stiffness Compensation Mechanism for Body Powered Hand Prostheses with Cosmetic Covering." In: *Journal of Medical Devices* 6.1, p. 011004. DOI: 10.1115/1.4005781.

de Visser, H. and J.L. Herder (2000). "Force-directed design of a voluntary closing hand prosthesis." In: *Journal of Rehabilitation Research and Development* 37.3, pp. 261–271. PMID: 10917258.

Wijsman, F. (2010). "The Design of a Glove Compensated Hand Prosthesis for Toddlers." Master's thesis. Delft University of Technology.

Part II

Literature Study

1 Cosmetic gloves **19**
- 1.1 History . . . 19
  - 1.1.1 Implementation & intention . . . 19
  - 1.1.2 Evolution of glove materials . . . 19
- 1.2 Interfering characteristics. . . . 20
  - 1.2.1 Viscoelasticity. . . . 20
  - 1.2.2 Stiffness . . . 20
  - 1.2.3 Hysteresis . . . 20
  - 1.2.4 Strain rate dependency . . . 21
  - 1.2.5 Glove characteristic . . . 21
- 1.3 Candidate materials . . . 22
  - 1.3.1 PVC . . . 22
  - 1.3.2 Silicone rubber . . . 23
  - 1.3.3 Polyurethane . . . 24
  - 1.3.4 Multi-layer materials . . . 24
- 1.4 Glove modification . . . 25
- 1.5 Concluding remarks. . . . 25

2 Compensation mechanisms **27**
- 2.1 On glove compensation . . . 27
- 2.2 Existing mechanisms . . . 29
  - 2.2.1 Preceding glove compensation mechanisms . . . 29
  - 2.2.2 Other compensation mechanisms . . . 30
- 2.3 Concluding remarks. . . . 34

3 Energy storage **35**
3.1 Fundamental energy sources 35
3.2 Counterweights 36
3.3 Mechanical springs 37
3.3.1 Constant spring rate 37
3.3.2 Variable spring rate 38
3.3.3 Constant force springs 40
3.4 Permanent magnets 40
3.4.1 Magnets with common axis 41
3.4.2 Sliding magnets 42
3.5 Gas springs 43
3.6 Concluding remarks. 45

4 Mechanical linkage **47**
4.1 Types of mechanisms 47
4.2 Four-bar linkages 47
4.2.1 Classification 48
4.2.2 Mechanical enhancement 48
4.3 Gears, rollers and pulleys 49
4.4 Concluding remarks. 50

5 Conclusions **51**

Chapter 1

Cosmetic gloves

Cosmetic gloves have been used for decades in order to improve the overall cosmetic appearance of upper limb prostheses. During these years several types of materials have been designed, manufactured, used, evaluated and eventually discarded or further developed, leading to today's standard. By evaluating the current status on cosmetic coverings of the artificial hand, its characteristics can be discussed and how it effects the overall performance of the terminal device.

1.1 History

Compared to the rich history in prostheses themselves, the history in cosmetic gloves is very short. The train of thought and the choices made, however, can still provide insight in why they are as they are now.

1.1.1 Implementation & intention

One of the earliest documentations on the general use and manufacturing of a cosmetic glove dates back to 1949. Consequently, this led to the introduction of the *social usefulness* of prosthetic devices, indicating that more emphasis must be put on the social effects of having a prosthesis (Research Division, College of Engineering, New York University, 1949; cited in Dembo and Tane-Baskin, 1955). For example, in the study of Dembo and Tane-Baskin (1955) it was shown that the mere presence of a natural looking hand can be sufficient in order to have it perceived as an ordinary hand. Even though being strongly dependent on the intensity of social and/or physical contact, a cosmetic glove can have the effect of becoming unrecognised as an amputee when dealing with everyday people in everyday life.

1.1.2 Evolution of glove materials

Most of the commercially available cosmetic gloves in the early '50s were made out of polyvinyl chloride (PVC) with added plasticiser for extra flexibility. It was, however, susceptible to wear, yellowing and the plasticiser made removing stains virtually impossible (Carnelli et al., 1955), but the wide field of application of PVC materials allowed it to be cheap and thus affordable for users. A new suitable candidate was introduced in the 1970s, when the increasing development in new types of silicone rubbers allowed for stronger solutions. Even though it was still more expensive than PVC and has lower tear strength, the superior stain resistance made silicone rubbers very attractive (Davies et al., 1977). Other materials such as natural and synthetic rubbers/latices (Klopsteg and Wilson, 1954; Fillauer and Quigley, 1979) and urethanes (Krouskop et al., 1974) were also shortly introduced. Even though some of them looked promising at the time, not much of them is seen again. As a result, cosmetic gloves were and still are mostly made by either PVC or silicone rubbers.

1.2 Interfering characteristics

Apart from being durable and suitable for cosmetic purposes, cosmetic gloves are also interfering with the intended functioning of the terminal device. As the glove will deform when opening or closing the artificial hand, it will require additional energy to do so. The materials used show viscoelastic behaviour, resulting in complex behaviour including non-linear stiffness and hysteresis.

1.2.1 Viscoelasticity

Both PVC and silicone rubbers—and other candidate materials (section 1.3)—are amorphous polymers. This means that, at low temperatures, they become a solid rubber and act like purely elastic materials. At high temperatures, the material becomes a liquid and shows viscous behaviour. However, if the temperature is somewhere in between (above glass temperature), a mixture of the two is experienced; *viscoelasticity*.

1.2.2 Stiffness

The stiffness of a material is a strain dependent quantity, causing larger deformations to require more energy. The problem with rubber-like materials as used in cosmetic gloves is their non-linear behaviour. Figure 1.1 shows recent measurements on a prosthesis from Tolou et al. (2012) with four different PVC gloves, showing its basic progressive shape. It also shows that, even though being from the same material and manufacturer, the gloves show different stiffnesses.

1.2.3 Hysteresis

Unlike the elasticity of a material, the viscosity is not able to store energy when deformed. Instead, energy is dissipated during deformation. Consequently, part of the energy which is put into opening or closing of the prosthesis is lost due to this dissipation. This also means that the force-displacement curve is different for loading and unloading the gloved prosthesis. Early tests from Herder et al. (1998) show this exact behaviour in a graph, which is verified later on with similar tests by Wijsman (2010).

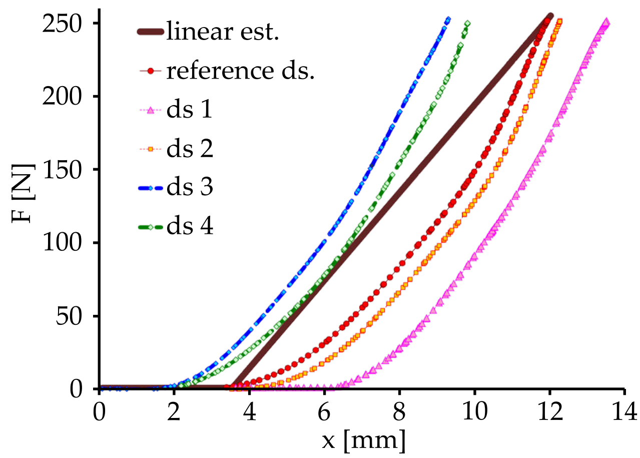

Figure 1.1: *Effective stiffness of a prostheses with four different gloves. An average force-displacement relationship (reference ds) is resultant from averaging each dataset (ds). A bilinear approximation is used to estimated this behaviour. (Adapted from Tolou et al., 2012, Fig. 2).*

The latter one is shown in Figure 1.2. The surface area between the loading and unloading curve is representative for the dissipated energy.

1.2.4 Strain rate dependency

The viscosity of the material also adds a time-dependent behaviour. This is making the process not only dependent on initial and final state, but also on its path towards this final state. The time-dependent behaviour of the material affects its stiffness and hysteresis. Higher velocities will increase viscous forces that resist deformation, whereas lower velocities enhance viscoelastic creep inside the material. In Herder et al. (1998), a series of tests have been performed on rectangular PVC specimen that show this behaviour. These results are shown in Figure 1.3, where it can be seen that both stiffness and hysteresis increase with strain rate.

1.2.5 Glove characteristic

The amount of added stiffness and hysteresis due to the cosmetic glove, can be seen by looking at the glove characteristic. This characteristic can be established by measuring the force and displacement of the Bowden cable while pulling it. An example of the resulting curve can be seen in Figure 1.4, showing its typical progressive shape. In this figure, a distinctive loading and unloading curve can be seen. The surface area between these two curves represents the amount of dissipated energy due to hysteresis.

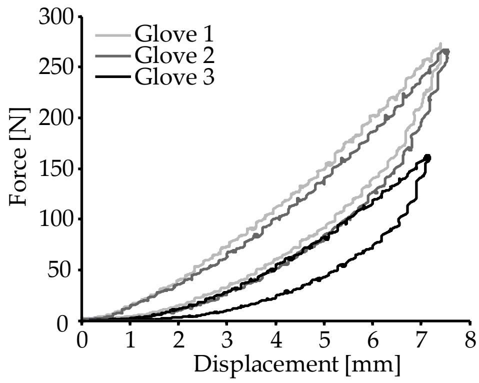

(a)

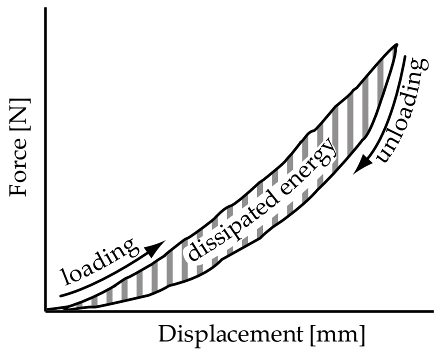

(b)

Figure 1.2: *Force-displacement characteristics of (a) measurement data of three different gloves, and (b) a generalised figure indicating the area between the loading and unloading curve, representing the dissipated energy (adapted from Wijsman, 2010, Fig. B.142).*

1.3 Candidate materials

As is previously stated, today's market in cosmetic gloves is dominated by either PVC or silicone rubbers. Typically, the choice will end up in a trade-off between "...availability, cost, appearance, functionality and durability." (Schweitzer, 2009). The next few sections discuss the cosmesis and mechanical properties of candidate materials, covering the appearance, functionality and durability of a glove using that material. Availability and cost are very dependent on the market status and are not elaborately discussed here.

1.3.1 PVC

Cosmesis PVC is able to fulfil the basic cosmetic requirements a cosmetic glove should have. For users, it is usually a simpler or more basic solution in order to reduce public attention towards the hand in general. However, stains are not that easily removed from the material, giving a faster degradation of cosmetic value and drawing more attention towards it. A possible available solution is to apply a certain micro-coating on the surface, it helps preventing stains from for example newspapers or pens to be absorbed in the material (Centri AB, 2011).

Mechanical properties What PVC loses in cosmesis, it gains in its mechanical properties. It is a very wear-resistant material, making it durable and suitable for extensive use. The exact product life of one glove is difficult to predict however, as the thickness within one batch can differ up to 50% (Wijsman, 2010). This does not only affect the product life, but also its mechanical behaviour.

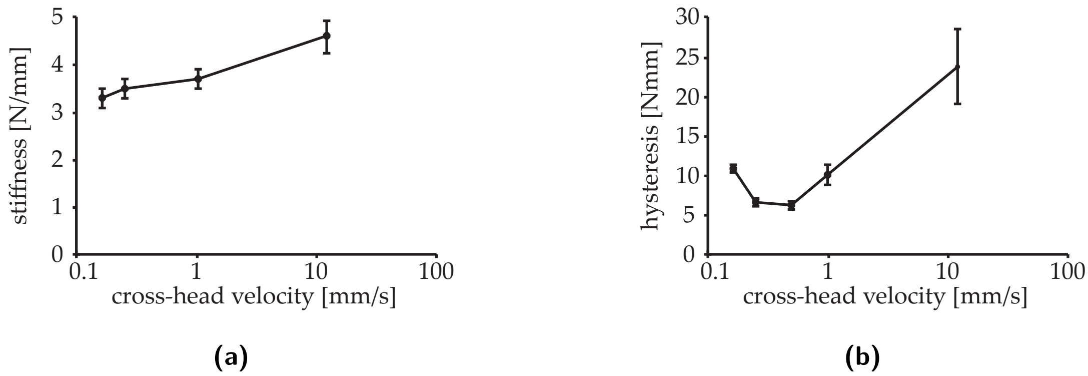

Figure 1.3: *Effect of cross-head velocity on (a) stiffness and (b) hysteresis (adapted from Herder et al., 1998, Fig. 8a&b).*

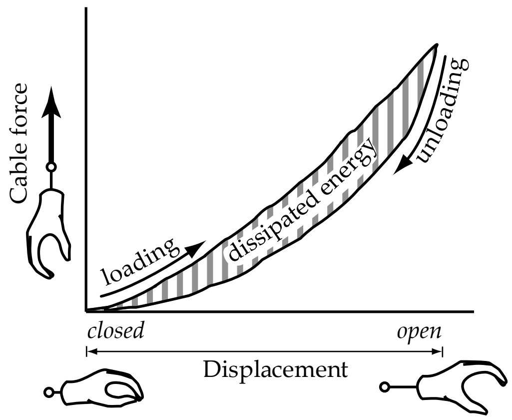

Figure 1.4: *Example of a glove characteristic, showing the loading and unloading curve. The difference between the two curves is termed the hysteresis and causes irreversible energy dissipation.*

1.3.2 Silicone rubber

Cosmesis Silicon gloves are widely seen as more realistic than their PVC counterparts. They are easier to clean and allow for more different skin tones. Also the texture gives the whole glove a better and more 'skin'-like feel. These properties, however, are not guaranteed for every random glove made out of silicone rubber, because it offers a wide range of qualities.

Mechanical properties One of the main concerns of using silicone rubbers, is that they tend to tear faster. Being more susceptible to wear, the overall texture fades away faster. Furthermore, silicon gloves generally have a higher coefficient of friction than PVC gloves, which can be seen as both an advantage as a disadvantage. Bilotto (1986) states that the higher coefficient of friction makes picking up smooth objects easier (e.g. glasses), while Schweitzer (2009) finds it annoying when donning and doffing coats and pullovers as it sticks to the sleeves. As is also done with PVC gloves, applying a micro-coating can reduce this effect (Centri AB, 2011) and is certainly better than covering it with a plastic bag. Unfortunately, this comes at extra costs and it is not available everywhere.

1.3.3 Polyurethane

Cosmesis There is no doubt that polyurethanes are able to mimic the appearances of the human skin. Apart from the early attempts that showed promise—for example by Krouskop et al. (1974)—it is also used in almost all cosmetic products, showing that it can hold its colour in numerous skin tones. Furthermore, there is a polyurethane solution in passive prostheses available by the company TRS, where this material is chosen for its elastic, shock-absorbent and durable properties (TRS Inc. 2012).

Mechanical properties Not a lot can be found when searching for polyurethanes as cosmetic coverings. But there are other examples that show that polyurethanes could be very suitable. For example, it shows high similarities with human skin behaviour, making it suitable for artificial skin (Bjellerup, 2005; Wang et al., 2006). In Plettenburg (2006a), it is used to provide for a coloured layer in certain prosthetic hooks for children. However, polyurethanes appeared to show more hysteresis and less compliance compared to silicon materials (Cabibihan et al., 2009; Cabibihan et al., 2011). As a result, polyurethanes do not show clear advantages over PVC or silicone gloves and are therefore not able to improve the current standard.

1.3.4 Multi-layer materials

There is also the possibility to use layers of different materials and combine their properties. This idea for laminating is barely used in current commercially available gloves, e.g. in the advanced i-LIMB Skin (Connolly, 2008), but there are similar examples that might contain useful information.

In a study towards approaching the viscoelastic behaviour of the human skin in maxillofacial prosthetics, the idea of using multi-layer solutions is used (Bellamy and Waters, 2005). The plan was to make a three-layer prosthetic skin with a high tear strength silicone rubber base layer, an inner gel layer and a yet-to-define outer polymeric layer (Figure 1.5). Due to the strong differences in mechanical behaviour of each layer, strengths are combined (Cabibihan et al., 2011). At this stage it is hard to conclude its applicability in cosmetic gloves, as the fixation between layers might still pose a problem. But the concept does show promise and further development is worth the effort.

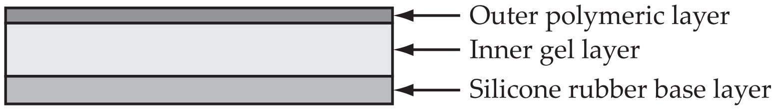

Figure 1.5: *Schematic view of a three-layered maxillofacial prosthesis (adapted from Bellamy and Waters (2005)).*

1.4 Glove modification

Apart from adjusting the glove material, it is also possible to adjust the shape of the glove. In Herder et al. (1998), the heat-wire treatment is discussed. In this study, it is proposed that a series of heated wires create grooves to locally reduce the glove's thickness. This would result in weak spots, requiring less energy to deform the glove. With rectangular specimen made out of PVC, it was shown that it is possible to half both stiffness and hysteresis. For a glove, a hysteresis reduction of 30% is reported by applying a set of grooves between the thumb and opposing fingers, without compromising too much in the glove's durability. Furthermore, because the grooves are applied on the inside of the glove, there should be no decrease in cosmetic value. This technique is, however, not as easily applicable on silicone gloves, because then the actual manufacturing process needs to be changed. Also, this method only partially addresses the problem caused by cosmetic gloves, indicating that there will always be stiffness and hysteresis interfering with the prosthesis.

1.5 Concluding remarks

From the available literature concerning cosmetic glove materials it may be clear that the viscoelastic behaviour of the glove is inevitable. From the candidate materials, PVC and silicone rubber remain the best candidates. They both show different pros and cons, allowing the user to choose a material according to his/her own preferences. The use of polyurethane seems to show potential, but not enough to be able to substantially improve the current standard. Multi-layer materials, however, are worth the effort to investigate, as the properties of different materials can be combined.

Glove modification—even though it is an interesting way of treating the problem—can never be a complete solution. It only reduces stiffness and hysteresis by a certain amount and is only feasible on PVC material. In other words, the application of grooves into the cosmetic glove is good for a supplementary solution, giving more freedom for other solutions if forces get too high.

Regardless of the choice in glove material or shape, its stiffness and hysteresis will always interfere with the intended prosthesis characteristics. Consequently, it is important to investigate the possibilities in an additional compensation mechanism that is able to compensate for these interfering characteristics.

CHAPTER 2

Compensation mechanisms

In general, the stiffness and hysteresis need to be reduced in order to improve the performance of a gloved prosthesis. Merely adapting the glove can be helpful, but does not provide for a complete solution. By compensating the stiffness of the glove with an additional mechanism, the effective stiffness of the whole system can, ideally, return to the ungloved equivalent (with added glove hysteresis).

To be able to approach the problem in a more fundamental view, one must first understand what exactly needs compensation and how to compensate it. Furthermore, several examples of existing compensation devices should provide more insight on already existing methods.

2.1 On glove compensation

In the literal sense, compensation means to offer an improvement to replace a mistake. In this case, the glove's stiffness and hysteresis are considered the "mistake" and need to be corrected. Unfortunately, hysteresis is an effect purely due to the viscoelastic behaviour of the material and can therefore not be avoided[1]. Stiffness, however, is a different story.

In terms of energy, a certain amount of input energy (E_{in}) is necessary to overcome the glove's stiffness, which opens the prosthesis and puts elastic energy into the glove ($E_{g,load}$). During closing of the prosthesis, the cosmetic glove is unloaded and energy is dissipated due to hysteresis (E_{hyst}), leaving a smaller amount of elastic energy ($E_{g,unload}$). When no compensation mechanism is used, the elastic energy that is left, $E_{g,unload}$, is completely lost (Figure 2.1a). The addition of a compensation mechanism, however, makes it possible to store this energy and reuse it, reducing necessary energy from the user to operate the prosthesis (Figure 2.1b).

An added compensation mechanism will act as a spring in parallel, so its stiffness is additive with the glove's stiffness. There are possibilities in creating force-displacement curves that approximate that of the glove, but mirrored around the x-axis. Such a *negative stiffness* characteristic can make the resultant stiffness be reduced to a minimum, compensating the glove's stiffness. The properties of the negative stiffness element are

[1] Although it can be reduced (Herder et al., 1998), it can never be fully *compensated*.

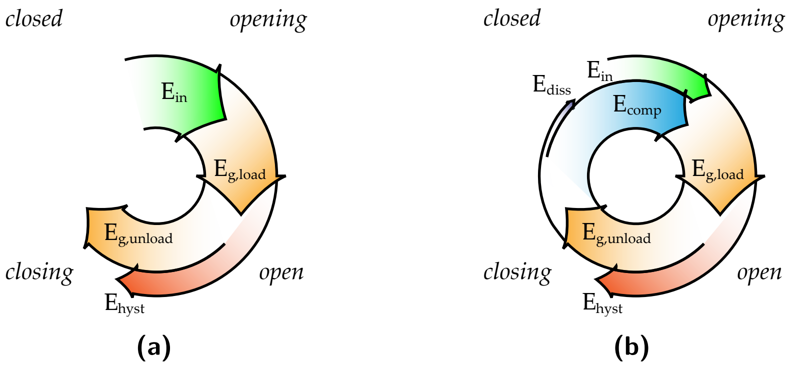

Figure 2.1: *Energy cycles for a voluntary opening prostheses. In (a) no compensation mechanism is used and elastic energy is lost. In (b) a compensation mechanism is used, conserving elastic energy from the glove and recycling it, reducing the necessary input energy (E_{in}) from the user.*

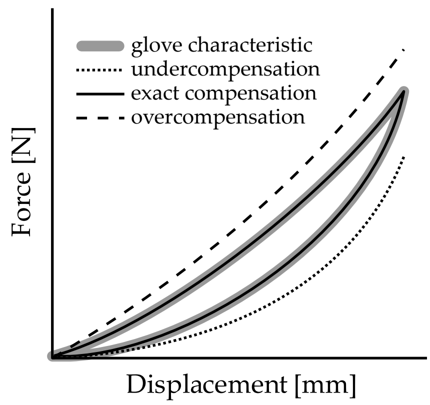

Figure 2.2: *Three different types of compensation characteristics, mirrored around the horizontal axis, compared to the glove characteristic.*

of high importance, as it should have the same characteristics as the glove material but in opposite direction. The exact shape of the compensation curve determines the effect on the device. One can divide this onto three possibilities:

- undercompensation: glove stiffness is still partly present, passively closing the prosthesis;
- exact compensation: system becomes indifferent, the terminal device will become statically balanced in every position;
- overcompensation: the overcompensated stiffness will passively open the prosthesis.

Figure 2.2 illustrates how these types of compensation correspond to the glove characteristic. For a voluntary closing prosthesis, undercompensation should be avoided as the glove's stiffness will still tend the prosthesis to close. Whereas overcompensation would have the opposite effect and should be avoided on a voluntary opening prosthesis.

The perfect compensation mechanism would show exact compensation, making the system indifferent. However, exact compensation would also imply that the exact same hysteresis behaviour is required. Also, different cosmetic gloves with the same size and manufacturer already show different characteristics (Herder et al., 1998; Wijsman, 2010; Tolou et al., 2012). Consequently, either over- or undercompensation is desired.

2.2 Existing mechanisms

From the already existing mechanisms, a few examples can be found in glove compensation mechanisms. Additionally, examples from other branches that require compensation can also prove as useful inspiration.

2.2.1 Preceding glove compensation mechanisms

Although not abundant, a few preceding methods have been proposed and implemented into hand prostheses in order to compensate the glove stiffness. In Kuntz (1995), several methods are discussed that are derived from one basic concept; an unstable spring-link system, using a linear tensile spring and the link represents the prosthesis' thumb (Figure 2.3a). This moment-compensating device originally shows a degressive behaviour, so an additional mechanism is needed to convert this into a progressive behaviour. As this relation is known, a four-bar linkage can be designed that shows the wanted behaviour (Figure 2.3b). In order to reduce the high energy losses due to the journal bearings, rolling links were used (Figure 2.4a).

In de Visser and Herder (2000), a similar mechanism can be seen. Here, each phalange of the prosthetic fingers connects with the previous one using rolling contact, where a band connects the rolling elements. Rubber bands are then used that tend to bend the phalanges where a cosmetic glove would want to stretch them (Figure 2.4b). However, it did not show the right compensation curve. This resulted in situations where the hand did not passively return to its initial position as it was designed to do. This does have the effect that energy losses due to hysteresis is absorbed outside the system, e.g. with the sound hand. Nevertheless, it might be annoying for users when trying to pick up small or thin objects like a piece of paper.

Plettenburg (2002) discusses the issue that the cosmetic glove does not only interfere in opening of a prosthesis, but also with closing. It seems that, in resting position, a gloved prosthesis prefers one particular situation that is not necessarily fully closed. A solution to this phenomenon is a set of two springs, where one spring aids in opening and the other in closing of the prosthesis (Figure 2.4c). However, the exact glove characteristic was not reached and an additional pneumatically powered energy source was used to overcome this difference. As the prosthesis for which it was designed was pneumatically powered, this proved useful.

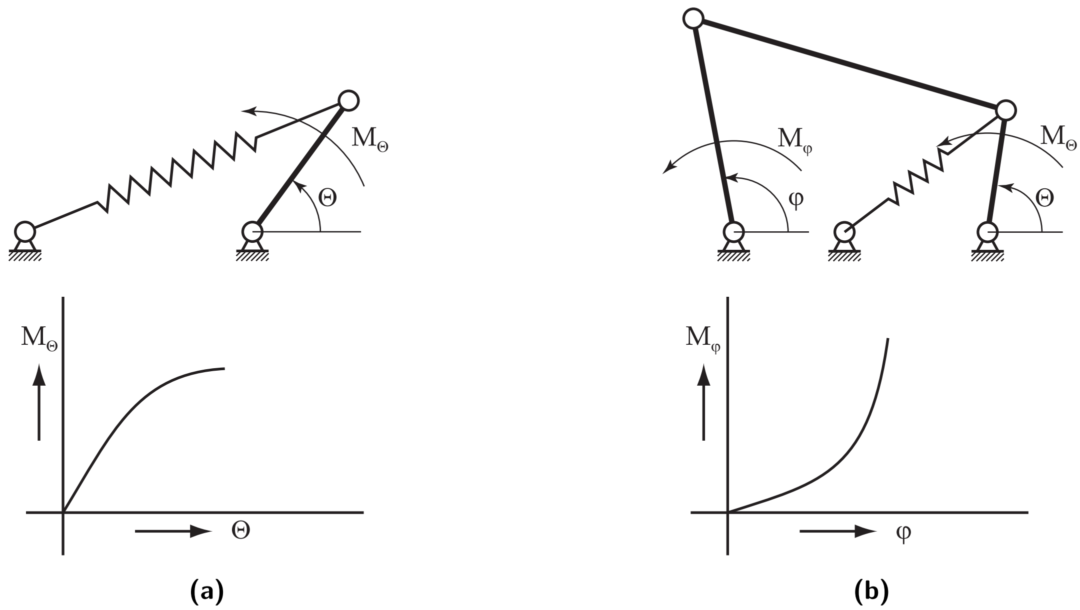

Figure 2.3: *Basic moment-compensation mechanisms with (a) a simple spring-link system with degressive behaviour, and (b) the same mechanism, but with added links to create a progressive behaviour (adapted from Kuntz, 1995, Figure 7.11 & 7.12).*

A knee-mechanism is known to show a progressive mechanical enhancement between the knee joint and slider. This concept is exploited in Wijsman (2010), where compression springs are used to store elastic energy and push against the knee. The slider is replaced by a rotating lever that approaches the straight line. This lever then transfers the mechanical enhancement to a push-rod that forces the hand to open, compensating the glove stiffness (Figure 2.4d). Unfortunately, this mechanism failed under the high forces that act on such small link elements. These forces where not redirected correctly and caused substantial losses due to friction, locking the mechanism.

A more recent mechanism is presented in Tolou et al. (2012). Here, a series of static balancers is used, where each static balancer is modelled as two opposing compression springs (Figure 2.4e). Each static balancer is able to exert a linear negative stiffness from its unstable, pretensed position (both springs vertical). This way, a progressive behaviour can be approximated with multiple linear characteristics with increasing slopes. A numerical example shows a decrease in stiffness of 96%, and continued research is done in using this principle in a compliant mechanism.

2.2.2 Other compensation mechanisms

From the preceding methods it may be concluded that there are not a lot of examples that focus on glove compensation particularly. The ones that are shown here also seem to come from the same location and group of researchers. This implies that, in order to gather as much information as possible, inspiration has to be sought elsewhere.

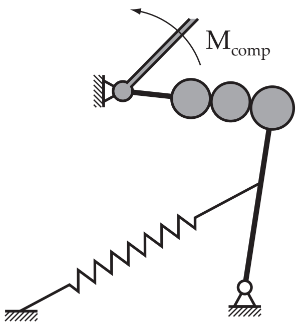

(a) *A spring-link system where additional links are added to create a progressive behavior (adapted from Kuntz, 1995, Figure 7.15).*

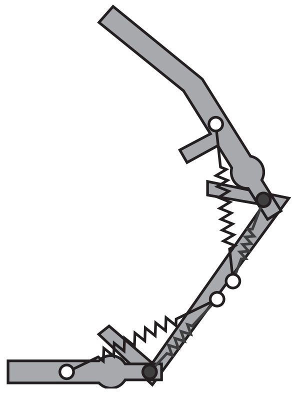

(b) *The glove stiffness (gray) is compensated at each joint by a tension spring (black) (adapted from de Visser and Herder, 2000, Figure 6b).*

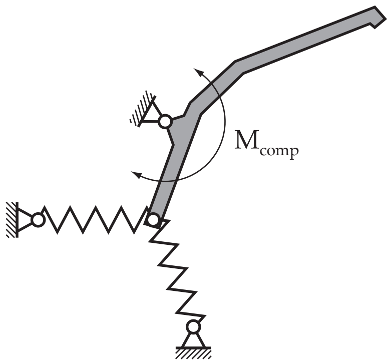

(c) *One spring forces the hand to open, at smaller angles the other spring will close the hand (adapted form Plettenburg, 2002, Figure A.3.3.06).*

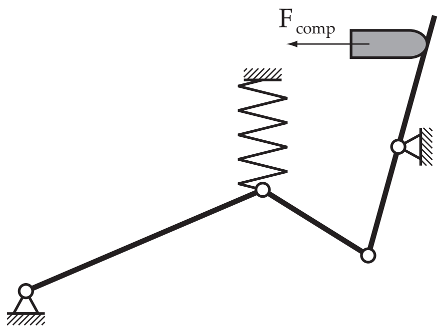

(d) *A knee-mechanism with a lever that transfers the compensation force to a push rod (adapted from Wijsman, 2010, Figure E.8.5 & E.11.1).*

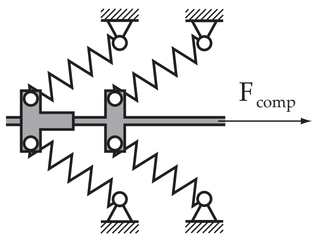

(e) *A series of static balancers, drawn in a stress-free position. When the left static balancer is pretensed such that both springs are vertical, the mechanism exerts a force towards the right (adapted from Tolou et al., 2012, Fig. 4).*

Figure 2.4: *Different types of glove compensation mechanisms found in literature.*

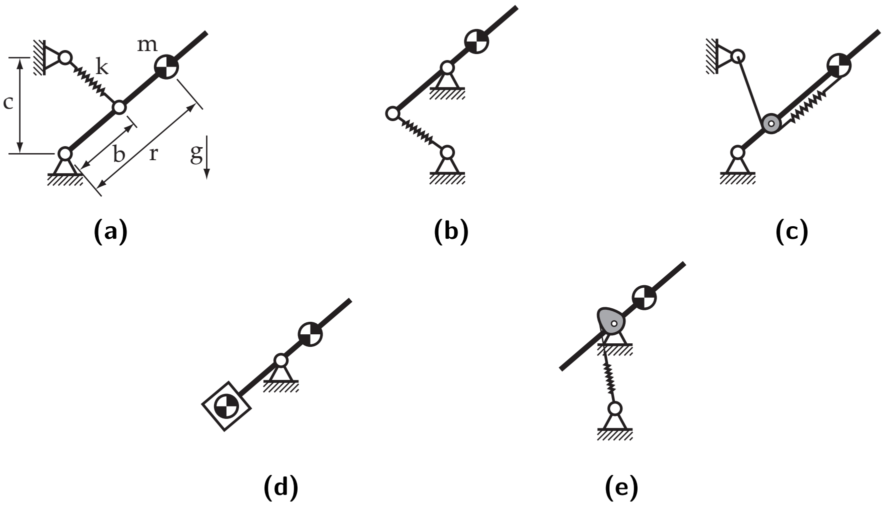

Figure 2.5: *Different types of gravity balancers.*

Weight & stiffness compensation The need to compensate weight or stiffness is one of the most popular reasons to include a compensation mechanism. This can result in a statically balanced mechanism in which it is stable in every position, or it simply reduces the energy demand. In principle, weight and stiffness compensation are very similar, because gravity can be modeled as a constant-force spring.

There are numerous types of gravity compensating devices (Lu et al., 2011), with the original Anglepoise desk lamp (Carwardine, 1937) being a successful example. The most basic form of weight compensation can be visualised with a pendulum with mass. Figure 2.5a shows a configuration using a spring. This configuration, however, assumes the use of a zero-free-length spring, meaning that the spring should have a constant stiffness over the whole spring length. In practice this is never the case because a spring has a certain minimal free length. This can be solved by using a pretensed helical extension spring, where the pretension is chosen such that its free length becomes zero (Herder, 2001). Other workarounds can include using a pulley (Figure 2.5c), a counterweight (Figure 2.5d) or a non-circular pulley (Figure 2.5e) (Endo et al., 2010). The latter one is interesting, as the shape of the pulley can be chosen freely in order to create the required characteristic, allowing more freedom in the overall design of the mechanism.

Stiffness compensation is a method quite similar to weight compensation, where spring forces with a certain spring rate are to be compensated instead of a constant force of gravity. The parasitic stiffness can be compensated in a spring-lever system, which can be adjusted by following a set of rules in order to remain a statically balanced situation (Herder, 2001).

Assistive devices An additional mechanism can help to lower the force needed to operate certain devices. A rather simple example for an assistive device can be found in a spring-assisted jack. In order to reduce manual effort, a pretensed spring assists in

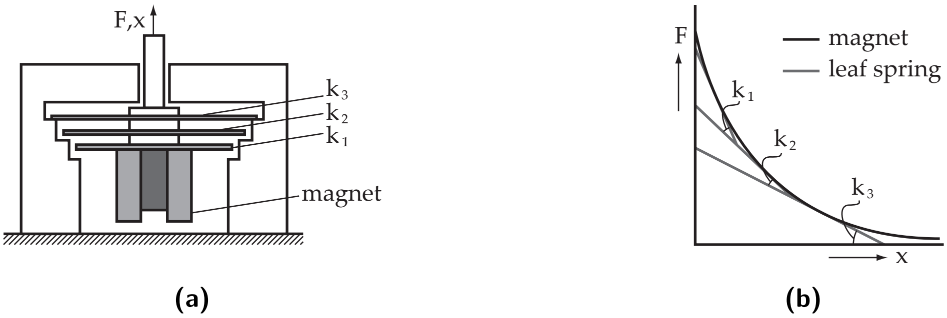

Figure 2.6: *(a) A magnetic sticking unit where the internal magnetic forces are compensated by a series of leaf springs, with (b) the resulting spring characteristic compared to the magnetic characteristic (adapted from Hirose et al., 1986, Fig. 13 & 14).*

raising heavy equipment (Chironis, 1965). A more sophisticated example can be found in a magnetic sticking unit, which is used by robots moving on vertical steel sheets (e.g. on large ships). The high magnetic force that is needed makes it hard to retract them from the wall again. In order to lower the force, without using electromagnets or compromising in magnetic force, a series of leaf springs are installed to lower the internal forces (Figure 2.6). Because the different sized linear leaf springs act after one another, the magnetic characteristic is approached (Hirose et al., 1986).

Vibration isolation The isolation of external vibrations is a necessity for high-precision equipment or experiments. For example, when making images with a scanning tunnelling microscope (STM), vibrations with amplitudes in the range of the light beam's wavelength already induce errors. Vibration isolation can be realised by using a very large mass, connected to the ground via a spring with very low stiffness. As a result, the system's natural frequencies remain in the very low frequency region so less resonance should occur.

Creating a large mass is easy, but the stiffness needs to be lowered by adding a negative stiffness element in series. An often used configuration is two opposing springs with equal spring rate (also applied by Tolou et al. (2012), Figure 2.4e). A third spring is then added to reduce the snap-through behaviour and to better control the net stiffness (Figure 2.7a). By varying parameters such as stiffness, pre-load and inclination angle of the opposing springs, different characteristics can be obtained (Carrella et al., 2007). An example of curves is shown in Figure 2.7b, where the inclination angle is varied.

Many other configurations of mechanical springs—or even magnets (Robertson et al., 2009)—can be used to create systems with a similar working principle (Park and Luu, 2007).

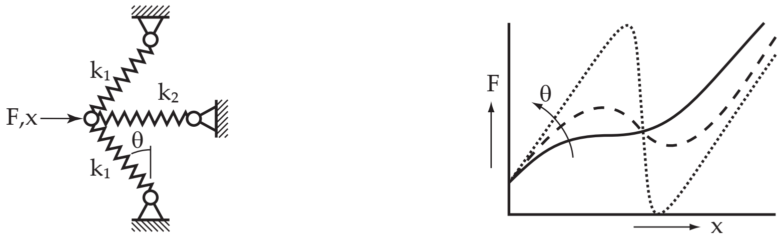

(a) (b)

Figure 2.7: *Vibration isolation system using a negative stiffness element (opposing springs), with (a) a common-used configuration, where (b) shows different characteristics that can be obtained by varying the initial angle θ (adapted from Carrella et al., 2007, Fig. 3).*

2.3 Concluding remarks

As for glove compensation devices, high forces act on small mechanisms and can lead to high friction losses or possibly even failure. From previous attempts it appeared that the exact compensation characteristic, efficiency and distribution of reaction forces determine its success.

All compensation mechanisms have one thing in common; energy is transferred from an energy source via some mechanical linkage. In other words, a working glove compensation mechanism should at least include an energy source and a mechanism to transfer it to the prosthesis with the right characteristic. This means that a correct combination must be made between them and should, together, show a high energy density. At the same time, energy losses should be reduced to a minimum and it needs to fit inside a small prosthesis.

The next two chapters elaborately discuss energy storages and mechanical linkages that might be used in a glove compensation device.

CHAPTER 3

Energy storage

With a compensation mechanism, energy has to come from somewhere in order to create a force that compensates the opposing stiffness of the cosmetic glove. This chapter discusses various methods of mechanical energy storage and how they would fit into a glove compensation mechanism.

First, different types of fundamental energy sources are discussed, where each type has its own subgroup of practical realisations. These are then discussed in the succeeding sections.

3.1 FUNDAMENTAL ENERGY SOURCES

In general, the phenomenon "energy" can be roughly subdivided into potential energy and kinetic energy. Here, potential energy is a function of a body's position, orientation or arrangement of the inner structure. Kinetic energy on the other hand requires movement—a velocity—of either of these. It can therefore be concluded that storing energy in the form of kinetic energy inside a prosthesis is impractical and potentially dangerous.

Potential energy is a different story and has many forms. The most basic forms are gravitational, elastic, electromagnetic, nuclear, chemical and intramolecular energy. At a first glance, the use of nuclear and chemical energy are immediately rejected due to safety, weight and scaling issues. This leaves exploiting gravitational, elastic, electromagnetic or intramolecular energy as possible candidates.

Each form of energy has their own practical realisations. Gravitational energy comprises of using counterweights in order to compensate for unwanted forces. The use of elastic energy is realised in the countless types of mechanical springs which are often used in engineering. Magnetic forces can prove very useful when using electromagnetic energy. Lastly, intramolecular energy implies the use of pressure in, for example, gas springs. Figure 3.1 shows a tree that starts with the concept "energy" and shows the subsequent steps that lead to these mechanisms.

When treating each of these different types of energy sources, an important parameter that must be taken in account is the energy density, as minimising weight and spatial occupation is very important in upper limb prosthetics. The minimal amount of energy required for the compensation device is rated at 0.9 J and energy dissipation due to hysteresis at 0.3 J by Wijsman (2010).

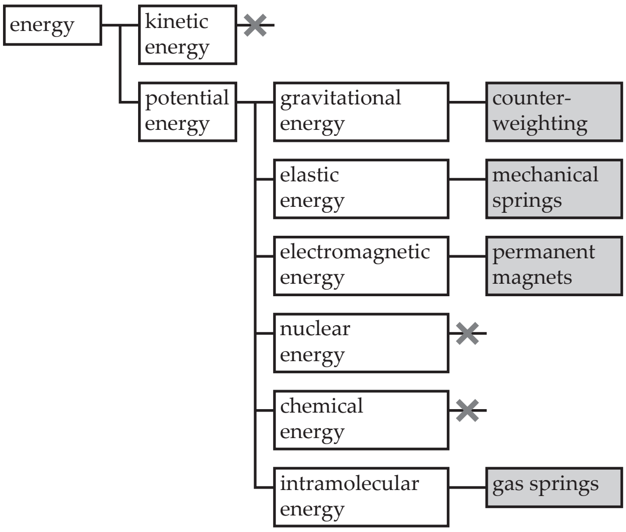

Figure 3.1: *Tree diagram that shows the process of choosing which methods of energy storage are worth investigating. A cross indicates that the preceding method of energy storage is not applicable in a glove compensation mechanism.*

3.2 COUNTERWEIGHTS

Counterweights are often used for compensating forces. Examples can be found in elevators, drawbridges or old scales where a certain amount of weight counterbalances a certain load. They all have one thing in common: the counterweight travels along a fixed path such that the gravitational potential used for counterbalancing can be precisely controlled. A hand prosthesis is continuously changing location and orientation during use, making it very hard to control this.

The gravitational potential can be calculated according to:

$$\Delta W_g = mg\Delta h \tag{3.1}$$

where:
$\Delta W_g =$ change in gravitational potential [J]
$m =$ mass of counterweight [kg]
$g =$ gravitational constant [$9.81\,\mathrm{m\,s^{-2}}$]
$\Delta h =$ change in height [m]

According to Equation (3.1), already a mass of 2 kg is needed over a change in height of 5 cm in order to reach a 1 J change in potential. This is approximately five times heavier than an average human hand. From here it can be concluded that the use of counterweighting is far from useful as a suitable form of energy storage.

3.3 Mechanical springs

Mechanical springs are widely used in order to store and release elastic energy. However, there are many different springs and each one has their own characteristics. According to EN ISO 26909:2010, springs can be classified according to a constant or variable spring rate, or constant spring force. The next few subsections discuss the best candidates with these different characteristics.

3.3.1 Constant spring rate

Springs with a constant spring rate are generally termed as linear springs. In general, the energy density of linear springs can be described according to:

$$\frac{W}{V} = \alpha \frac{\sigma^2}{E} \tag{3.2}$$

where: $\frac{W}{V} =$ energy density [$\mathrm{J\,m^{-3}}$]
$\alpha =$ a spring dependent factor [-]
$\sigma =$ maximum allowable stress [$\mathrm{N\,m^{-2}}$]
$E =$ modulus of elasticity (Young's modulus) [$\mathrm{N\,m^{-2}}$]

From Equation (3.2) it can be seen that, presuming equal material properties, only the factor α is different for each type of spring. From all mechanical springs, a tensile bar would possess the most attractive energy density ($\alpha = 1/2$). When made of metal, a tensile bar is unfortunately too stiff with very small displacements. This means that a less stiff material should be used, say a purely elastic rubber. The second best option would be to introduce helical springs ($\alpha = 1/4$), their high energy densities and wide varieties make them very suitable candidates. A rectangular leaf spring is the least attractive option ($\alpha = 1/18$). Even though the buckling effect of a leaf spring can still be interesting in producing negative stiffness characteristics (van Eijk and Dijksman, 1979), it reduces the possibilities of being able to scale the mechanism down substantially. Other springs show moderate energy densities ($1/8 \leq \alpha \leq 1/6$), but can still distinguish themselves from other methods in its working principle (e.g. torsion spring) (Cool, 2006)).

When assuming the use of spring steel, except for the tensile bar, the energy densities of the springs can be calculated according to Equation (3.2). Table 3.1 shows a list of energy densities accompanied by the volume and weight in relevant orders of magnitude, which the springs would have when fulfilling an energy demand of 1 J. Maximum allowable stresses are approximated at 50% of the material's tensile strength. Consequently, for the tensile bar, a natural rubber (vulcanised) material is assumed with $\sigma = 14 \times 10^6$ $\mathrm{N\,m^{-2}}$, $E = 0.00150 \times 10^9$ $\mathrm{N\,m^{-2}}$ and $\rho = 950$ $\mathrm{kg\,m^{-3}}$ (MatWeb, 2012). For spring steel, reference values are taken according to EN 10270-1:2011 using a dynamically loaded spring with maximum wire thickness of 2.0 mm, such that the

Table 3.1: *Energy densities for selected linear springs according to Equation* (3.2). *Material properties are according to MatWeb (2012) for natural rubber and EN 10270-1:2011 for spring steel.*

Spring type	Material	α [-]	W/V [$\mathrm{MJ\,m^{-3}}$]	V [$\mathrm{cm^3}$]	m [g]
Tensile bar	Natural rubber	$\frac{1}{2}$	65.3	0.0153	0.0145
Rectangular leaf spring	Spring steel	$\frac{1}{18}$	0.270	3.71	29.1
Triangular leaf spring	Spring steel	$\frac{1}{6}$	0.809	1.24	9.70
Helical spring	Spring steel	$\frac{1}{4}$	1.21	0.82	6.47
Helical torsion spring	Spring steel	$\frac{1}{8}$	0.607	1.65	12.9
Spiral torsion spring	Spring steel	$\frac{1}{6}$	0.809	1.24	9.70

minimum tensile strength is about 2000 MPa. This results in $\sigma = 1000 \times 10^6\ \mathrm{N\,m^{-2}}$, $E = 206 \times 10^9\ \mathrm{N\,m^{-2}}$ and $\rho = 7{,}85 \times 10^3\ \mathrm{kg\,m^{-3}}$ for spring steel.

This table shows a remarkable head start for tensile bars made of a natural rubber. However, the low elastic modulus of this material results in high relative elongations of the spring. Moreover, there no such thing as a purely elastic rubber, so it would introduce additional hysteresis. As hysteresis is one of the things that needs to be minimised, this is not a suitable solution. Furthermore, the differences in weight in between the spring steel springs are not big (except for the rectangular leaf spring), perhaps even negligible compared to the total weight of a prosthesis. The use of helical springs provides an advantage over all others, as it offers a wide range of mass-produced products.

3.3.2 Variable spring rate

Springs with a variable spring rate, or non-linear springs, are less common than linear springs, as they usually require more specific characteristics. Some springs are non-linear by nature, while a lot of other springs are so by introducing non-linearities to linear springs.

Progressive helical springs Helical springs can show progressive behaviour by varying diameter, pitch or wire cross-section. Coils with bigger diameter, thinner wire or smaller pitch tend to collapse sooner than others and show a lower stiffness. This means that the spring's total stiffness is dependent on the force already applied on the spring, introducing a non-linear—in this case progressive—behaviour. As for conical, barrel or waisted springs, if the coil diameter reduces sufficiently with each new winding, each coil is able to fall into the previous one upon compression (telescoping). This can reduce the minimal spring length to about twice the wire thickness, meaning that a large portion of the spring length is used. The challenge with these kind of springs

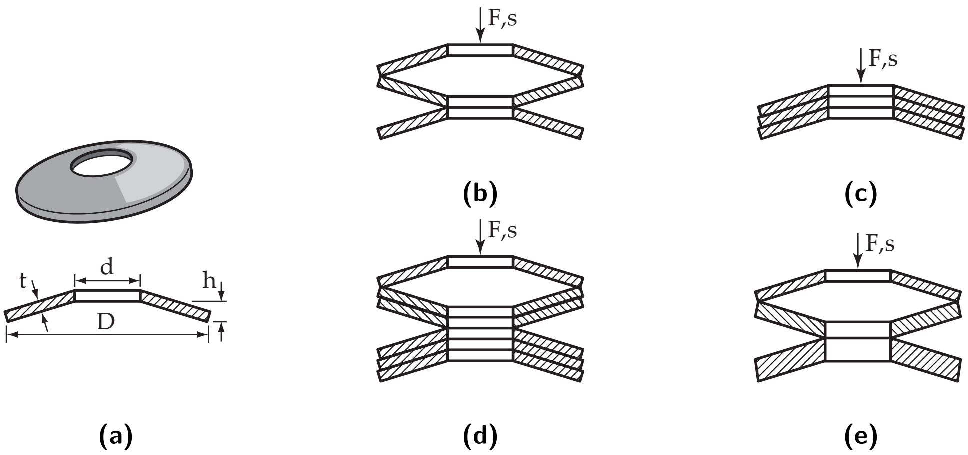

Figure 3.2: *A disc spring, where the overall shape is shown in (a). Disc springs can be stacked in order to increase (b) total deflection s or (c) total spring load F. Progressive characteristics can be obtained by stacking with (d) varying amount of springs in series or (e) varying spring thickness.*

is their particular characteristics, resulting in the very probable need for custom-made springs. The energy densities for these type of springs remain the same as normal helical springs, the only difference lies in the shape they take in and may be less efficient.

Disc springs A disc spring, also called Belleville washer, can show both a linear as a degressive characteristic, depending on the ratio h/t (see Figure 3.2a). It is even possible to create a negative stiffness due to its buckling behaviour. It is a very small spring that can withstand high forces over a short deflection. In itself, this deflection would be too small, but stacking multiple disc springs in series can enhance this deflection (Figure 3.2b). Moreover, stacking disc springs in parallel increases the spring load (Figure 3.2c). This results in spring columns, where different types of disc springs can be stacked in different ways to create almost any characteristic.

A linear characteristic for a single disc spring can be obtained by maintaining $h/t = 0.4$. A normal degressive characteristic can be created by maintaining $0.4 < h/t \leq 1.4$. For $h/t > 1.4$ the spring is also degressive, but starts to buckle at a certain threshold and thus showing a negative stiffness from that point on. Lastly, a progressive characteristic can be obtained by varying the amount of parallel stacked springs in a single spring column (Figure 3.2d) or by varying the spring thickness in a single spring column (Figure 3.2e) (Schnorr Corporation, 2003).

There is no explicit expression for the energy density of these type of springs, but one can get an approximate estimate. As an example, a certain disc spring from Tevema Technical Springs (article number S82490) shows a spring load of $F = 200$ N at a deflection of $s = 0.20$ mm. Consequently, when assuming a linear characteristic (so $E = 1/2k\Delta L^2$), one such disc spring is able to store 20 mJ. The inner and outer diameter are respectively $d = 6.48$ mm and $D = 12.7$ mm, with a material thickness of $t = 0.46$ mm. This gives a volume estimation of 172 mm^3. As a result, the energy density is approximated at 0.116 $\mathrm{MJ\,m^{-3}}$ and a column of disc springs would not occupy more than 8.6 $\mathrm{cm^3}$ when fulfilling the 1 J demand. Even though this energy density serves as a minimum, as a degressive characteristic would contain a higher energy density, it is already much lower than other mechanical springs.

3.3.3 Constant force springs

The most basic type of spring that is able to exert a constant force, regardless the spring's deflection, is a Neg'ator. It consists of a rolled, pre-stressed, flat ribbon made of spring steel. The force it takes to unroll remains approximately constant, thus it is often termed as a constant-force spring.

The energy density is once again estimated by using an example from Tevema Technical Springs (article number KK1050). Here, a steel ribbon of 0.25 mm thick, 25.4 mm wide and a free length of 864 mm is used, thus having a total volume of $5.49 \times 10^3\ \mathrm{mm^3}$. It is able to exert a constant force of 15.57 N over 686 mm, thus storing a maximum amount of energy of 10.7 J. This results in an energy density of 1.95 $\mathrm{MJ\,m^{-3}}$, so a constant-force spring would occupy approximately 0.514 $\mathrm{cm^3}$ when fulfilling the 1 J demand. It should be noted however, that these springs need a very long range of deflection. This method is therefore only worth considering in a hand prosthesis when it is wound onto another axis, i.e. as a spring motor, despite its high energy density.

3.4 Permanent magnets

The use of electromagnetic energy allows for exploiting forces between two bodies without establishing physical contact. As a result, it can offer possibilities in low friction compensation mechanisms. Moreover, the phenomenon is known to contain non-linear characteristics which are specifically interesting in this case. The use of electric components is, however, an unwanted approach in body-powered prostheses as it will lose its advantages that separates it from externally-powered prostheses. In order to open possibilities of using magnetic forces in body-powered prostheses, permanent magnets should be investigated.

In general, at least two permanent magnets are needed that can either translate or rotate with respect to each other. Figure 3.3 shows two opposing cuboid magnets where one magnet is fixed and the other is free to move in all directions. When moving solely in z-direction, both magnets maintain the common axis and a approaching characteristic emerges. When moving in either x- or y-direction, one magnet then slides past the other, so they will be treated as sliding magnets. Rotation is not treated, as rotation in φ and θ are considered to have similar effect to sliding magnets, and rotation in ψ is considered to have negligible effect.

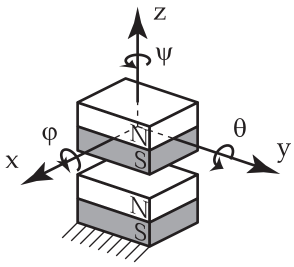

Figure 3.3: *Two cuboid permanent magnets can translate and rotate with respect to each other in all directions to create different characteristics.*

3.4.1 Magnets with common axis

Two magnets that approach each other on their common axis is an easy way of using magnetic forces. A perfect theoretical description of the resulting behaviour is, however, not at all easy. In Vokoun et al. (2009), an approximation is presented for two identical cylindrical magnets (see Figure 3.4a):

$$F_z = -\frac{1}{2}\pi K_d R^4 \left[\frac{1}{z^2} + \frac{1}{(z+2t)^2} - \frac{2}{(z+t)^2}\right] \tag{3.3}$$

where:
$F_z =$ force in z-direction [N]
$R =$ magnet radius [m]
$z =$ distance between magnets in z-direction [m]
$t =$ magnet thickness [m]
$K_d =$ $\mu_0 M^2/2 =$ magnetostatic energy constant
$\mu_0 =$ permeability of vacuum [$4\pi \times 10^{-7}$ H m^{-1}]
$M =$ $B_0/\mu_0 =$ saturation magnetisation [A m^{-1}]
$B_0 =$ magnet strength [T]

Equation (3.3) is an approximation only valid for larger distances. However, the force F_z only starts to become of significant magnitude at distances smaller than 3 mm. At 1 mm, the actual magnet force is about two times smaller than this approximation. Figure 3.4b shows the result for two magnets with $R = 5$ mm and $t = 2$ mm. Magnet strength is taken at $B = 1$ T, because modern rare-earth magnets, e.g. sintered neodymium magnets, are able to reach a magnet strength of over 1 T (International Magnetics Association). From this figure, the advantage of using magnets in a glove compensation mechanism shows itself, because it already shows a progressive behaviour without the need of physical contact.

The figure shows that, according to the approximation, forces of higher than 300 N are possible. The accumulated energy, calculated as the surface area under the graph, is around 0.2 J. This requires two magnets occupying a total volume of 3.14×10^{-7} m^3. In other words, the energy density in this situation is estimated at less than 0.637 MJ m^{-3},

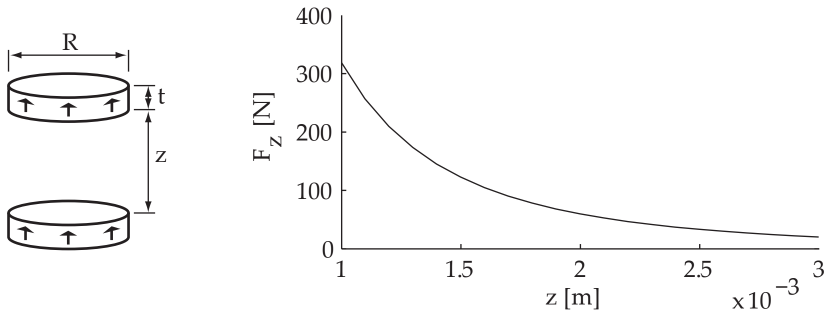

(a) **(b)**

Figure 3.4: *(a) Two identical cylinder magnets approaching along the common axis (arrows indicate direction of poles), with (b) an approximation of forces according to Equation* (3.3)*, using $R = 5$ mm, $t = 2$ mm and $B = 1$ T.*

because the approximation is based on an equation that can overestimate the force by a factor two. Despite its overestimation, it is already much lower than using the best mechanical springs.

3.4.2 Sliding magnets

Sliding magnets show a different characteristic from magnets that approach each other on a common axis. The approximation of the force-displacement curve is more complex but offers more possibilities. It can be calculated by using the following equations (Yonnet et al., 1993):

$$F_x(x,y) = t\left(\varphi_x(x,y) - \varphi_x(x,y-b) - \varphi_x(x,y+b)\right) \tag{3.4}$$

$$\begin{aligned} \varphi_x(x,y) = \frac{M^2}{4\pi\mu_0} \Bigg\{ &(x+a)\ln\left((x+a)^2+y^2\right) + \\ &-2x\ln\left(x^2+y^2\right) + (x-a)\ln\left((x-a)^2+y^2\right) + \\ &+2y\left(\arctan\frac{x+a}{y} - 2\arctan\frac{x}{y} + \arctan\frac{x-a}{y}\right)\Bigg\} \end{aligned} \tag{3.5}$$

where: $F_x =$ force in x-direction [N]
$t =$ magnet thickness [m]
$a =$ magnet width [m]
$b =$ magnet height [m]
$x =$ longitudinal distance between centers of magnets [m]
$y =$ transverse distance between centers of magnets [m]

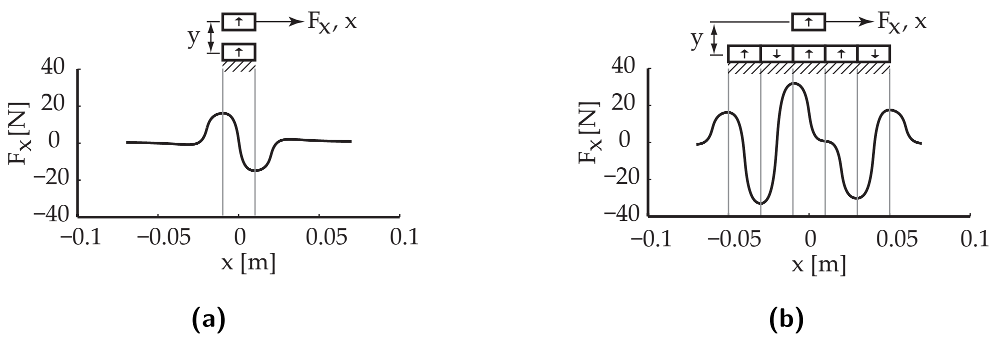

Figure 3.5: *Sliding magnets with a distance of 0.5 mm between them, where (a) shows the characteristic for one pair of attracting cuboid magnets (20×10×10 mm^3), (b) shows a possible characteristic when an array of 5 magnets is used. The arrows in the magnets indicate the direction of the poles.*

For two opposing magnets with strength $B = 1$ T, dimensions $a = 20$ mm, $b = 20$ mm and $t = 10$ mm and a distance of 0.5 mm between them ($y = 10.5$ mm), the characteristic in Figure 3.5a emerges according to Equation (3.4) & (3.5). It shows that only one pair of magnets does not suffice in reaching high forces or large displacements. However, one is not restricted by using only one pair, as it is also possible to guide one magnet along an array of magnets. The resulting characteristic would then be a summation of the individual characteristics of each magnet which the moving magnet passes. For example, an array of 5 magnets can be used where the direction of the poles is antisymmetric with respect to the middle one. This resulting characteristic becomes as shown in Figure 3.5b.

The advantage of this method is that virtually any characteristic can be obtained by tweaking the direction and strength of each magnet. One particular array is a Halbach-array, where due to the direction of the magnet poles the magnetic flux is concentrated on one side of the array and cancels the flux on the other side (providing intrinsic shielding) (Allag et al., 2009).

However, both Figure 3.5b and the results from Allag et al. (2009) show that an array of 5 magnets with each a strength of $B = 1$ T, is only capable of reaching a maximum of $F_x = 30$ to 40 N. Moreover, only a small portion of the curve will be used to obtain the progressive characteristic (e.g. between $0.01 \leq x \leq 0.03$). The accumulated energy in this portion—being the surface area between the curve and x-axis—reaches a value of 0.30 J. This requires a total of 6 magnets, each having a volume of 2.0×10^{-6} m^3, resulting in an energy density of 0.025 MJ m^{-3}. One can immediately conclude that this is far less than the previously described methods of energy storage.

3.5 Gas springs

A gas spring is nothing more than a cylinder filled with air, where the compressibility of a gas is exploited to obtain a spring-like behaviour. In this case, the ideal gas law can be used to describe the process. More specifically, the compression or expansion of gas can be described as a polytropic process:

$$pV^n = \text{constant} \tag{3.6}$$

where: $p =$ air pressure inside the cylinder [N m^{-2}]
$V =$ air volume inside the cylinder [m^3]
$n =$ polytropic exponent [-]

Assuming a certain initial volume, V_0, and initial pressure, p_0, one can use Equation (3.6) and obtain an expression for the accumulated energy:

$$p(V) = p_0 \left(\frac{V_0}{V}\right)^n \tag{3.7}$$

$$\begin{aligned} W &= -\int_{V_0}^{V} p(V)dV \\ &= \frac{p_0 V_0}{n-1} \int_{V_0}^{V} \left(\frac{1}{V}\right)^n dV \\ &= \frac{p_0 V_0}{n-1} \left(\left(\frac{V_0}{V}\right)^{n-1} - 1\right) \\ &= \frac{p_0 V_0}{n-1} \left(\left(\frac{p}{p_0}\right)^{\frac{n-1}{n}} - 1\right) \end{aligned} \tag{3.8}$$

Equation (3.7) implies how the characteristic curve would look like, where the force can be obtained by multiplying p with the piston's surface area. Upon compression, the volume decreases and approaches the vertical asymptote where $V = 0$, resulting in a progressive characteristic. The polytropic exponential n then determines the exact shape of the curve. It is also worth mentioning that increasing p_0 increases the slope of the curve, but also adds a threshold value for when the cylinder starts to compress.

The last expression from Equation (3.8) is especially convenient, because when loaded in compression, V_0 can be representative for the total volume occupied by the cylinder. In other words, dividing this expression by V_0 results in a direct relation for energy density as a function of pressure. Assuming an adiabatic process ($n = 1.4$ for air), a maximum pressure of $p = 100$ bar and that p_0 equals atmospheric pressure, the energy density equals 0.687 MJ m^{-3}.

The main disadvantage of using a gas spring, however, is that it contains a certain viscosity. This introduces a velocity-dependent force that counteracts the intended movement acting on the cylinder. This may be experienced as annoying by the user of the prosthesis.

Table 3.2: *Summary of most important methods of energy storage, comparing energy density and other important remarks.*

	W/V [MJ m^{-3}]	Important remarks
Helical spring	1.21	variable pitch/thickness/diameter
Disc spring	≥ 0.116	stackable in multiple configurations
Neg'ator	1.95	large deflections
Magnets with common axis	< 0.637	no physical contact needed
Sliding magnets	0.025	no physical contact needed
Gas spring	0.687	velocity-dependent

3.6 Concluding remarks

Several methods of energy storage have been discussed and are weighed by their energy density and applicability. It appeared that counterweights are far from useful when used in hand prosthetics and tensile bars are either too stiff or add hysteresis. However, helical springs have proven to be very useful in both energy density and due to their numerous variations. Disc springs can be stacked in multiple configurations to create almost any characteristic, but show a moderate energy density. The constant force spring, or Neg'ator, showed one of the highest energy densities, but it also requires large deflections and therefore an additional mechanism with high transmission ratio. Both concepts using permanent magnets do not need any physical contact, but the energy densities appeared disappointing. Lastly, the use of a gas spring shows an average energy density, but introduces viscous effects. Table 3.2 summarises these methods of energy storage with their energy density.

Combining the values for energy density and whether they are applicable in a small hand prosthesis, the best candidate for energy storage would be a helical spring. It has the single highest energy density and offers a wide range of variations. When requiring a progressive characteristic, the pitch, wire thickness or diameter can be varied.

CHAPTER 4

Mechanical linkage

In order to transfer the stored potential energy into compensating the glove, a mechanical linkage is required. Such a linkage accepts some input characteristic and transfers it into an output characteristic. This transfer function is a result of several principle methods—the most important ones in this case being decomposition of forces and leverage—and is called the mechanical enhancement.

As it appeared in Chapter 3, the output characteristic from the energy storage can be either progressive, linear, degressive or even constant. Each type of curve will be multiplied by the mechanical enhancement and should match the glove characteristic. Consequently, the mechanical enhancement can also be progressive, linear, degressive, or constant, depending on the given input.

4.1 Types of mechanisms

There are almost countless different types of mechanical linkages, making it virtually impossible to treat them all and select the best candidates. However, four-bar linkages are a very good starting point due to their wide range of applications and simplicity. Additional links can then be added in order to improve the linkage's performance and/or reduce the reaction forces on the joints. Other possible linkages include the use of gears, rollers and pulleys. They distinct themselves from n-bar linkages because they can offer varying moment arms by using non-circular shapes.

4.2 Four-bar linkages

Four-bar linkages are probably the most popular kind when it comes to n-bar linkages. It consists of an input link, coupler link, output link and a fixed link. The next few sections describe a crude classification of four-bar linkages and how the mechanical enhancement can be determined, from which a few possible candidates emerge.

4.2.1 Classification

The relation between the bar lengths determine the range of motion for each bar and thus the working principle of the linkage. Four-bar linkages can be classified according to these relations by using the Grashof Condition, which says that the shortest link can make a full rotation if:

$$s + l \leq p + q \tag{4.1}$$

where:
$s =$ shortest bar length [m]
$l =$ longest bar length [m]
$p, q =$ intermediate bar lengths [m]

Linkages that satisfy the condition from Equation (4.1) are categorised as *Grashof* linkages, whereas those that do not are coined *non-Grashof*. A special case emerges when $s + l = p + q$, as the bars are then able to situate themselves in one line. From this point, the four-bar linkage can make two different motions, which is why these mechanisms are called *change-point* mechanisms (Barker, 1985).

A four-bar linkage can take the shape of a crank-rocker, double-crank or double-rocker mechanism and is determined by the purpose of the shortest link. In the case of a glove compensation mechanism, it is not needed to make a full rotation because the prehension of the hand does not include such a motion. Consequently, double-rockers are also possible candidates.

4.2.2 Mechanical enhancement

Figure 4.1 shows a basic four-bar mechanism with bars a, b, c and d as input, coupler, output and fixed link, respectively. They are connected by joints with coordinates $\boldsymbol{A}$, $\boldsymbol{B}$, $\boldsymbol{C}$ and $\boldsymbol{D}$. The mechanism is constrained by the coupler bar, resulting in the following constraint equation:

$$(\boldsymbol{C} - \boldsymbol{B})^T \cdot (\boldsymbol{C} - \boldsymbol{B}) - b^2 = 0 \tag{4.2}$$

A second constraint equation can be obtained by differentiating Equation (4.2). The mechanical enhancement is then determined by the relation between input torque M_θ and output torque M_ψ, which is inversively related with the speed ratio:

$$ME = \frac{M_\psi}{M_\theta} = \frac{\dot{\theta}}{\dot{\psi}} = \frac{ad\sin(\theta) - ac\sin(\psi - \theta)}{cd\sin(\psi) - ac\sin(\psi - \theta)} \tag{4.3}$$

Equation (4.3) can be used to determine the mechanical enhancement curves for a set of possible linkages. Figure 4.2 shows some examples of possible four-bar linkages that show a progressive, linear or degressive curve.

All previously described four-bar linkages are based on four linkages connected with four revolute joints, or RRRR-linkages. It is also possible to include prismatic

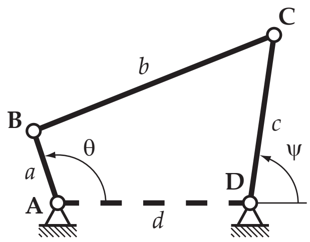

Figure 4.1: *A basic four-bar linkage with input link a, coupler link b, output link c and fixed link d, determining the relation between input angle θ and output angle ψ.*

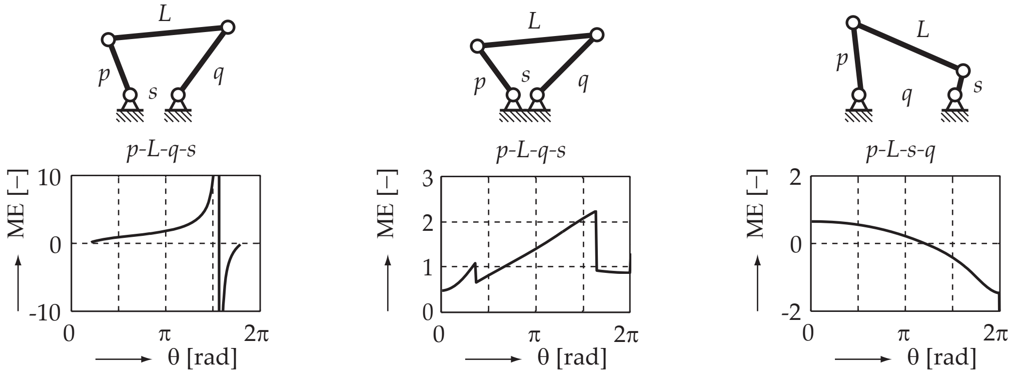

(a) $s = 0.4$, $L = 1$, $p = 0.5$, $q = 0.7$

(b) $s = 0.2$, $L = 1$, $p = 0.5$, $q = 0.7$

(c) $s = 0.2$, $L = 1$, $p = 0.5$, $q = 0.7$

Figure 4.2: *Examples of four-bar linkages with (a) a progressive curve, (b) a linear curve and (c) a degressive curve. Note the different scales on the vertical axes for a better view on the curve shape.*

joints for sliding motions. This may result in either a *slider-crank* linkage (RRRP-linkage) or a *double-slider* linkage (PRRP-linkage). These situations can be approximated using Equation (4.3) by implementing very large—or infinite—bar lengths. For example, the motion of an RRRP-linkage can be approached with an RRRR-linkage (e.g. a crank-rocker mechanism with a relatively long rocker).

4.3 Gears, rollers and pulleys

A four-bar linkage creates mechanical advantage by a combination of leverage and decomposition of forces. A gear, roller or pulley on the other hand works on pure leverage, making it easier to predict the reaction forces on the joints. They can also take on non-circular shapes, such that different kinds of characteristics can be made.

Gears and rolling links work according to the same principle, where the mechanical enhancement is dependent on the ratio between the radii. However, rolling links—as the name suggests—only experience friction due to rolling contact, whereas gears

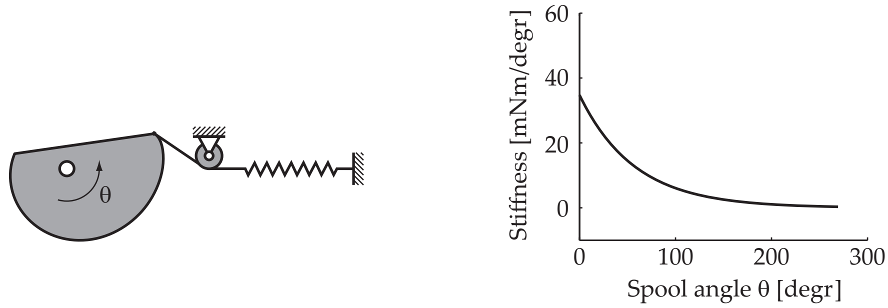

(a) **(b)**

Figure 4.3: *(a) A non-circular pulley in combination with a linear spring, with (b) the resulting (progressive) characteristic (adapted from Schmit and Okada, 2012, Figure 4).*

also have sliding contact. The advantage of rolling links over gears are therefore immediately clear as the amount of dissipated energy due to friction can be dramatically reduced (Kuntz, 1995). An example of a working rolling link mechanism was already shown in Figure 2.4a, which also shows that any linkage can be converted into a rolling link mechanism.

In Schmit and Okada (2012), non-circular pulleys are used to convert a linear spring into any other characteristic. Figure 4.3 shows such a mechanism, where the shape of the pulley is calculated in such a way that it exerts a desired rotational stiffness characteristic. In the given example, a progressive characteristic emerges from pretensed state. This same principle can be used for creating non-circular rolling elements.

4.4 Concluding remarks

It appeared that four-bar linkages are able to create a wide range of characteristics, only by tweaking with bar lengths and kinematic inversions. This makes them very suitable candidates, but also difficult to choose a single best option. Rolling links are considered as better options in comparison with gears, due to the absence of sliding friction. They can replace regular links or take on non-circular shapes for more specific characteristics, where the latter is also possible with non-circular pulleys.

Because of the great diversity within mechanical linkages, a definitive choice or recommendation cannot be made. For this, a more elaborate analysis is needed in which reaction forces should be studied. This is because high reaction forces induce more friction losses on the vital points, e.g. joints, degrading the usability of the total mechanism. However, the effect of reaction forces on the mechanism can be reduced by using rolling links.

CHAPTER 5

Conclusions

Based on all presented literature and calculations, a few conclusions and recommendations can be made for any attempt in designing a glove compensation mechanism for body-powered upper limb prostheses.

The cosmetic glove The first element that needs to be considered, is the cosmetic glove. It appeared from previous methods that only a few materials pose as possible candidates for a realistic and durable cosmetic glove. The most popular ones are made of either PVC or silicone. Although they both show some considerable disadvantages, alternative materials such as polyurethane do not show any clear superior properties.

The choice between PVC and silicone gloves remains an everlasting trade-off and can hardly be made objectively. Because the user will eventually have his/her own preference, the ideal glove compensation mechanism should be compatible with both. However, additional and more recent glove measurements should be performed to see of this is even possible.

Furthermore, techniques such as glove modification and multi-layer materials should be able to improve the mechanical properties of a cosmetic glove and are definitely worth investigating in the future.

The energy storage Perhaps the most important part of the compensation mechanism, the energy storage greatly influences the mechanism's efficiency and safety. From different principles of energy storage, it appeared that mechanical springs show higher energy densities than others and offer numerous variations.

Based on a combination of energy density and applicability, the conventional helical spring is the best option. It is also possible to create progressive characteristics by making changes in diameter, pitch or wire thickness. By avoiding this, however, off-the-shelf products can be implemented which is preferred.

The mechanical linkage The mechanical linkage between energy storage and cosmetic glove needs to deal with fairly high forces. The perfect method should therefore be able to distribute these forces evenly over the whole system, preventing high reaction forces on the joints that may result in jamming or failing.

A raw analysis of four-bar linkages has been made, which showed that many particular characteristics are possible. Furthermore, non-circular rolling links and pulleys are—in theory—able to create any characteristic with only rolling contact. The right choice should result from a more extensive force analysis, where reaction forces are of high importance. With the latter in mind, rolling links are very useful for reducing friction – its magnitude being closely related to reaction forces.

Part III

Appendices

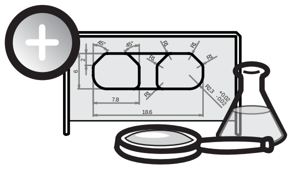

A Cosmetic glove measurements **57**
A.1 Materials . . . 57
A.2 Methods . . . 58
A.3 Results . . . 59
A.4 Discussion . . . 59

B Concept synthesis **63**
B.1 Design criteria . . . 63
B.1.1 Resultant force . . . 63
B.1.2 Glove material . . . 63
B.1.3 Energy storage . . . 64
B.1.4 Friction losses . . . 64
B.1.5 Mechanical enhancement . . . 65
B.1.6 Volume & mass . . . 65
B.1.7 Safety & strength . . . 66
B.2 Design philosophies . . . 66
B.2.1 On a roll . . . 66
B.2.2 Divide & conquer . . . 66
B.2.3 Keep it simple . . . 66
B.3 Devising concept . . . 67
B.3.1 Asymptotic behaviour . . . 67
B.3.2 Exploiting rolling friction . . . 68
B.3.3 Modelling behaviour . . . 69

B.4 Energy dissipation 74
B.4.1 Sources of rolling resistance 74
B.4.2 Hertzian contact. 75
B.4.3 Effect on reaction forces 77
B.4.4 Friction amount 79
B.5 Optimisation procedure 79

C Manufacturing & assembling **81**
C.1 Design embodiment. 81
C.1.1 Dimensioning. 81
C.1.2 Stabilisation 83
C.1.3 Assembly strategy 84
C.2 Technical drawings 86

D Prototype performance **87**
D.1 Spring measurements 87
D.1.1 Method 87
D.1.2 Results 87
D.1.3 Discussion 88
D.2 Prototype measurements 88
D.2.1 Method 88
D.2.2 Results 89
D.2.3 Discussion 90
D.3 Prototype with prosthesis measurements 91
D.3.1 Method 91
D.3.2 Results 92
D.3.3 Discussion 92

E Future work **95**
E.1 Practical adjustments 95
E.2 Refining contour shape 97
E.2.1 Determining correction angle 98
E.2.2 Defining contour shape 99
E.3 Interactive compensation mechanism design 101
E.4 Integration with WILMER WHD-4 103
E.4.1 The WILMER WHD-4 mechanism 103
E.4.2 Connecting the compensation mechanism 104
E.4.3 Added energy dissipation 105
E.4.4 3D CAD model 106

F Technical drawings **109**

Appendix A
Cosmetic glove measurements

Several cosmetic gloves were measured in order to provide for average data on stiffness and hysteresis. Consequently, the best choice for cosmetic glove material can be made and with it the range of energy requirements for the compensation mechanism.

A.1 Materials

The gloves were tested by using a test bench readily available at the Delft Insitute of Prosthetics & Orthotics (DIPO), where a force sensor is able to pull a cable while another sensor measures an absolute position. A voluntary opening prosthesis (WILMER WHD-4) was then added and fixed to this measurement set-up, equipped with either of the measured cosmetic gloves. By putting upon a position, a force/displacement-characteristic can be determined. It should be noted that this resulting characteristic not only describes the glove behaviour, but also incorporates the prosthesis mechanism, cable and coupling wire between the cable and load cell. Figure A.1 shows the measurement set-up, where these additional parts can also be seen.

With this measurement set-up, it can be assumed that the stiffness of the prosthesis mechanism and that of the cosmetic glove act in parallel, whereas the cable and coupling wire are stiffness elements in series (see Figure A.2). If the prosthesis mechanism's stiffness is as low as possible and the cable and coupling wire have a very high stiffness, then these additional components should have the smallest effect on the results in this configuration.

The force at the end of the cable was measured by a load cell (model: B3G-C3-50kg-6B, Zemic, Etten-Leur, The Netherlands) and the position by a linear position transducer (model: LCIT 2000, S/N: J 0069, Schaevitz, Hampton, VA). Both force and position measurements were fed to a data acquisition (DAQ) device (model: NI USB-6008, 12-bit, 10 kS/s, National Instruments, Austin, TX) and into the computer, using LabView version 10.0.1 (National Instruments, Austin, TX) for visualisation and storing of the measured values.

A total of ten different pediatric gloves were measured, each having the same or compatible size. Six gloves were made of PVC (Otto Bock, size 8S6=142x50, thickness of 0.8–1.3 mm), two were made of silicone (Otto Bock, size 8S6=142x50, thickness of

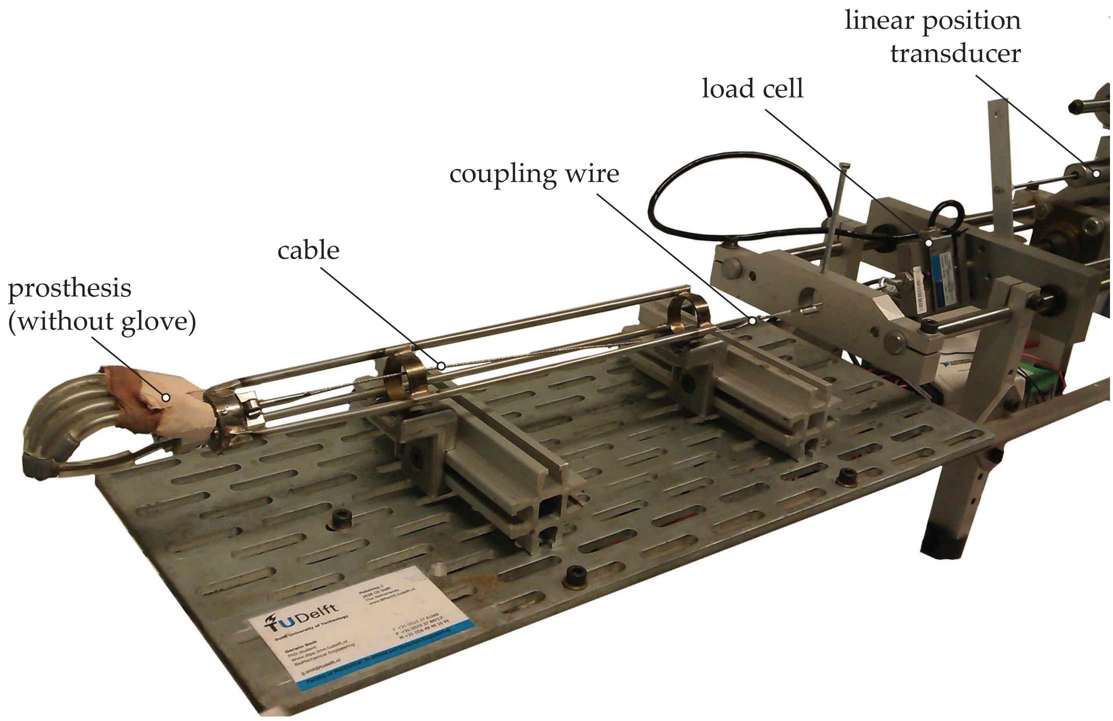

Figure A.1: *The set-up that is used for measuring the force/displacement-characteristic of the different cosmetic gloves. The measured characteristic is also affected by the stiffness of the prosthesis, cable and coupling wire.*

2.2–2.5 mm) and two were made of silicone with applied smooth-coating (Regal, size CS, thickness of 2.8–3.0 mm).

A.2 Methods

Before the cosmetic gloves were measured, the prosthesis without glove and solely the coupling wire were measured separately[1]. Both measurements were repeated five times, from which a linear fit would determine the average stiffness. It was assumed that the cable and coupling wire have a constant stiffness.

Each glove was measured five times, where each repetition was fitted separately. Due to the expected progressive shape, exponential and polynomial fits were tested. An average of these five fits would then provide for a single fit for the corresponding glove. Consequently, energy values can be calculated by determining the surface area enclosed by the characteristic. The first glove was also measured at a fast (as fast as the set-up would allow) and slow speed, in order to indicate any differences due to strain rate dependency of the glove material.

[1]Unfortunately, the prosthesis mechanism and cable were inseparable.

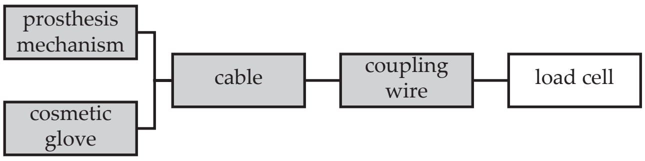

Figure A.2: *Schematic view of the different components with respect to the load cell where the force is measured and the position is put upon. The prosthesis mechanism and cosmetic glove are connected in parallel, which is then connected to the cable and coupling wire in series.*

A.3 RESULTS

The average stiffness of the coupling wire was measured at 93 $\mathrm{N\,mm^{-1}}$. With the ungloved prosthesis, the measured force did not exceed 10 N until it was fully open and was building up force.

The raw data for all gloves and their fits are shown in Figures A.3, A.4 and A.5, along with relevant values that indicate the quality of the fit and its corresponding energy values. A fifth order polynomial fit has shown to be the most accurate and efficient method for fitting all characteristics, based on the adjusted R-squared values.

Figure A.6 shows the average fits for all three glove materials in one figure. PVC gloves showed an average necessary input energy of $E_{in} = 833$ N mm and an average amount of hysteresis of $E_{hyst} = 259$ N mm. Silicone gloves showed an average input energy of $E_{in} = 277$ N mm and an average hysteresis of $E_{hyst} = 105$ N mm. The smooth-coated silicone gloves from Regal showed an average input energy of $E_{in} = 388$ N mm and an average hysteresis of $E_{hyst} = 133$ N mm.

Lastly, an average increase in stiffness of 4% is measured between the slow (0.08 mm/s) and fast (2 mm/s) speed at which the hand is opened. This number is in the same order of magnitude in which two different gloves of the same material can differ.

A.4 DISCUSSION

As for the used measurement set-up, the used additional components seem to have minimal influence on the measured stiffness. The prosthesis mechanism showed a very low stiffness and seemed more dependent on gravity and overcoming the static friction within its own hinges. Due to the parallel connection with the glove stiffness, its effect can be neglected. The coupling wire showed to be fairly stiff, but might have slightly affected the glove measurements towards the higher force region. Consequently, the resulting force/displacement-characteristics were corrected by this stiffness.

The results also indicate that slight differences in speed of displacement are in the same order of magnitude as two gloves would differ from each other. This means that all repeated measures can indeed be compared with each other and averaged.

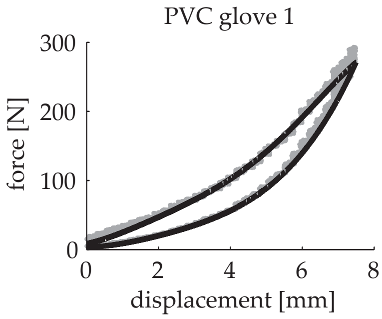

(a) *adjusted* $R^2 = 0.998$, $RMSE = 3.7$ *N*, $E_{in} = 859$ *N mm*, $E_{hyst} = 251$ *N mm*

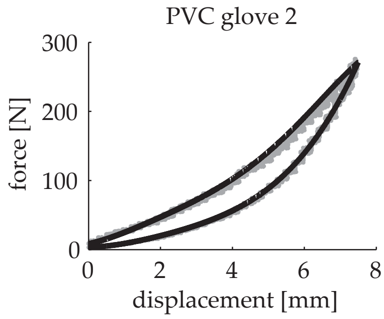

(b) *adjusted* $R^2 = 0.998$, $RMSE = 3.1$ *N*, $E_{in} = 796$ *N mm*, $E_{hyst} = 234$ *N mm*

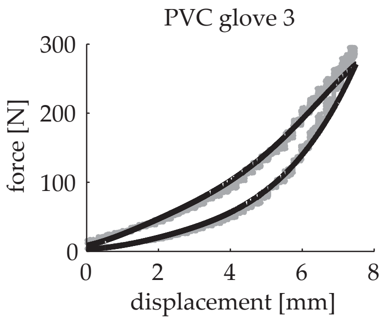

(c) *adjusted* $R^2 = 0.998$, $RMSE = 3.8$ *N*, $E_{in} = 829$ *N mm*, $E_{hyst} = 250$ *N mm*

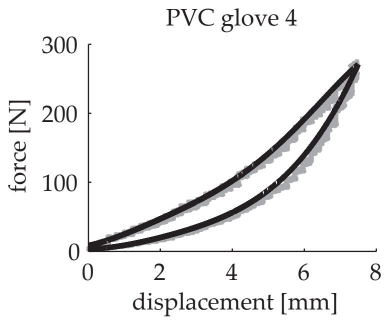

(d) *adjusted* $R^2 = 0.998$, $RMSE = 3.5$ *N*, $E_{in} = 796$ *N mm*, $E_{hyst} = 268$ *N mm*

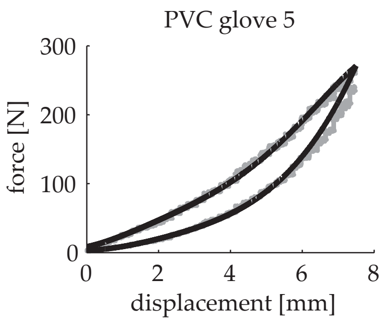

(e) *adjusted* $R^2 = 0.996$, $RMSE = 4.2$ *N*, $E_{in} = 816$ *N mm*, $E_{hyst} = 269$ *N mm*

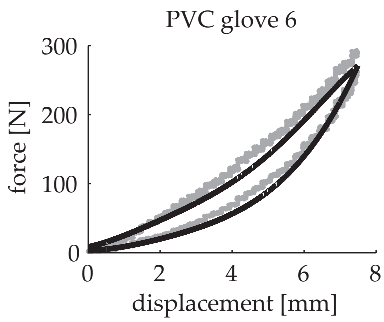

(f) *adjusted* $R^2 = 0.996$, $RMSE = 4.7$ *N*, $E_{in} = 900$ *N mm*, $E_{hyst} = 279$ *N mm*

Figure A.3: *Raw data and fifth order polynomial fits for all PVC gloves. The grey area indicates the range of raw data, the black line represents the fitting curve.*

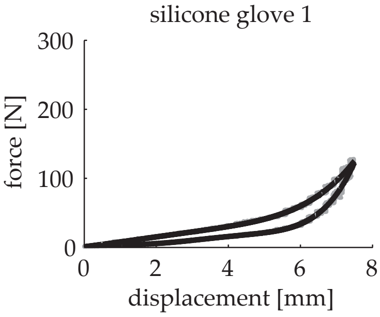

(a) *adjusted* $R^2 = 0.994$*,*
$RMSE = 2.2$ *N,*
$E_{in} = 279$ *N mm,*
$E_{hyst} = 106$ *N mm*

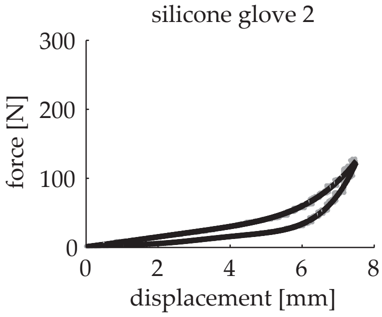

(b) *adjusted* $R^2 = 0.996$*,*
$RMSE = 2.0$ *N,*
$E_{in} = 276$ *N mm,*
$E_{hyst} = 103$ *N mm*

Figure A.4: *Raw data and fifth order polynomial fits for all silicone gloves. The grey area indicates the range of raw data, the black line represents the fitting curve.*

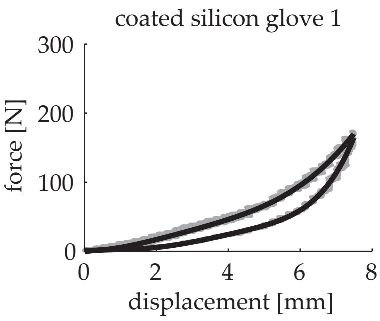

(a) *adjusted* $R^2 = 0.997$*,*
$RMSE = 2.3$ *N,*
$E_{in} = 398$ *N mm,*
$E_{hyst} = 142$ *N mm*

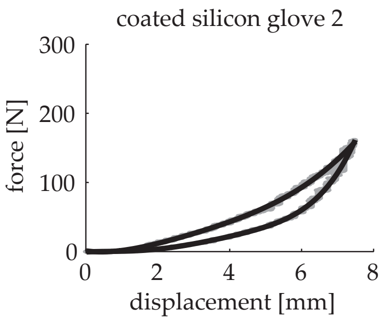

(b) *adjusted* $R^2 = 0.998$*,*
$RMSE = 2.1$ *N,*
$E_{in} = 378$ *N mm,*
$E_{hyst} = 124$ *N mm*

Figure A.5: *Raw data and fifth order polynomial fits for all coated silicone gloves. The grey area indicates the range of raw data, the black line represents the fitting curve.*

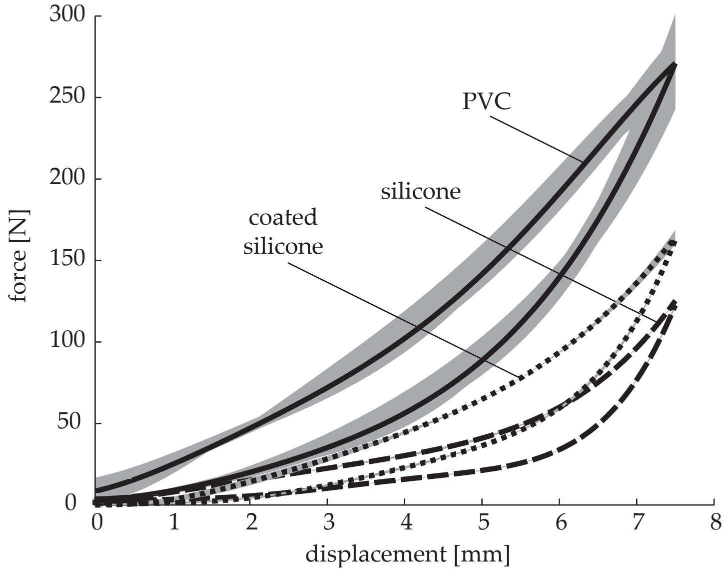

Figure A.6: *The average fit (black) compared to the range of different fits (grey) for all types of glove material. Average energy values are for PVC: E_{in} = 833 N mm, E_{hyst} = 259 N mm, for silicone: E_{in} = 277 N mm, E_{hyst} = 105 N mm, for coated silicone: E_{in} = 388 N mm, E_{hyst} = 133 N mm*

From the glove measurements it appeared that the different gloves within the same material do not differ that much from each other as is found in literature. A possible explanation for this can be that their thicknesses are more alike and only gloves from the same manufacturer are averaged.

A more important result is that the silicone gloves show a much lower stiffness than their PVC counterparts, despite the fact that they are at least twice as thick. Within these silicone gloves, however, the added smooth-coating and extra thickness on the Regal gloves seem to increase the stiffness. On the other hand, the regular silicone gloves from Otto Bock appear to be more non-linear, consequently showing greater relative losses in hysteresis. Absolute losses are, however, in this case more important. Based on these observations, the use of regular silicone gloves would be the best option when designing a compensation device as it would require a lower amount of energy storage.

Appendix B

Concept synthesis

With the glove characteristics known, a set of design criteria can be established and quantified. This list determines the goals and limits of the design. Furthermore, some design philosophies can be noted to serve as guidelines, which can help in aiming for the optimal solution. Eventually, a possible concept emerges and can be optimised towards its purpose. This whole process is directed towards the dimensions and working principle of a toddler-sized WILMER WHD-4 prosthetic hand.

B.1 Design criteria

Before devising concepts, it is important to quantify limitations and design choices that influence the outcome of the mechanism. Table B.1 summarises these criteria in order of importance, whereas the following subsections elaborate them.

B.1.1 Resultant force

The resultant force represents the eventual goal of the compensation mechanism. Its purpose is to reduce operation forces to a minimum, but a boundary must be quantified in order to know whether it succeeded. In Hichert (2010) and Plettenburg et al. (2011), a comfortable limit is defined at 40 N for body-powered prosthesis. Consequently, the maximum resultant force of the prosthesis should remain below this value.

B.1.2 Glove material

From the glove measurements it appeared that both PVC and silicone gloves show a non-linear, progressive curve with a certain amount of hysteresis. In general, gloves made out of silicone showed to be more non-linear and have a higher percentual hysteresis. However, compared to PVC gloves, the total required energy for the loading curve is lower by 67% and hysteresis is lower by 18%. These drastic differences imply that, when a compensation device is to implemented in a body-powered prosthesis, this should be accompanied by a silicone glove.

Table B.1: *List of design criteria and their quantifications, in order of importance.*

Descriptive	Criterium
Resultant force	Resultant operation force < 40 N
Glove material	Silicone glove.
Energy storage	Linear helical tension/compression spring(s), *minimum* energy storage of 337 J.
Friction losses	Total energy dissipation $\leq 11\%$.
Mechanical enhancement	Strongly progressive/asymptotic behaviour.
Volume	Total volume < $\varnothing 30 \times 30$ mm.
Mass	Total mass of prosthesis < 100 g.
Safety	No possibility to harm users or others.
Strength	Withstand a 500 N load from all directions.

B.1.3 Energy storage

As appeared from the literature study, helical springs are in this case the most practical and efficient methods of energy storage. Linear springs (no variation in diameter/pitch/wire) are in this case preferred, as it offers off-the-shelf products and makes slight adjustments to the mechanism easier.

When using a silicone glove, a total of 277 N mm is needed to overcome the glove stiffness and friction losses in the hand mechanism itself. Additionally, the compensation mechanism needs to overcome the friction inside the Bowden cable and any losses within the compensation mechanism. From the glove measurements (Appendix A), the ungloved prosthesis showed operating forces of lower than 10 N. This can be approximated with an average force of 8 N over a range of 7.5 mm of displacement. If the friction losses in the compensation device must be kept at the same level, an additional storage of energy of 60 N mm is required. Consequently, a minimum total amount of energy storage of 337 N mm is required.

B.1.4 Friction losses

A glove compensation mechanism experiences high forces on small dimensions. If these forces get too high, the source of energy storage needs to be overdimensioned or the whole mechanism might jam. In order to prevent these effects, the total dissipation of energy due to friction must kept under a certain level.

As mentioned above, an average force of 8 N is deemed necessary to overcome friction losses over the whole range of motion. This is partly due to losses in the Bowden cable. In Smit and Plettenburg (2010), a force of 3 N is reported to overcome Bowden cable friction in a TRS hook – being the most successful terminal device among tested voluntary closing prostheses. Consequently, only 5 N is due to friction in the mechanism itself. This is equivalent to 37.5 N mm of energy dissipation, being approximately

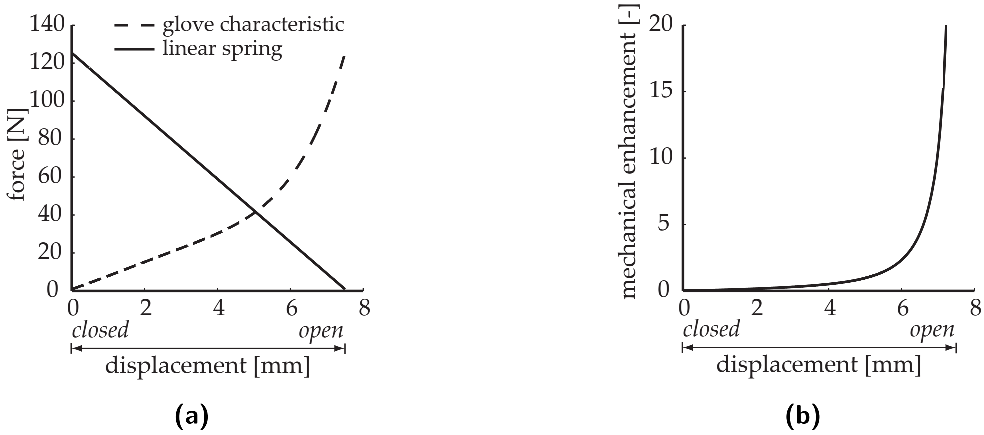

Figure B.1: *Figures showing (a) the glove and mirrored energy storage characteristic, and (b) the resulting necessary mechanical enhancement curve, showing asymptotic behavior.*

11% of the minimum amount of energy storage. It is therefore concluded that energy dissipation due to friction losses *within the compensation mechanism* should remain equal or lower than 11% of the total energy storage.

B.1.5 Mechanical enhancement

The expected progressive glove characteristic is confirmed by the glove measurements, and the energy storage characteristic is assumed to be linear. The energy storage, however, must be in resting state when the hand is opened and in fully tensed state when the hand is closed. This way, the compensation mechanism will reverse the equilibrium position of the hand, turning it into a voluntary closing device. Consequently, the mechanical enhancement must be zero when the hand is closed and infinitely large when the hand is open. A division of the glove characteristic by the energy storage characteristic confirms this, resulting in the need of an asymptotic, or at least strongly progressive mechanical enhancement curve (see Figure B.1).

B.1.6 Volume & mass

The total volume of the mechanism should be able to fit inside a children's prosthesis. The WILMER WHD-4 is taken as a reference measure, in which a volume of approximately $\varnothing 30 \times 30$ is available in the smallest size wrist (Plettenburg, n.d.).

The added mass of the mechanism should have a negligible effect on the comfort of the prosthesis. Taking the original WILMER WHD-4 weight as a reference, approximately 80 g, a maximum increase of 25% is considered acceptable. This results in a total maximum mass of 100 g. With the average hand being around 0.6% of the total body mass (Dempster and Gaughran, 1967)—the average body mass of a child of age 12-13 being around 50 kg (DINED anthropometric database, 1993)—this is still only 1/3 of the average child's hand mass.

B.1.7 Safety & strength

Apart from functioning, the mechanism should also not put the user or any other into possible harm. This would mean that sharp objects should be avoided and no gaps should be exposed in which fingers can get stuck.

Furthermore, the mechanism should be able to withstand forces due to daily use of the prosthesis. Using a child's average body mass (age 12-13) of 50 kg (DINED anthropometric database, 1993) as a reference point, the mechanism should be able withstand a 500 N load.

B.2 Design philosophies

A concept should follow must-have design criteria as mentioned above, but the addition of some 'like-to-have' aspects can also enhance the chance of success. These 'design philosophies' are described in this section.

B.2.1 On a roll

The amount of energy losses due to friction can be dramatically decreased by using rolling contact instead of sliding contact. Consequently, rolling elements should always be preferred over sliding elements. This would also avoid the use of bearings and lubrication and would make the whole mechanism very simplistic. Therefore, during the design process, the omission of sliding contact and bearing points should always be pursued. However, it should be realised that it also introduces other problems, such as the necessity of stabilising the rolling elements with an additional band.

B.2.2 Divide & conquer

The small dimensions and high forces pose a problem for the mechanism as it increases the chance of failing and/or jamming. To decrease these risks, forces should be spread over the mechanism as much as possible. This can be done by using multiple, smaller springs, instead of using one large spring. Furthermore, the conservation of energy can be exploited by increasing deflection and decreasing force, while maintaining the same level of energy.

B.2.3 Keep it simple

Due to the high non-linearities that are necessary, one can easily drift towards more complex systems. The simplest design, however, is often the most successful one as it lacks in any of these unnecessary complexities. In the case of a compensation mechanism, this means to reduce the amount of (moving) parts to a minimum and make it simple to implement and adjust the mechanism when necessary. Also, by placing the compensation mechanism as close to the source as possible, energy losses due to additional parts along the way (e.g. levers, pushrods, bearings) are reduced to a minimum.

B.3 DEVISING CONCEPT

Using design criteria & philosophies as the limits & guidelines, a concept can be created. Ideally, the mechanism will show an asymptotic compensation curve in order to exactly match the glove characteristic. Secondly, the use of rolling elements allow for a omission of sliding friction. Lastly, an analytical model can be made to determine the exact compensation characteristic and investigate the effects of making basic changes in geometry.

B.3.1 Asymptotic behaviour

The asymptotic behaviour of the glove compensation mechanism is one of the key properties in order to get the best compensation characteristic. Such an asymptotic behaviour is, however, only possible by using decomposition of forces. This rules out the use of (non-circular) pulleys or gears, as they only rely on leverage[1]. The answer can, however, be found in using four-bar linkages.

Due to the conversation of energy, the mechanical enhancement for a four-bar linkage is equal to the inverse of the speed ratio between in- and output bar:

$$M_{in}\dot{\phi}_{in} = M_{out}\dot{\phi}_{out} \longrightarrow \frac{M_{out}}{M_{in}} = \frac{\dot{\phi}_{in}}{\dot{\phi}_{out}} \tag{B.1}$$

where: $M_{in}, M_{out} =$ in- and output torque [N m]
$\dot{\phi}_{in}, \dot{\phi}_{out} =$ in- and output angular velocity [rad s^{-1}]

Equation (B.1) shows that, if the output angular velocity goes to zero, the mechanical enhancement approaches an asymptote. This occurs when the output link changes direction of movement, as its angular velocity will then briefly be equal to zero. When drawing such a situation, one comes across the conclusion that it greatly resembles the working principle of a knee mechanism. Figure B.2a shows a four-bar linkage in this situation, where the two bars in line is almost identical to a knee-mechanism as shown in Figure B.2b. In other words, it appears that a knee mechanism is the generalised shape of a mechanism showing an asymptotic mechanical enhancement curve.

The same conclusion can also be obtained by using a more fundamental starting point. As stated earlier, an asymptotic mechanical enhancement curve is the result of decomposition of forces, which, in turn, is the result of forces acting in an angle. If a force is divided by a sine or cosine—this includes the use of the tangent—of such an angle, a division by zero occurs and an asymptote emerges. In practise, this translates to a situation where the input force is *all but* the hypotenuse component in a force triangle. Figure B.3 illustrates this, where Equations (B.2a)–(B.2c) are methods in which the left-hand side denotes a force that shows asymptotic behaviour as a function of angle α. The

[1] Also, these methods require an overdimensioned source of energy storage and become impractical at small scales

Figure B.2: *(a) A four-bar linkage approaching an asymptote, compared to (b) a knee mechanism, showing similarities with this situation.*

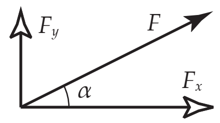

Figure B.3: *A decomposition of force F into two perpendicular components.*

$$F = \frac{F_x}{\cos\alpha} \tag{B.2a}$$

$$F = \frac{F_y}{\sin\alpha} \tag{B.2b}$$

$$F_y = F_x \tan\alpha \tag{B.2c}$$

simplest method of realising this is by using a double slider (Figure B.4). As a result, Equation (B.2c) can be applied.

The double slider from Figure B.4 is, in fact, one half of a symmetric knee mechanism. It can therefore be concluded that a mechanism containing an asymptotic mechanical enhancement curve should be derived from a knee mechanism or, even simpler, a double slider. This basis coincides with the preceding glove compensation mechanism from Wijsman (2010).

B.3.2 Exploiting rolling friction

The problem with hinged and sliding joints is the amount of friction they can experience. As friction is especially important to reduce in a glove compensation mechanism, it is of top priority to avoid any of these connections. Rolling links on the other hand, only experience rolling friction and do not need lubrication. As a side-effect, the rolling links need to be stabilised by the addition of a stabilisation band. This band is subject to tensile stresses in order to prevent (micro-)slip between the links.

In general, the sliding joints in the double slider (Figure B.5a) can be omitted by mirroring the mechanism around these points, resulting in a parallelogram (Figure B.5b–

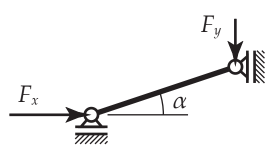

Figure B.4: *A double slider, where $F_y = F_x \tan\alpha$ in order to maintain equilibrium.*

B.5c). Then, the hinged joints can be replaced by contact points between rolling links, resulting in a mechanism using only rolling friction (Figure B.5d). The mechanism can be fixed to the outside world by adding additional bodies between two rolling links on opposite sides (Figure B.5e). If these additional bodies move in one line and one of them is fixed, the mechanism is left with one degree of freedom.

The result is a concept that uses only rolling friction and has a asymptotic mechanical enhancement curve. The force in vertical direction (F_y), however, is always the tangent component of the contact force between the rolling links. This increases the chance of slip and therefore increases friction. Instead, the same working principle can be kept by having circular rollers following a circular contour (Figure B.5f). This way, the normal force between the rolling links is the main component that creates the vertical force, dramatically reducing tangent forces and slip.

The final result not only reduces slip between rolling elements, but also decreases in volume. The input force from the energy storage can be applied by spanning linear helical extension springs between the roller centres. By using springs on both sides (front & back) for symmetric loading of the rollers, a total of four springs can be used that evenly distribute the necessary compensation force over the mechanism. The vertical force can be transferred to the prosthesis' pushrod and serves as the eventual compensation force. The exact shape of the mechanical enhancement curve is dependent on the circular roller radius and contour shape of the intermediate body. Figure B.6 illustrates the basic working principle of the concept.

B.3.3 Modelling behaviour

In order to better understand how a design works, one must first know how slight changes affect its behaviour. This can be done by modelling its behaviour in an analytical model, and observe the consequences in the compensation characteristic after such modifications.

B.3.3.1 Defining forces & geometry

Figure B.7 shows free body diagrams with forces acting on the different elements. As the line of action of all forces need to go through one point for equilibrium, the following set of equations can be obtained:

$$F_r = F_s \tan\alpha \tag{B.3a}$$

$$F_R = \frac{F_s}{\cos\alpha} \tag{B.3b}$$

$$F_v = 2F_R \sin\alpha = 2F_s \tan\alpha \tag{B.3c}$$

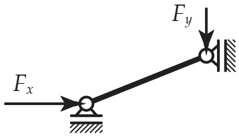

(a) *Double slider is taken as reference point.*

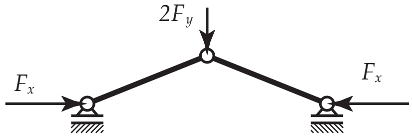

(b) *Vertical slider is eliminated by vertically mirroring the mechanism.*

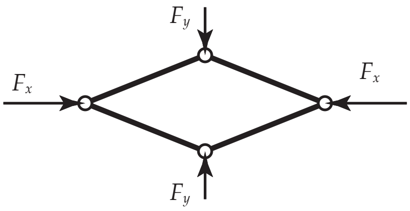

(c) *Horizontal sliders are eliminated by horizontally mirroring the mechanism.*

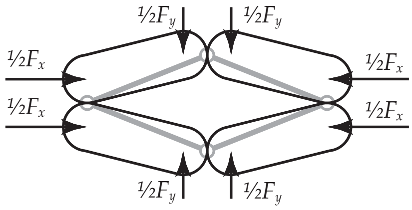

(d) *Hinged joints are replaced by contact points between rolling links.*

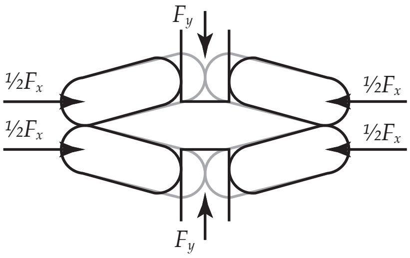

(e) *Additional bodies are added for fixation.*

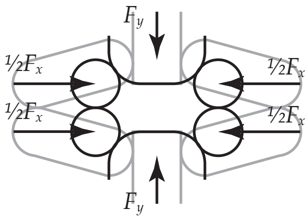

(f) *Shapes of bodies are adjusted to minimise slip.*

Figure B.5: *Steps that are taken to come to a possible solution for a glove compensation mechanism. All forces are in reference to the forces F_x and F_y from the initial double slider.*

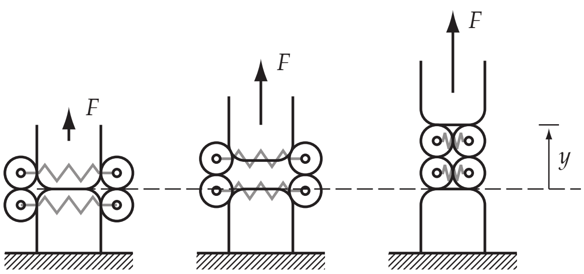

Figure B.6: *Basic working principle of the concept using rollers. The compensation force F asymptotically increases with gap size y.*

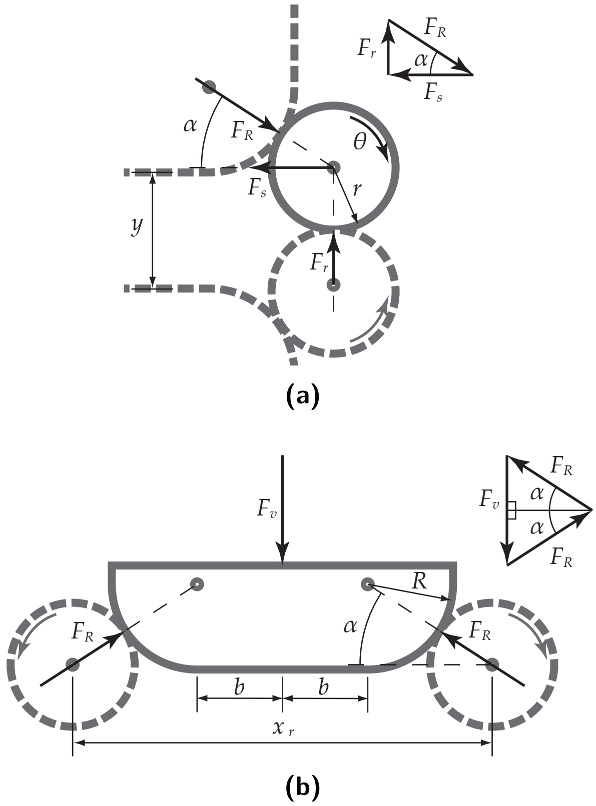

Figure B.7: *Free body diagrams with (a) the forces acting on the roller r and with (b) the forces acting on the intermediate body.*

where:
$F_s =$ spring force acting on roller center [N]
$\alpha =$ contact angle [rad]
$F_r =$ reaction force from roller [N]
$F_R =$ reaction force from intermediate body [N]
$F_v =$ vertical force / compensation force [N]

Furthermore, the geometric relations need to be defined. For this, it is easiest to express all measures as a function of contact angle α:

$$x_r = 2\left((R+r)\cos\alpha + b\right) \tag{B.4a}$$
$$y = 2\left((R+r)\sin\alpha - R + r\right) \tag{B.4b}$$

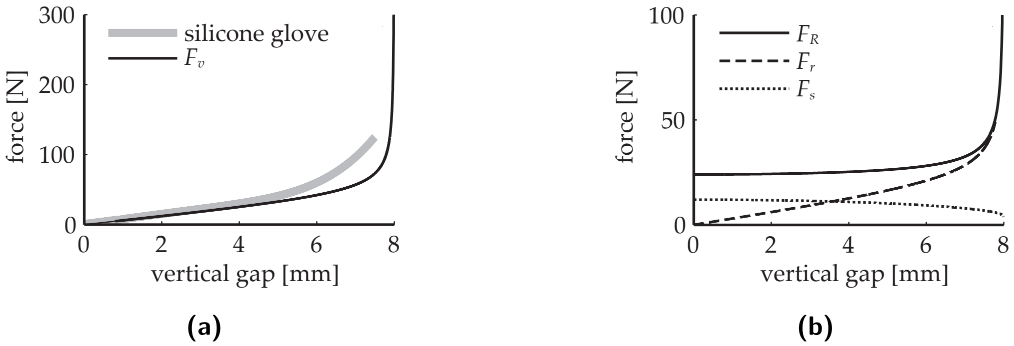

Figure B.8: *Basic characteristic of the concept with (a) the compensation force compared to the glove characteristic, and (b) the spring force and reaction forces.*

where: $R =$ contour radius [m]
$r =$ roller radius [m]
$b =$ additional width of intermediate body [m]
$x_r =$ distance between roller centers / spring length [m]
$y =$ vertical gap between intermediate bodies [m]

B.3.3.2 Initial measures and characteristic

The roller radius, r, determines the maximum size of the vertical gap, y. From the glove measurements, a total translation of 7.5 mm is measured in the cable. Therefore, the roller radius is initially taken at 2 mm such that a gap size of 8 mm is possible. Furthermore, the contour radius is also taken at 2 mm and parameter b equal to the roller radius r – this way, angle α makes a full 90 ° rotation. Lastly, a zero-free-length spring is chosen with a spring rate of $k = 1\,\mathrm{N\,mm^{-1}}$. Because each roller is connected to two identical springs on either side, the effective stiffness is doubled. The resulting characteristic is compared to the average glove characteristic of silicone gloves in Figure B.8.

From this figure it can be seen that the basic shape of the silicone glove characteristic can be found in the compensation characteristic. It initially shows a seemingly linear behaviour—such as the toe-region of the glove characteristic—followed by a fast increase in compensation force towards the asymptote at $y = 8$ mm.

B.3.3.3 Varying parameters

As the rollers determine the total gap size of the mechanism, their radius should not be varied. The radius R and width b of the intermediate body, however, *can* be varied. Additionally, the spring rate and pretension can also be varied that have an influence on the eventual compensation characteristic. Figure B.9 shows how these variations

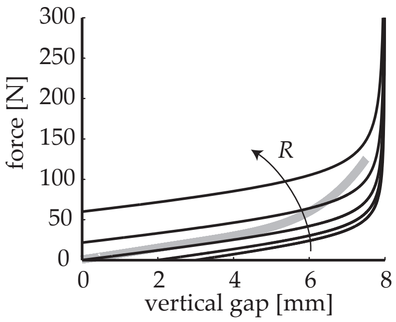

(a) *Contour radius* R *is varied between* 0.5, 1, 2, 4 *and* 8 *mm.*

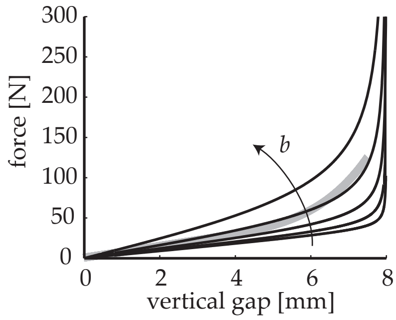

(b) *Width* b *is varied between* 0.5, 1, 2, 4 *and* 8 *mm.*

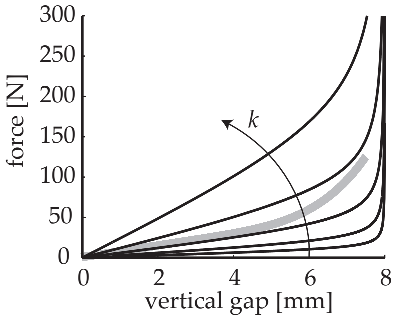

(c) *Spring rate* k *is varied between* 0.25, 0.5, 1, 2 *and* 4 $N\,mm^{-1}$.

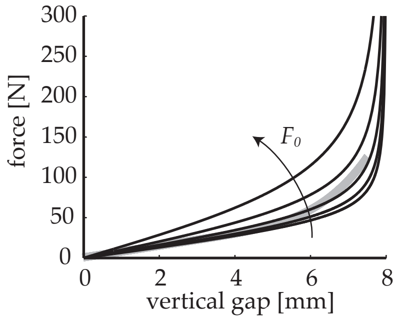

(d) *Spring pretension* F_0 *is added and varied between* 1, 2, 4, 8 *and* 16 *N.*

Figure B.9: *Figures showing the effects on the compensation characteristic by varying several parameters. The grey line indicates the averaged silicone glove characteristic as comparison.*

affect the compensation characteristic. Here, R, b and k are varied at 1/4, 1/2, 1, 2 and 4 times the initial value. The pretension is varied at 1, 2, 4, 8 and 16 N *per spring*.

From these results it can be seen that an increase in contour radius R adds an initial force to the mechanism at zero displacement. This is because the contact angle α will always be greater than zero if $R > r$, resulting in the compensation force being always greater than zero. Increasing the width b smoothens the transition towards the asymptote, but also increases spring force. This is because it increases the spring's initial elongation and consequently more energy is used. Increasing the spring rate k also increases the slope of the characteristic. Lastly, adding pretension to the spring is almost identical to increasing b, as it is just a different method to add pretension to the spring.

The ideal shape can be determined by performing an optimisation procedure, searching for the ideal combination of parameters. This, however, is only useful when friction and tolerances are taken in account. For this reason, the next section will discuss energy dissipation in the concept, followed by an optimisation procedure.

B.4 Energy dissipation

As is made clear by the preceding attempts in glove compensation mechanisms, the prediction of energy dissipation is of great importance. It is not only important to determine the magnitude, it is at least as important to investigate where these losses go to and how they are distributed. The sources and consequences of these losses magnify the weaknesses of the design, such that the least amount of surprises occur at a later stage.

In this case, rolling friction is considered to be the dominating friction phenomenon, which occurs between the rolling elements and at the spring attachments. At first, the sources of rolling resistance are investigated to determine what theories apply. Secondly, Hertzian contact theory can be used to determine the contact area and pressure distribution of the rolling contact. Thirdly, the effects of adding friction to the reaction force calculations can be determined. Lastly, by determining the amount of friction quantitatively, the effects on the resulting compensation characteristic can be determined.

B.4.1 Sources of rolling resistance

Micro-slip One cause of rolling resistance is micro-slip within the contact area. Forms of micro-slip are Reynolds slip and Heathcote slip (van Beek, 2009), which are not essentially a consequence of transmitted normal or tangential force – although they are dependent on them. Namely, they both are the consequence of separate stick and slip zones within the contact area. Reynolds slip occurs when the two interacting bodies have different elastic and geometric properties, whereas Heathcote slip occurs when one body rolls inside a closely conformed grooved surface (possibly due to *running in*). It appears, however, that due to the elastic properties of the surface material—which were not included in Heathcote's theory—a grooved runway only reduces rolling friction (Kuntz, 1995). Consequently, the effects due to Heathcote slip can be neglected. Furthermore, it is assumed that all rollers and intermediate bodies are made of the same material and show little differences in radius, such that Reynolds slip can also be neglected.

An additional form of micro-slip occurs when tangential forces are transmitted. Such forces create shear stresses parallel to the surface, resulting in creepage. Such creepages result in slight differences in mean velocity between the two contacting bodies and induce amounts of slip that are not visible to the eye. In this case, however, there is no transmission of tangential forces because there is no transmission of torque. As a result, the process can be described according to *free rolling*. It may therefore be concluded that any dissipation of energy due to rolling, is only a result from the normal force at the contact areas.

Hysteresis losses Normal forces induce compressive stresses on the interacting bodies. As a result, small deformations occur and will counteract the rolling motion.

More specifically, during rolling, material deforms at the front end and recovers at the back end of the contact area. Even when this deformation remains in the elastic region, energy is lost due to the material's hysteretic properties and the material does not fully recover at the back end. In effect, the amount of energy loss is dependent on the combination of materials and amount of stress, which is expressed in the hysteresis loss factor (Greenwood et al., 1961).

Plastic deformation When the load on the rolling elements exceeds a certain limit, plastic deformation around the rolling contact will occur. This does not only affect the mechanism's geometry, it will also result in a drastic increase in energy dissipation as no energy is recovered from the deformation. Any occurrence of plastic deformation should therefore be avoided at all costs.

B.4.2 Hertzian contact

Contact area In the case of above-mentioned concept, all rolling contacts between the rolling elements concern line contacts (two parallel cylinders), whereas the spring attachments concern point contacts (two crossing cylinders). Using Hertzian contact theory, the dimensions of the contact area can be defined according to:

$$a_{line} = 2\sqrt{\frac{2F_N R'}{\pi L E'}} \tag{B.5a}$$

$$a_{point} = \sqrt[3]{\frac{3F_N R'}{E'}} \tag{B.5b}$$

$$\text{with:} \quad \frac{1}{R'} = \frac{1}{r} + \frac{1}{R}, \qquad \frac{1}{E'} = \frac{1-v_r^2}{2E_r} + \frac{1-v_R^2}{2E_R}$$

where:

a_{line}	=	half contact area width for line contact [m]
L	=	contact area length for line contact [m]
a_{point}	=	contact area radius for point contact [m]
F_N	=	normal force [m]
R'	=	effective radius [m]
E'	=	effective elastic modulus [N m^{-2}]
E_r, E_R		elastic moduli of roller and intermediate body modulus [N m^{-2}]
v_r, v_R		Poisson's ratio of roller and intermediate body [-]

Pressure distribution Using Equation (B.5a), the mean pressure can be determined by dividing the normal force by contact area. Also, the pressure distribution over the contact width can be calculated, as Hertzian pressure is half-elliptic within the contact area (van Beek, 2009). Consequently, the maximum pressure occurring at the contact area can be calculated. Because the highest forces will occur at the line contacts between the rolling elements, they are considered to be the most important ones. With x pointing in the rolling direction and being zero at the contact area's centre, the pressure values for a line contact can be calculated according to:

$$p_{mean} = \frac{F_N}{2aL} = \frac{1}{4}\sqrt{\frac{\pi F_N E'}{2LR'}} \tag{B.6a}$$

$$p(x) = p_{max}\sqrt{1 - \frac{x^2}{a^2}} \tag{B.6b}$$

$$p_{max} = \frac{4}{\pi} p_{mean} \tag{B.6c}$$

Maximum Hertzian load Due to this contact pressure, high compressive stress occur at the contact surface. The material is, however, most probably a ductile metal and will more likely fail under the shear stresses below the contact area. In van Beek (2009) it is said that, for a line contact, initial yielding of the material will occur due to the shear stress at $0.786 \times a$ m below the contact surface. Its magnitude is approximately $0.304 p_{max}$ N m^{-2}, which should remain below the critical value for shear stress. According to Tresca's yield criterion, this critical shear stress is equal to half the material's yield strength (Hibbeler, 2008). This translates to the following:

$$\begin{aligned} \tau_{max} &= 0.304 \frac{4}{\pi} p_{mean} \\ &= 0.304 \sqrt{\frac{F_N E'}{2\pi L R'}} < \frac{\sigma_Y}{2} \end{aligned} \tag{B.7}$$

where: $\sigma_Y =$ material's yield strength modulus [N m^{-2}]

Or, more importantly, Equation (B.7) can be used to explicitly limit the normal force by this criterion:

$$\frac{F_N}{L} < \frac{\pi R'}{2E'} \left(\frac{\sigma_Y}{0.304}\right)^2 \tag{B.8}$$

In Equation (B.8), the normal force is limited in the units of force-per-length. This is because the depth of the concept, and consequently length L of the contact area, can still be adjusted. As can be seen from Figure B.8b, maximum normal forces are not likely to exceed 50 N. Consequently, a stainless steel with $E = 200$ GPa and say $\sigma_Y = 240$ MPa, results in the need for $L > 8.5$ mm. With $\sigma_Y \geq 350$ MPa, however, the mechanism is already capable of carrying the load with $L = 4$ mm due to the square in Equation (B.8). Stronger steels such as AISI 314 are able to provide such higher yield strengths (Ashby and Cebon, 2012).

Figure B.10: *A roller on a flat surface, loaded by a force F downwards, showing indicative shapes of pressure distributions for (a) stationary contact and (b) rolling contact (adapted from Hibbeler, 2008, Fig.8-26b). During rolling, an additional force F_f is required which is equal to the amount of rolling resistance.*

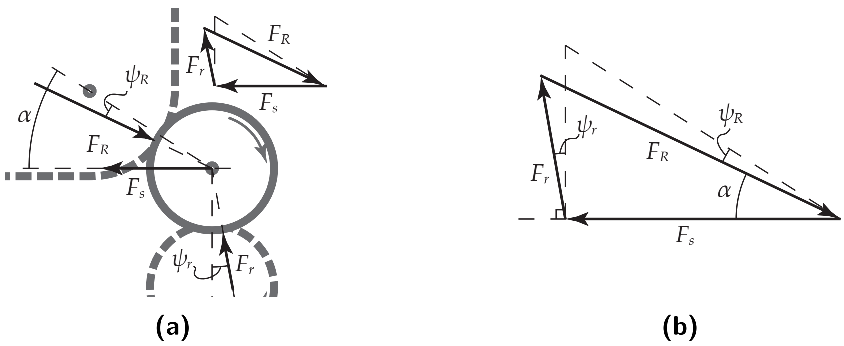

Figure B.11: *The addition of rolling resistance changes the direction and magnitude of the reaction forces, such that (a) an adjusted free body diagram emerges. In (b), the force triangle is magnified in which the friction angles ψ_R and ψ_r can be used to calculate the resulting reaction forces.*

B.4.3 Effect on reaction forces

The symmetric, half-elliptic pressure distribution from Equation (B.6b) is only valid under stationary loading. Because, as mentioned before, material is deformed and not fully restored within this contact area. As a consequence, the pressure distribution loses its symmetry and the average normal force is not perpendicular to the surface, but slightly rotated. As a result, an additional driving force is needed to keep the body rolling, which is equal to the rolling friction. Figure B.10 illustrates this effect.

In the case of current concept, this additional driving force needs to be provided by the energy storage, i.e. the springs. This also results in a change in direction of reaction forces, of which only the normal component contributes to the compensation force. The difference between the eventual reaction force and its normal component is denoted with its friction angle ψ, such that the amount of friction is equal to $F_N \tan\psi$. Consequently, the free body diagram and the resulting force triangle need to be adjusted again, as shown in Figure B.11.

Using the force triangle from Figure B.11b, a new definition for the reaction forces can be made. From the sine rule, the following can be stated:

$$\frac{F_r}{\sin(\alpha - \psi_R)} = \frac{F_R}{\sin(\pi/2 + \psi_r)} = \frac{F_s}{\sin(\pi - (\alpha - \psi_R) - (\pi/2 + \psi_r))} \tag{B.9}$$

From Equation (B.9), implicit definitions for the reaction forces can be determined. Also, by using $\sin(x + \pi/2) = \cos(x)$ and $\cos(-x) = \cos(x)$, a simpler set of definitions emerges:

$$F_r = \frac{\sin(\alpha - \psi_R)}{\sin(\pi/2 - \alpha + \psi_R - \psi_r)} F_s = \frac{\sin(\alpha - \psi_R)}{\cos(\alpha - \psi_R + \psi_r)} F_s \tag{B.10a}$$

$$F_R = \frac{\sin(\pi/2 + \psi_r)}{\sin(\pi/2 - \alpha + \psi_R - \psi_r)} F_s = \frac{\cos(\psi_r)}{\cos(\alpha - \psi_R + \psi_r)} F_s \tag{B.10b}$$

The compensation force, F_v, is the result of the vertical components of the normal forces on either side of the intermediate body, $F_{R,N}$ – *not* the vertical component of F_R. Consequently, it is calculated according to:

$$\begin{aligned} F_v &= 2F_{R,N}\sin(\alpha) \\ &= 2F_R\cos(\psi_R)\sin(\alpha) \\ &= 2\frac{\cos(\psi_r)\cos(\psi_R)\sin(\alpha)}{\cos(\alpha - \psi_R + \psi_r)} F_s \end{aligned} \tag{B.11}$$

Lastly, the rolling friction at the spring attachments needs to be included. From Figure B.8b, it can be seen that the reaction forces at these contact points are relatively low. Because of the expected low amount of rolling friction, it is simply estimated by multiplying the spring force, F_s, with the tangent of the friction angle, $\tan\psi_r$. As a result, the effective spring force can be calculated according to $F_{s,eff} = F_s\cos\psi_s$. This results in the final definitions for reaction and compensation forces, as a function of contact angle α:

$$F_r = \frac{\sin(\alpha - \psi_R)}{\cos(\alpha - \psi_R + \psi_r)} F_s\cos\psi_s \tag{B.12a}$$

$$F_R = \frac{\cos(\psi_r)}{\cos(\alpha - \psi_R + \psi_r)} F_s\cos\psi_s \tag{B.12b}$$

$$F_v = 2\frac{\cos(\psi_r)\cos(\psi_R)\sin(\alpha)}{\cos(\alpha - \psi_R + \psi_r)} F_s\cos\psi_s \tag{B.12c}$$

It can indeed be seen that when friction is neglected, i.e. $\psi_r = \psi_R = \psi_s = 0$, Equations (B.12a), (B.12b) and (B.12c) become identical to Equations (B.3a), (B.3b) and (B.3c), respectively.

B.4.4 Friction amount

Because of the dependence on material, geometry and loading, it is hard to determine the amount of rolling friction for a general case. It is therefore impossible to find a suiting tabulated value for ψ_R, ψ_r and ψ_s such that it applies to the current situation. They can be calculated using the hysteresis loss factor, as described in section B.4.1. However, reliable values for this factor are very hard to find. The exact amount of rolling friction can therefore only be estimated, using existing values from comparable situations.

In many cases, the amount of rolling friction is expressed in the *coefficient of rolling resistance*, which has length as dimension. It relates to the friction angle according to:

$$f = \tan \psi = \delta / r \tag{B.13}$$

where: $f =$ friction coefficient [-]
$\delta =$ coefficient of rolling resistance [m]
$r =$ radius [m]

Values for δ are difficult to measure and reported values are hard to rely on (Hibbeler, 2007). In Cool (2006), a value of 0.05 mm is reported for railroad steel wheels and several millimetres for rubber tires. Assuming this situation is somewhere between the two situations, a value of $\delta = 0.1$ mm is taken as an (over–)approximation. This results in a friction coefficient of approximately $f = 0.05$. Using these values in the model, this results in a meagre 0.4% of energy dissipation due to rolling friction.

B.5 Optimisation procedure

In order to find the ideal solution, an optimisation procedure can be performed. This is done by minimising a certain error function while varying the most important parameters that determine the compensation characteristic: contour radius R, roller radius r, spring stiffness k and spring pretension F_0.

The basic error function is defined as the the difference between the glove characteristic and the minimised compensation characteristic. However, it is also important that the result *overcompensates* the glove characteristic, as well as follow a shape very similar to it. For this reason, the compensation characteristic is compared to the glove characteristic +8 N, where any remaining values lower than the compensation characteristic are weighed by a factor 100 more. Also the first derivative in length is included in the error function and more emphasis is put at larger displacements, i.e. multiplication by displacement y. After some proper scaling of these terms—such that all conditions appear in the same order of magnitude—the error function is defined as follows:

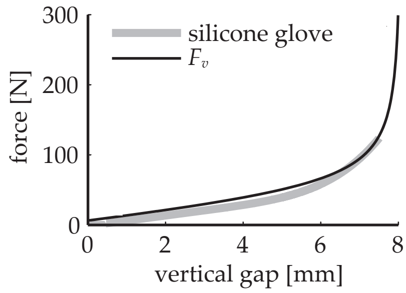

Figure B.12: *Resulting compensation characteristic after an optimisation procedure, which is mirrored around the horizontal axis and compared to the glove characteristic. Used parameters are R = 2.58 mm, r = 2.02 mm, k = 0.76 N mm^{-1}, F_0 = 8.23 N.*

$$e\left(R, r, k, F_0, y\right) = \left(C_1 e_1 + C_2 e_2\right) y \tag{B.14a}$$

$$\text{with: } e_1 = \frac{dF_v}{dy} - \frac{dF_{glove}}{dy} \tag{B.14b}$$

$$e_2 = F_v - \left(F_{glove} + 8\right) \tag{B.14c}$$

where:
$e =$ error function [-]
$F_v =$ compensation characteristic [N]
$F_{glove} =$ (measured) glove characteristic [N]
$y =$ vertical displacement [mm]
$C_1 =$ 500 [-]
$C_2 =$ 1 if $e_2 > 0$, 100 if $e_2 < 0$ [-]

A gradient search is then performed to find a solution with the lowest value for the error function. The result is shown in Figure B.12, using the following values:

$$\begin{aligned} R &= 2.58\,\mathrm{mm} \\ r &= 2.02\,\mathrm{mm} \\ k &= 0.76\,\mathrm{N\,mm^{-1}} \\ F_0 &= 8.23\,\mathrm{N} \end{aligned}$$

It can be seen that the resultant characteristic from the optimisation procedure closely follows the glove characteristic with full overcompensation. However, this does not necessarily mean that the found parameter values are the most ideal ones in practice. For example, it is practically impossible to find a spring with a (low) spring constant of $k = 0.76\,\mathrm{N\,mm^{-1}}$ combined with a pretension of over 8 N. The available types of springs and feasible tolerances will eventually determine the available dimensions. This process is initiated in Appendix C. Nonetheless, this optimisation procedure shows that the theoretical concept *is* able to achieve a working compensation characteristic.

APPENDIX C

Manufacturing & assembling

After concept synthesis, the resulting mechanism has proven to be able to function as a glove compensation device in theory. However, the mathematical model that is used to predict its behaviour is not yet validated. Furthermore, in practice, other factors—like manufacturing and assembling—become important in order to be able to build a physical concept. For this reason, it is chosen to build an initial prototype, not yet integrated in a prosthesis mechanism. Its purpose is to serve as a proof-of-concept, testing its manufacturability, its compensation characteristic and how it relates to the predicted behaviour from the model.

At first, Figure C.1 shows a short recapitulation of the concept's working principle, also showing often-used terminology, in order to provide for an overview. Furthermore, the process of translating the concept into a mechanism that is possible to manufacture and assemble is described. Additionally, the resulting technical drawings are presented. Lastly, the performance of the prototype is tested and compared to the model.

C.1 Design embodiment

In order to go from a theoretical concept towards a working mechanism, the design needs to be altered to make this possible. At first, the overall dimensions of the concept need to be determined. Secondly, the concept needs to be stabilised so that it only performs the motion path as intended. Lastly, a strategy needs to be thought of in which the mechanism can be assembled.

C.1.1 Dimensioning

Springs The components that influence the dimensions the most are the springs. As minimising volume is still an important aspect, an ideal zero-free-length spring is preferred with a relatively large possible elongation. Unfortunately, this either requires custom-made springs or is not possible at all, whereas at this stage off-the-shelf products are preferred. As a result, the optimised values as determined in section B.5 need to be reconsidered into more practical values.

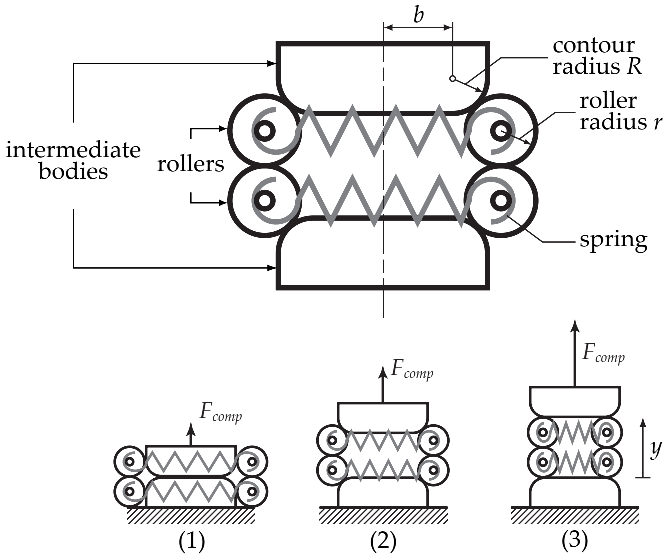

Figure C.1: *Recapitulation of the concept's working principle, showing often-used terminology and parameters. In situation (1), the mechanism exerts minimal to no compensation force, despite the tension in the springs. Situation (2) shows an arbitrary situation between minimum and maximum vertical displacement. In situation (3), the mechanism reaches its maximum vertical displacement and compensation force.*

The total required elongation of the spring is equal to twice the contour radius, plus twice the roller radius. The order of magnitude for the roller and contour radius lies between 2–2.5 mm, resulting in an elongation of approximately 10 mm. When looking for such a helical tension spring with minimum free length, one comes across the springs T30840 (spring steel) and T40840 (stainless steel) from Tevema Technical Springs. They both show the same dimensions: a free length of 12.5 mm, diameter of 3 mm and the maximum elongation ranges between 9.85–10.09 mm. Their pretension at zero elongation and spring rate differ from each other, allowing to test different spring properties while maintaining the same dimensions.

Rolling elements With the spring dimensions known, the dimensioning of the rolling elements can be done. At maximum vertical displacement of the intermediate bodies, the distance between the rollers' centres need to be slightly longer than the spring's free length of 12.5 mm. Also, at this position, the tension that is left in the spring should be as high as possible in order to better reach the high compensation force. For this reason, the total elongation of the spring should be as short as possible, in order to leave more tension available in this critical position.

As a result, the roller radius is taken at $r = 1.9$ mm, as this is the smallest dimension available with a 0.1 mm accuracy. This is because a total vertical displacement of 7.5 mm is necessary, which, in turn, should be equal or lower than four times the roller radius. The contour radius is taken at $R = 2.3$ mm, which is the smallest value before undercompensation starts to occur for a larger portion of the glove characteristic. Lastly, the width b is taken at 7 mm.

Thickness As appeared from the maximum Hertzian load in section B.4.2, a total length of 4 mm for the line contacts is enough to withstand the reaction forces without failing. However, this does require a stronger steel with a larger yield strength than usual. Several types of steels can be used, but the preference lies in using either austenitic or duplex steels due to their superior corrosion resistance. Examples of usable austenitic steels are AISI 205, AISI 216, AISI 314 or AISI 303 (cold drawn) (Ashby and Cebon, 2012).

C.1.2 Stabilisation

The stability of the mechanism is a very important aspect that has a great influence on its ability to function in practice. In this case, the term *stability* concerns the stability of the rolling elements, which is solved by using stabilisation bands, but also the stability of the opposing intermediate bodies, which should be vertically aligned and limited in rotation.

Stabilisation bands The main challenge with using rolling link elements, is the necessity to use stabilisation bands. They need to follow a certain woven path through the rolling elements and require some pretension to press all the parts together. By fixating their endpoints they are able to remain in place and contain this pretension. In order to lower the chance of these fixations to loosen, they should be free from other components that can possibly damage these points. Furthermore, a minimum of two crossing bands are necessary to provide for the desired stability.

All these requirements make it hard to include such stabilisation bands, especially when it is impossible to make a fixation onto either of the rollers as their rotation exceeds 180°. Therefore, a protruded shape needs to be added to the intermediate bodies, such that the fixation points can be led to a point free of disturbance. Figure C.2 shows how the bands can be woven through the rolling elements, using protrusions and an indentation to create space for the endpoint fixations. Furthermore, a wide groove should be added on the rollers, in which the bands can be guided in the rollers' axial direction.

Vertical alignment & rotation limit In a perfectly symmetric situation and where the compensation force is exactly vertical, the concept as shown in Figure C.1 can work. In practice, however, slight disturbances and variations will occur, causing the upper intermediate body to translate and rotate in multiple directions and making it impossible to function correctly. For this reason, the centres of the upper intermediate bodies need to be vertically aligned and rotation needs to be limited to a minimum.

Constraining two parts relative to each other in all but one degree of freedom—without significantly interfering with the mechanism's compensation characteristic—is

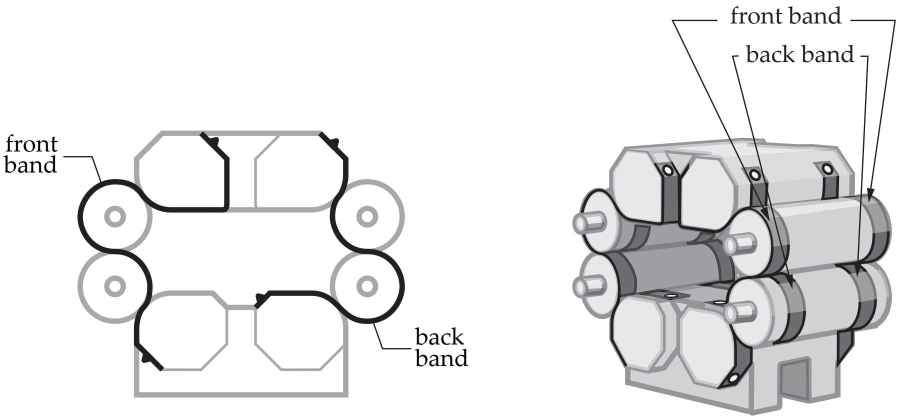

(a) (b)

Figure C.2: *The woven path for front and back stabilisation bands, shown (a) in 2D and (b) in 3D. Protrusions on the intermediate bodies act as guidance for the bands. Note that both left and right side of the mechanism contain both a front and back band that cross each other at the contact points.*

inevitably attended with the introduction of additional sources of friction. To minimise this, again, rolling friction is exploited.

An additional oblong part is added through the middle of the mechanism in order to provide for this stability. The mid piece is fixed on the upper intermediate body and is guided between two rolling pins on the lower intermediate body. As an additional advantage, this part is able to provide for a physical stop to prevent the rollers from rolling to much inwards. Also, it adds a point to which a cable can be attached, such that the mechanism can be operated. Figure C.3 illustrates the situation.

C.1.3 Assembly strategy

Stabilisation bands The bands that are used are steel sheets with a thickness of 20 and 50 μm, such that micro spot welding can be used to fixate their endpoints. Their minimum width are—for now—taken at 2 mm due to limits in manufacturing.

Because of the need to pretension the bands, the following procedure is inevitable during assembly:

1. spot weld one endpoint of the band;
2. weave the band according to its designated path;
3. pretension the band with a certain force and fix its position;
4. spot weld other endpoint of the band.

It should therefore be possible to tension the bands with a certain force, before the other endpoint is fixated. The exact amount of pretension is not of high importance, only its presence and that is approximately the same for every band. For this reason,

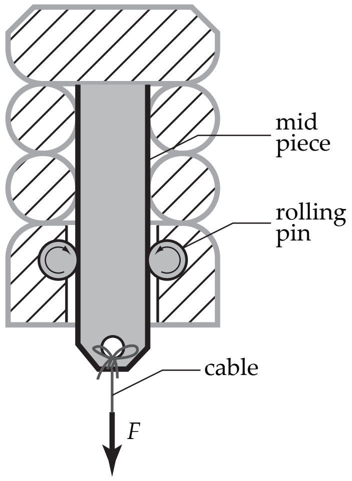

Figure C.3: *The additional mid piece, guided by rolling pins, provides for a vertical alignment of the intermediate bodies and limits their rotation. Its width prevents the rollers from rolling inward at maximum displacement. At the very end, a cable can be attached for operating the mechanism.*

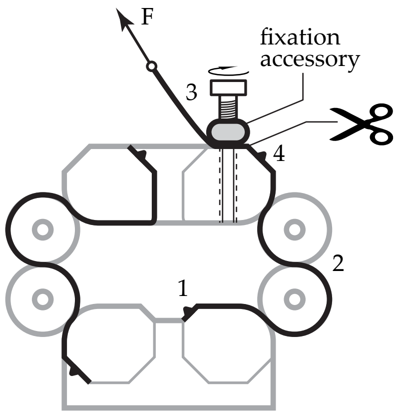

Figure C.4: *Method for fixation of the stabilisation bands, including the addition and control of the pretension. The numbers indicate the order of steps. 1: spot weld one endpoint, 2: weave the band, 3: pretense the band and fix position, 4: spot weld final endpoint.*

the stabilisation bands are tensed up to a certain force F, followed by the addition of a fixation accessory that is screwed tight onto the band. This way, the bands can be spot welded at pretension F. As a final step, the band can be cut to size right after the fixated endpoint. Figure C.4 shows these steps, where the numbers are equivalent to the above-mentioned steps.

Null position Before the bands can be woven trough the rolling elements and tensioned, the mechanism needs to be fixed in a certain position. Otherwise, it is prac-

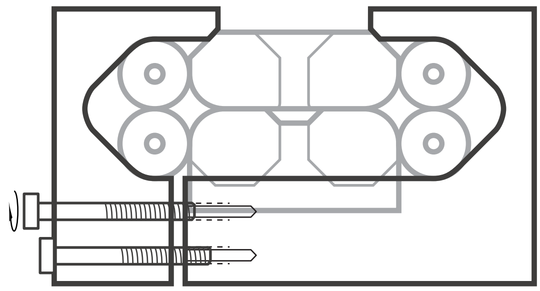

Figure C.5: *Method for fixing the mechanism in a null position with the addition of a brace. The U-shaped parts embrace the rolling elements and intermediate bodies at the same time, which will be fixed by tightening the set of screws.*

tically impossible to obtain a symmetrical placement of the rollers. In order to make it easier, an additional brace is needed that fixes all elements in a null position, upon which the bands can be woven, tensioned and fixed. Figure C.5 shows the shape of this brace, and how the mechanism is fixed by using a set of screws.

C.2 Technical drawings

Using all methods from previous sections, a 3D CAD model is made using SolidWorks version 2012 (Dassault Systèmes, Waltham, MA). Appendix F shows the 2D technical drawings that have emerged from this model. Part no. 4 is an exact copy of a part used in the WILMER WHD-4, hence its drawing is recycled in a different format.

Appendix D
Prototype performance

In order to measure the performance of the mechanism and how it relates to the model, several measurements were performed in the same test bench as described in Appendix A. First, the springs' mechanical properties were measured. Second, the mechanism's compensation characteristic is measured and compared to the model. Lastly, the mechanism in combination with a gloved prosthesis is measured and compared to a prediction resulting from the model and previous glove measurements.

D.1 Spring measurements

Before the prototype was fully tested, the springs' mechanical properties were measured such that the model could be adjusted to the actual spring rate that was used.

D.1.1 Method

Two different types of springs from Tevema Technical Springs (2008) were chosen that share the same dimensions, but vary in mechanical properties due to difference in material – one stainless steel (product code T40480) and one spring steel (product code T30480). A total of 10 springs of each type were measured with five repetitions. A set of four springs were then selected that resemble each other the most.

The same test bench as used in Appendix A was used. The springs were fixated on both ends with small-sized keyrings, which allowed for easy interchangeability of the different springs. The keyrings were first measured separately, such that the spring measurements could be corrected in order to extract the actual spring stiffness.

The data was processed by fitting a linear function to the raw data points for each repetition. The average fit over all repetitions then described the spring's mechanical behaviour. The slope of this fit represented the stiffness and the offset from the horizontal axis represented the pretension.

D.1.2 Results

The force at which the springs were pulled never exceeded 15 N. In this working area, the keyrings showed a linear stiffness of 23.4 $\mathrm{N\,mm^{-1}}$.

Table D.1: *Measured mechanical properties of 10 springs for each type. The top row shows the rated properties as indicated by the manufacturer.*

	stainless steel (T40480)		spring steel (T30480)	
spring	k [N mm^{-1}]	F_0 [N]	k [N mm^{-1}]	F_0 [N]
rated	*1.35*	*1.8*	*1.57*	*2.13*
1	1.02	1.09	1.18	0.91
2	0.98	1.48	1.10	1.04
3	1.01	1.12	1.18	0.83
4	1.00	1.29	1.17	0.64
5	1.05	0.95	1.18	1.08
6	1.05	0.71	1.16	0.75
7	1.05	0.55	1.14	1.07
8	1.01	0.94	1.08	1.62
9	1.05	0.65	1.09	1.42
10	1.05	0.62	1.09	1.61

Table D.1 shows the results from the spring measurements—corrected for the key-rings—where it can be seen that for both types of springs the actual stiffness (k) is systematically lower than the rated stiffness. The amount of pretension (F_0) is also systematically lower than intended and shows an additional random variation.

D.1.3 Discussion

Clearly, the measured pretension and spring rate largely differ from their rated values. Nonetheless, four springs of each type need to be chosen that most resemble each other. Moreover, it is preferable that the difference between the two types of springs is as big as possible.

As for the stainless steel variant, springs 6, 7, 9 & 10 were chosen as they mostly resemble each other's spring rate. This results in an average stiffness of 1.05 N mm^{-1} and pretension of 0.63 N. For the spring steel springs, springs 1, 3, 4 & 5 were chosen, resulting in an average of 1.18 N mm^{-1} and 0.86 N for stiffness and pretension, respectively.

D.2 Prototype measurements

With the actual spring properties known, the prototype could be measured and correctly compared to the predicted values from the model.

D.2.1 Method

At first, the overall mass and dimensions of the prototype were measured and compared to the original design criteria made in section B.1.

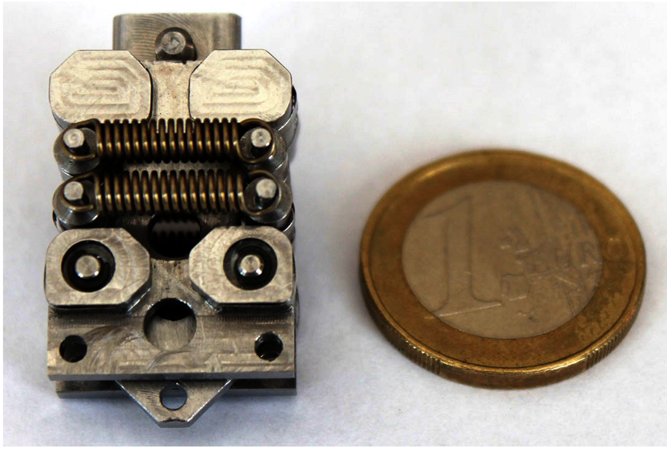

Figure D.1: *The manufactured prototype in its rest position alongside a Euro coin for scale.*

Next, the compensation characteristic of the prototype was measured. In order to test the effect of different components of the prototype on this characteristic, the spring rate and stabilisation band thickness were varied. From the spring measurements it appeared that a variation between 1.05 and 1.18 $\mathrm{N\,mm^{-1}}$ in spring rate was possible using off-the-shelf helical springs. The stabilisation band thickness was varied between 20 and 50 µm. Each measurement was repeated five times.

Again, the test bench from Appendix A was used. The prototype was fixed into position and a thick steel cable was used to put upon the displacement. The cable was first measured separately, such that its stiffness could be corrected for during prototype measurements.

The data was processed by dividing the raw data into discrete bins of 0.5 mm for each repetition. Within these bins, an average force level was calculated over all repetitions.

D.2.2 Results

The resulting prototype is shown in Figure D.1 in rest position. In this position, i.e. the springs are relaxed, the outer dimensions (length$\times$width$\times$depth) are equal to $33 \times 18.6 \times 19$ mm. When the springs are fully tensed, the dimensions are equal to $33 \times 26.2 \times 19$ mm. This slightly exceeds the length criteria of 30 mm by 3 mm. Additionally, although the width and depth do not exceed 30 m, it does not fit into a $\varnothing$30 wrist. Namely, it requires a $\varnothing$33 wrist. The total mass of the mechanism is equal to 26 g. Combined with the adjusted pushrod-operated WILMER WHD-4, the total mass is 95 g.

The cable showed a stiffness of 80 $\mathrm{N\,mm^{-1}}$ within the working area of the measurements. The absolute compensation characteristics for the first prototype compared with the model output are presented in Figure D.2.

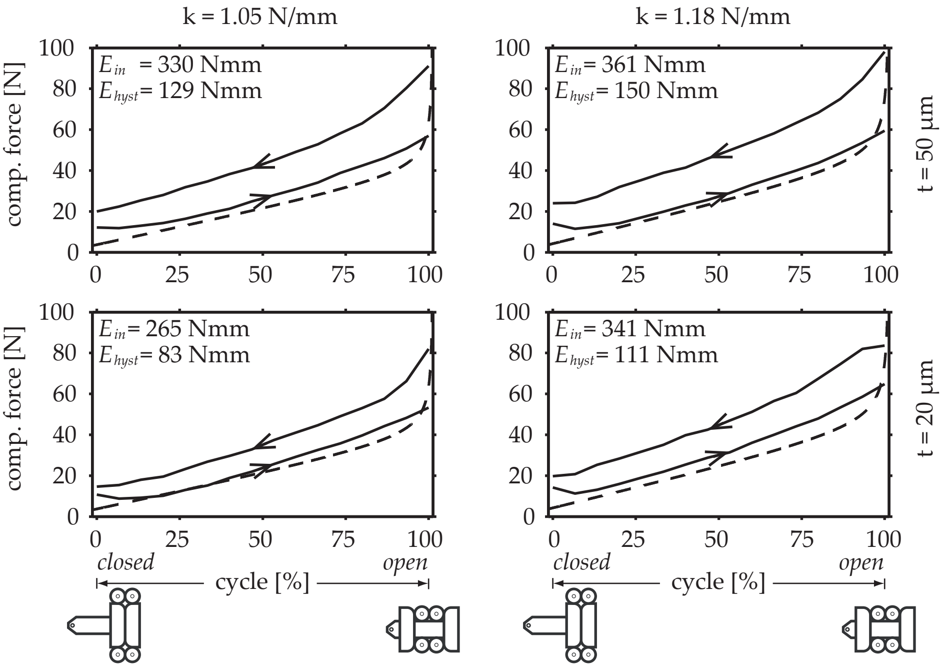

Figure D.2: *Figures showing the measured absolute compensation characteristic (solid) and the predicted outcome by the model (dashed. Spring stiffness (k) is varied left–right and stabilisation band thickness (t) is varied top–bottom.*

D.2.3 Discussion

The volume slightly exceeds the design criterium by several millimetres, whereas the mass has remained below 100 g. These differences are, however, not dramatically large and might still change if the compensation mechanism is integrated inside a prosthesis. Moreover, small reductions to the mechanism's depth can be made to reduce volume and mass, as well as adding several holes to the midpiece and upper intermediate body. The maximum width of the mechanism, on the other hand, is related to the springs that are used and is therefore harder to reduce.

All graphs show that the model is largely comparable to the measured values. However, there is a clear difference in offset and a large hysteresis loop is present. Both factors are directly linked to multiple sources of energy dissipation which were not included in the model. The most important sources are believed to be due to the stabilisation bands and misalignment of parts. Additionally, any source of friction directly increases the hysteresis loop. These effects are further explained below.

Effect of stabilisation bands The stabilisation bands have an effect on the compensation characteristic due to elastic and plastic deformation inside the material. The magnitudes of these effects are directly related to the band's thickness, because a thicker band would be more rigid. This introduces additional stiffness to the mechanism due to elastic deformation and energy dissipation (expressed as hysteresis) due to plastic deformation. Moreover, thicker bands are more likely to reach plastic deformation when bent around small radii, increasing its effect on the characteristic.

Effect of misalignment The misalignment of the different parts is mainly caused by play in the stabilisation bands. By pretensing the bands during assembly, this amount of play is minimised but only up to a certain extent. Too much pretension would result in high load on the fixations at the ends of the bands causing them to fail. As a result, the pretension is limited and parts can get misaligned. Its effect is one of the most prominent amongst sources of friction in rolling link mechanisms due to non-parallel axes of the rolling elements (Kuntz, 1995). It is therefore very likely to largely contribute to the hysteresis loop as is seen from the results in Figure D.2.

Effect of other friction sources Within this mechanism, any source of friction directly translates itself in a hysteresis loop. This is because the loading and unloading curve are not reversed identical, but show a different path. The total amount of energy necessary to operate the mechanism is equal to the loading energy of the springs *plus* the energy dissipation due to friction. The compensation energy, however, is determined by the unloading energy of the springs *minus* energy dissipation due to friction. In other words, any occurrence of friction expresses itself twice in opposite directions, causing a larger hysteresis loop.

D.3 Prototype with prosthesis measurements

Lastly, by putting the prototype in series with the pushrod inside the WILMER WHD-4 prosthesis, a glimpse on the possible resultant characteristic can be obtained.

D.3.1 Method

A additional wrist unit was designed and manufactured that allowed the compensation mechanism to be connected to the prosthesis mechanism, which operates by a central pushrod. The compensation mechanism could push against this pushrod via its midpiece, passively opening the hand (see Figure D.3). The prosthesis was fitted with a silicone glove (Otto Bock, size 8S6=142x50), so by pulling on the compensation mechanism with a cable, the compensation force decreased and the hand started to close. Resultingly, the force that is exerted by the cable is now equal to the resultant force.

The predicted characteristic from the model was defined as the measured glove stiffness characteristic minus the modelled compensation characteristic. Further variations and methods of data acquisition and processing were identical to those described in section D.2. In this case, however, the force from the cable was processed as a negative force, because the working principle of the prosthesis was reversed.

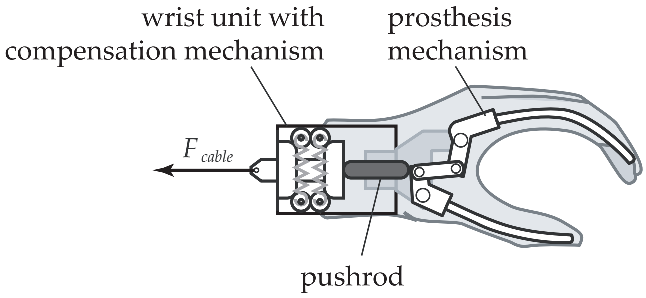

Figure D.3: *Drawing showing how the compensation mechanism is connected to the prosthesis mechanism via an additional wrist unit and central pushrod.*

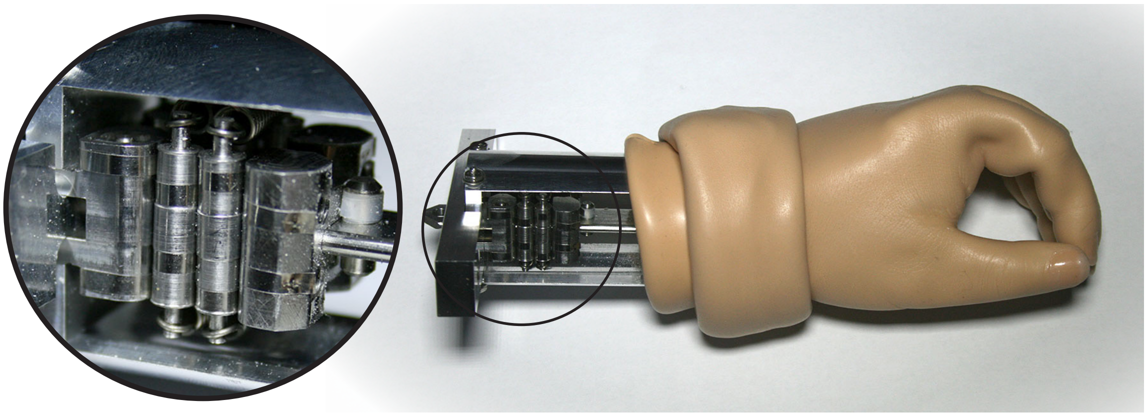

Figure D.4: *The manufactured prototype in series with a gloved WILMER WHD-4.*

D.3.2 Results

Figure D.4 shows the resulting wrist unit connected to the prosthesis, which is fitted with the silicone glove. The glove was partially rolled up, such that there was no chance it could influence the compensation mechanism.

The resultant characteristics are presented in Figure D.5, where the measured values are compared to the predicted outcome.

D.3.3 Discussion

The most important observation from these measurements is that the compensation mechanism has succeeded in compensating the cosmetic glove's stiffness, as well as converting the prosthesis into a voluntary closing device. The configuration with $k = 1.05\ \mathrm{N\,mm^{-1}}$ and $t = 20\ \mu\mathrm{m}$ even shows that resultant forces of lower than 40 N are possible.

The same effect of changing the spring stiffness and stabilisation band thickness can be observed in both Figure D.2 and Figure D.5. Their effects on the maximum operation forces, however, become more apparent in Figure D.5. It illustrates the importance of

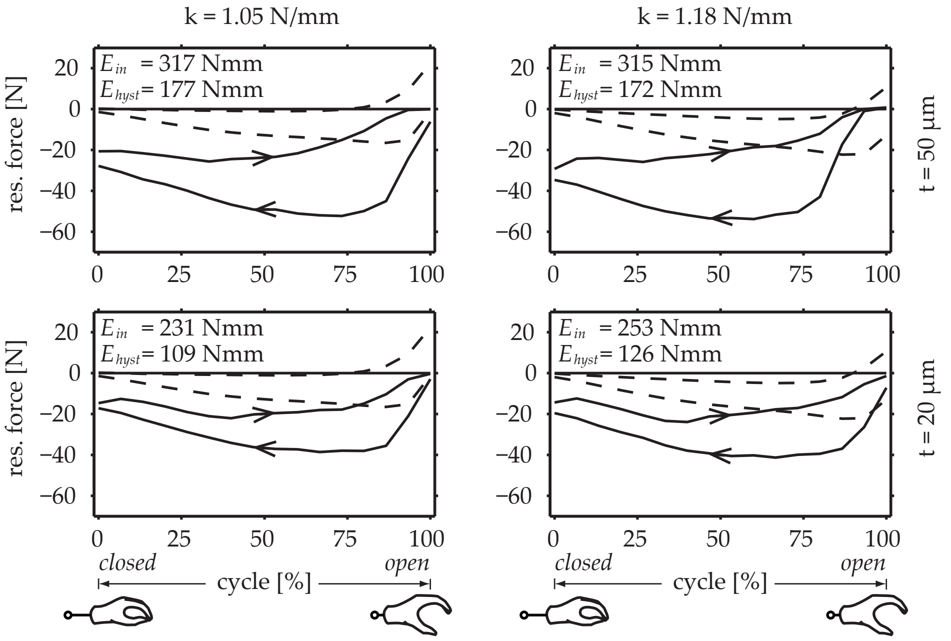

Figure D.5: *Figures showing the predicted outcome by subtracting the model from glove measurements (dashed) and measured values (solid) for the resultant characteristic. Spring stiffness (k) is varied left–right and stabilisation band thickness (t) is varied top–bottom.*

reducing the stabilisation band thickness to a minimum, as a decrease of 30 μm in band thickness already results in a decrease of 15 N in resultant force.

The precise amount of compensation is, however, not ideal. There are still discrepancies between the predicted and measured output of at least 20 N, caused by the influence of the stabilisation band, misalignment and other sources of energy dissipation (see the discussion in section D.2). Furthermore, the connection between the compensation mechanism and prosthesis was an easy but not ideal solution, as it lacked in stability and firmness. Unfortunately, a more solid solution did not fit into the time span of this thesis.

An additional observation is that the resultant hysteresis is lower than expected. For example, in the case where $k = 1.05\ \mathrm{N\,mm^{-1}}$ and $t = 50$ μm, it should be equal to approximately 234 N mm – being the glove's hysteresis (105 N mm) plus the compensation mechanism's hysteresis (129 N mm). The measured value, however, lies at 177 N mm. The main cause for this difference is the fact that the pulling force from the cable was not perfectly in line with the mechanism. As a result, the rolling elements became more misaligned when operation forces are higher, causing the hysteresis to increase. Because operation forces are substantially lower in combination with the prosthesis, this effect is reduced and the hysteresis is lower.

Detailed suggestions to improve the efficiency, stability and overall usability of the compensation mechanism are described in Appendix E, such that the drawbacks as discussed above can be reduced to a minimum.

APPENDIX E

Future work

The final conclusions as presented in this report are limited to those based on the prototype's performance. However, a considerable amount of thought is also put into the possible adjustments of the concept and how they may improve the mechanism's efficiency, stability and overall usability. These adjustments range from subtle changes in the concept's geometry to adaptations for integration in an existing prosthesis.

E.1 Practical adjustments

Prevent form-lock One major issue in current design is its tendency to end up in a form-lock. In this situation, the rollers make a contact angle of 90° and the mechanism can no longer be moved by normal operation. As a result, the mechanism needs an initial 'push' to get past this point. This action never goes smoothly because high forces are involved, hence a relatively large range of displacement is lost, effectively skipping the high-force region. This can all be prevented by widening the midpiece, which limits the movement of the rollers and thus their maximum contact angle. As shown in Figure E.1, this only slightly reduces the amount of vertical displacement.

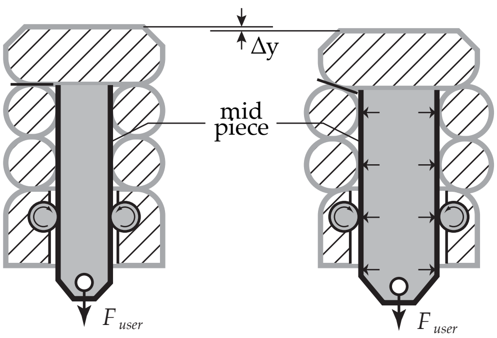

Figure E.1: *A wider midpiece reduces the maximum contact angle, prevents a form-lock and only slightly reduces the vertical displacement by Δy.*

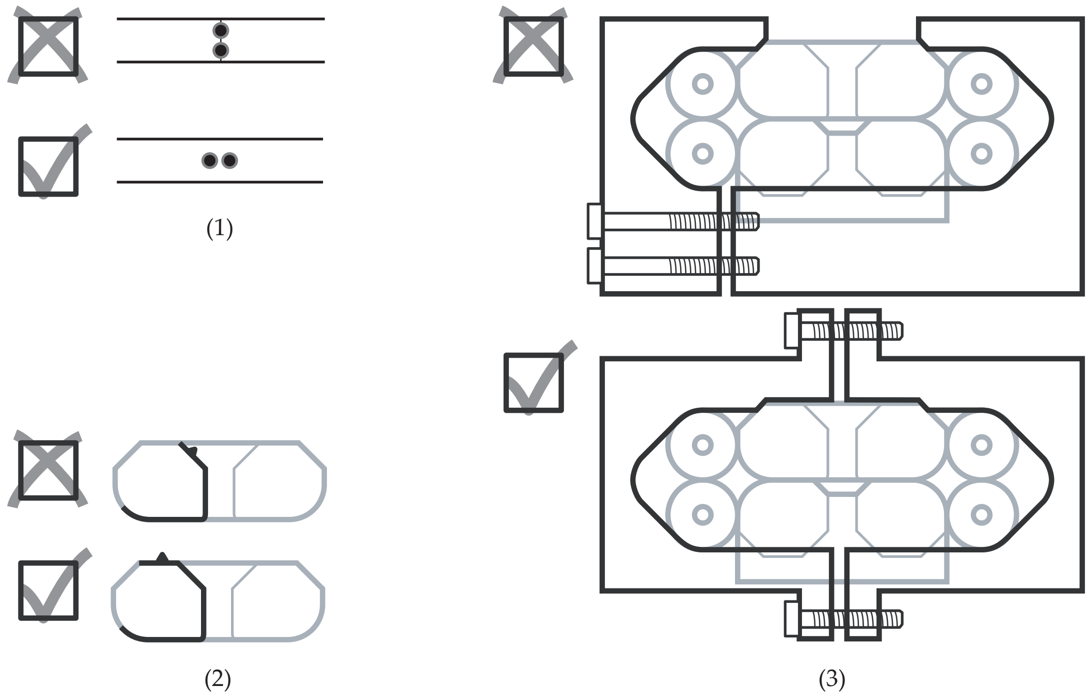

Figure E.2: *Suggestions that improve the quality of the spot welds by (1) only welding in the length of the band, (2) only welding on a flat surface and (3) better fixation of the rolling elements.*

On stabilisation bands As discussed multiple times in Appendix D, the stabilisation bands pose a problem for the mechanism. They make an essential part for it to work, but their thickness, placement, pretension and fixations largely influence the overall quality of the mechanism.

As appeared from the measurements of the prototype, the bands need to be as thin as possible to minimise their influence on the mechanism. Current minimal thickness is set at 20 µm, any thinner would be hard to find and too weak to add enough pretension. More importantly, it is already hard to apply strong spot welds to a 20 µm band as fixations. By experience, the following suggestions can be made to make the spot welds as strong as possible:

(1) always apply the spot welds in the *length* of the band, otherwise the pressure from the electrodes will crease the band and cause a weak spot;

(2) always weld under a straight angle on a flat surface, this makes it easier to place the electrodes perpendicular to the surface and for them to reach the surface properly; and,

(3) make sure all rolling elements are firmly fixed into place, such that they are unable to move when pretension is added to the bands (current fixation brace can be improved);

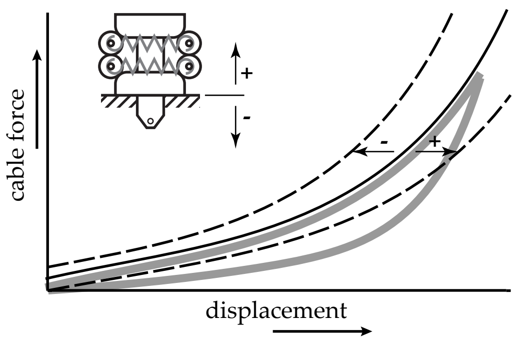

Figure E.3: *By increasing the workspace of the compensation mechanism, one can adjust its relative base position and tweak the compensation characteristic.*

These suggestions are illustrated in Figure E.2, where a suggested improved shape of the fixation brace is also shown. Additionally, it is believed that adding multiple layers of material at the location of the spot weld might improve its strength. This is, however, not tested.

Add intrinsic alignment Misalignment of parts is considered to be a substantial contributor to energy dissipation and needs to be prevented as much as possible. The assembly of the stabilisation bands is a challenging task and small discrepancies may already result in misalignment. To reduce this effect, an intrinsic alignment can be added to the rolling elements, such that misalignment is less bound to happen. For example, this can be done by locally increasing the diameter of the rollers. These protrusions can then fit inside a groove of the adjacent rolling element. It is unknown, however, whether this would have an effect that is worth the added complexity in the design.

Enlarge workspace The current design lacks in adaptability, so it cannot cope with changes of the cosmetic glove or miscellaneous inaccuracies. This can be improved by enlarging the workspace of the mechanism. By increasing the rollers radius r, the total range of displacement of the compensation mechanism increases and becomes larger than required. As a result, one can tweak the relative position in combination with the prosthesis, for example by the means of metric threading. This moves the compensation characteristic over the horizontal axis (see Figure E.3): towards the left results in higher compensation forces and towards the right results in lower compensation forces.

E.2 Refining contour shape

In section B.3.3, a model is described in which the general characteristic can be predicted. The effect of different variations in geometry and spring properties are examined and from there on optimised. These variations to the characteristic are, however, limited by the functional geometry of the concept and availability of particular spring

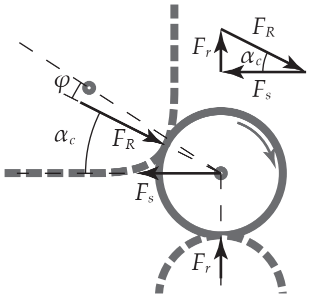

Figure E.4: *Adjusted free body diagram, showing the correction angle φ due to the non-circular contour shape of the intermediate body.*

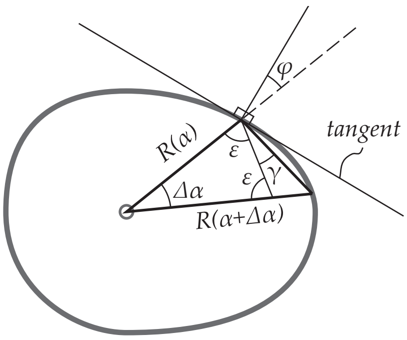

Figure E.5: *An arbitrary non-circular body, showing relevant line segments and angles in order to determine the correction angle φ.*

properties. One option that does not interfere with the concept's working principle, is altering the contour shape R to a non-circular shape. As a result, a concept with feasible dimensions can be further moulded into the desired curve.

Rolling elements that have a non-circular shape show different characteristics from those with a circular shape. This is because the tangent line is no longer perpendicular to the radius, a deviation which can be expressed into a correction angle. With the correction angle known, boundary conditions can be set in order to determine which types of contour shapes are allowed in this application. Lastly, an optimisation procedure is then able to find the ideal shape.

E.2.1 Determining correction angle

Due to the non-circular shape of the contour, the normal force no longer coincides with the radius. The angle α therefore needs to be adjusted with a correction angle φ, such that a corrected contact angle α_c is obtained. Figure E.4 illustrates this in the free body diagram.

In order to determine this correction angle, an arbitrary non-circular body is shown in Figure E.5. In this figure the angle $\Delta\alpha$ is exaggerated, but the limit case where it approaches zero is of importance.

If $\Delta\alpha \rightarrow 0$, the tangent line will coincide with the chord between the radii $R(\alpha)$ and $R(\alpha+\Delta\alpha)$. Furthermore, the angle ϵ is added to create an isosceles triangle, such that:

$$\lim_{\Delta\alpha \rightarrow 0} \epsilon = \pi/2 \tag{E.1}$$

When this is true, a right-angled triangle occurs with angle γ. As the adjacent side is now perpendicular to the radius $R(\alpha)$, it can also be concluded that $\gamma = \varphi$[1]. Using this, the correction angle φ can be approximated using the tangent equation:

$$\begin{aligned} \tan\varphi &= \frac{R(\alpha+\Delta\alpha) - R(\alpha)}{R(\alpha)\Delta\alpha} \\ &= \frac{1}{R(\alpha)}\frac{dR(\alpha)}{d\alpha} \end{aligned} \tag{E.2}$$

Using Equation (E.2) and how it relates to angle α in Figure E.4, the corrected contact angle α_c can be defined as:

$$\begin{aligned} \alpha_c &= \alpha - \varphi \\ &= \alpha - \arctan\left(\frac{1}{R(\alpha)}\frac{dR(\alpha)}{d\alpha}\right) \end{aligned} \tag{E.3}$$

E.2.2 Defining contour shape

The contour of the intermediate body cannot take any arbitrary shape. It is important that the (corrected) contact angle remains between 0 and 90°, such that the vertical component of the contact forces remains acting in the right direction. In other words:

$$\begin{aligned} &0 \leq \alpha_c \leq \pi/2 \\ &0 \leq \alpha - \arctan\left(\frac{1}{R(\alpha)}\frac{dR(\alpha)}{d\alpha}\right) \leq \pi/2 \end{aligned} \tag{E.4}$$

Furthermore, the main property of this concept is that no force is exerted when $\alpha = 0$ and maximum force is exerted when $\alpha = \pi/2$. This should not be affected by the addition of the correction angle, resulting in the following boundary conditions:

$$\alpha_c(\alpha = 0) = 0 \rightarrow \frac{dR(0)}{d\alpha} = 0 \tag{E.5a}$$

$$\alpha_c(\alpha = \pi/2) = 0 \rightarrow \frac{dR(\pi/2)}{d\alpha} = 0 \tag{E.5b}$$

[1] In said limit case, the tangent line coincides with the chord between the radii $R(\alpha)$ and $R(\alpha+\Delta\alpha)$. Resultingly, $\pi - \epsilon - \gamma = \pi/2 - \phi$, with $\epsilon = \pi/2$ this gives $\gamma = \phi$.

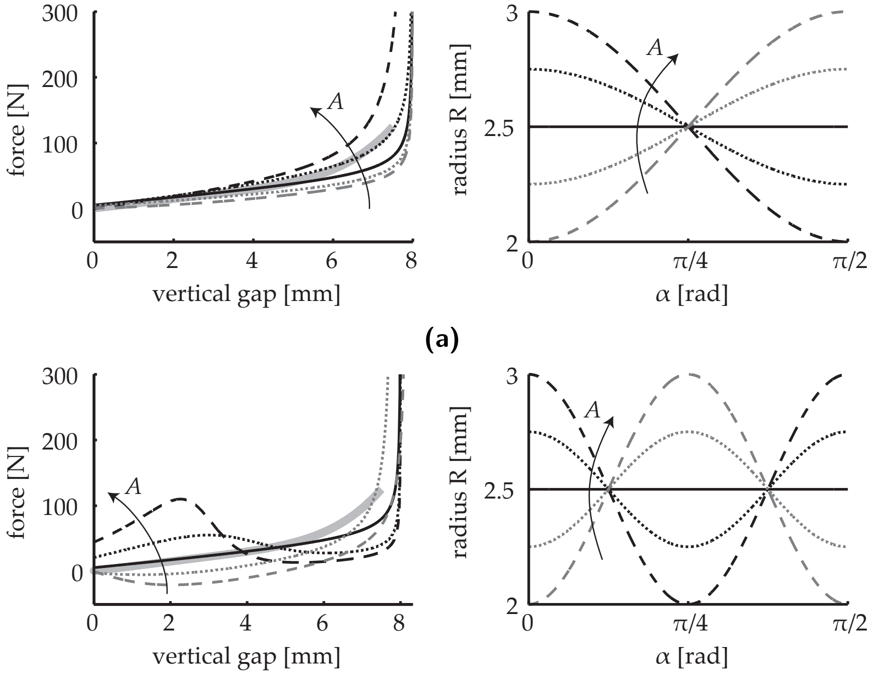

(a)

(b)

Figure E.6: *Figures showing compensation characteristics, compared to the glove characteristic, with corresponding contour profiles using a cosine function. The cosine is varied in period between (a) π and (b) $\pi/2$ radians. Moreover, amplitude (A) is varied between -0.5, -0.25, 0, 0.25 and 0.5 mm.*

One function that fulfils these conditions is a cosine with a period of π or $\pi/2$ – shorter periods are considered impractical due to the small scale. Additionally, the average value and amplitude can be varied as well as the polarity. Varying the average value was practically already covered and shown in Figure B.9a, where it can be seen that an increased value for R increases the vertical offset. The effects of varying period, amplitude and polarity are shown in Figure E.6. From these figures, it can be seen that a period of $\pi/2$ radians becomes impractical and not usable for this application. A period of π radians, on the other hand, shows how the compensation characteristic can be altered in a more subtle manner. An amplitude with positive polarity smoothens the transition towards the asymptote, making it more non-linear. An amplitude with negative polarity sharpens this region, making the majority of the curve more linear, but also reducing in compensation force. The best choice depends on the desired compensation characteristic. In this case, an amplitude between 0.25 and 0.5 mm with positive polarity seems ideal.

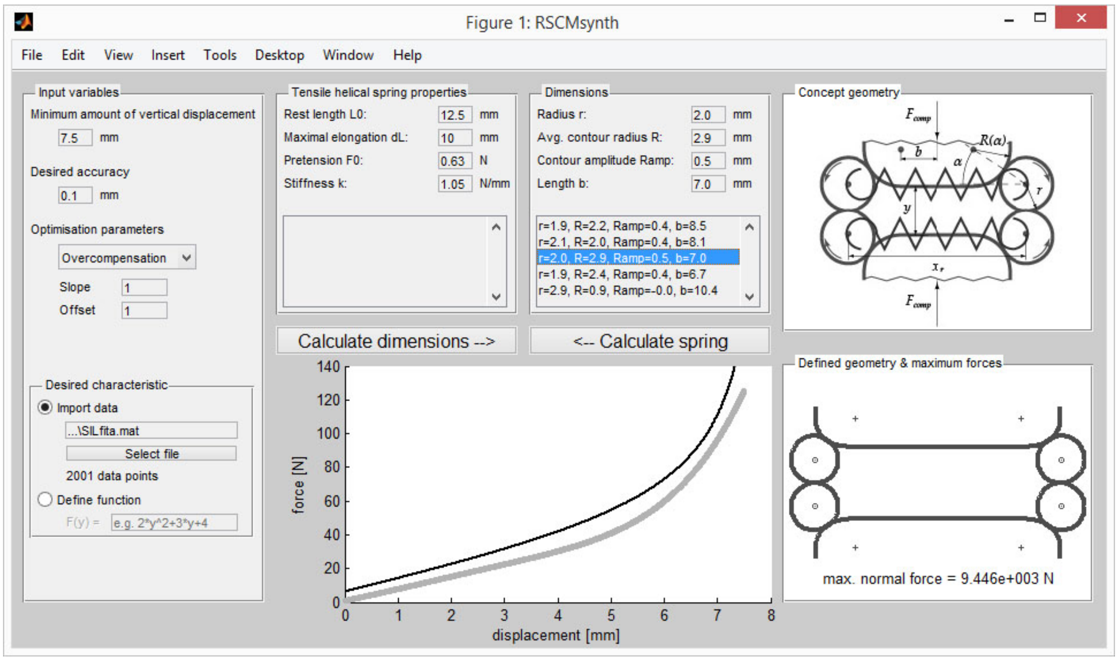

Figure E.7: *Screen capture of the custom GUI built in Matlab, named `RSCMsynth`. `RSCMsynth` can be used to interactively design and optimise a compensation mechanism. A set of input variables (left panel), spring properties and dimensions (top-mid panels) are used to predict the compensation characteristic (black) next to the desired characteristic (grey). Moreover, the overall shape and maximum normal force are shown (bottom right).*

E.3 Interactive compensation mechanism design

The exact shape of the compensaton mechanism, only now with non-circular shapes, can be determined by performing another optimisation procedure, searching for the ideal combination of parameters. However, it was found that performing several specific optimisation procedures throughout the thesis project was very cumbersome. For future efforts, a custom GUI was built in a Matlab environment that allows for interactive dimensioning and optimisation. In Figure E.7, a screen capture of this program is shown. The compensation mechanism was coined as a Rolling Stiffness Compensation Mechanism (RSCM), hence the program has been named `RSCMsynth`.

`RSCMsynth` accepts a variety of input variables and can be used in multiple ways. In any case, the user has to define a minimum amount of vertical displacement that is necessary, desired accuracy of the results, a few parameters related to the optimisation algorithm and the desired characteristic itself (left panel). In its easiest way, the user can now define the mechanical properties of the used springs and the dimensions of the mechanism (top-mid panels). The program will then call on the numerical model and predicts the absolute compensation characteristic of this particular configuration, plotting it next to the desired characteristic (bottom figure). Moreover, the overall shape of the mechanism is drawn and the maximum occurring normal force is shown (bottom-right panel). By changing either of the input variables, the compensation characteristic will be updated and the induced change will be visible.

RSCMsynth is, however, also able to perform an optimisation procedure. Based on given spring properties, an ideal set of dimensions can be determined. Vice versa is also possible, but this will most likely result in a spring that does not exist, thus it is not recommended. In either way, the algorithm uses the same principle, namely a constrained minimalisation procedure. The constraints are resultant from feasible combinations of spring properties and dimensions[2], as well as the minimum amount of displacement. The function to be minimised is identical to Equation (B.14), which is:

$$e\left(R, r, k, F_0, y\right) = \left(C_1 e_1 + C_2 e_2\right) y \tag{E.6a}$$

$$\text{with: } e_1 = \frac{dF_v}{dy} - \frac{dF_{glove}}{dy} \tag{E.6b}$$

$$e_2 = F_v - \left(F_{glove} + 8C_3\right) \tag{E.6c}$$

where:

$e =$ error function to be minimised [-]
$F_v =$ compensation characteristic [N]
$F_{glove} =$ (measured) glove characteristic [N]
$y =$ vertical displacement [mm]

Only now, the parameters C_1 and C_2 can be tweaked interactively, controlling the weighting on slope and offset, respectively. Additionally, with $C_3 = 1$ the program optimises for overcompensation, with $C_3 = -1$ it optimises for undercompensation.

The results from the minimalisation procedure are largely dependent on the initial values, as it is sensitive to local minima. For this reason, a large set of initial values is taken: one educated guess and an additional 20 randomly chosen values. The latter step adds a random aspect to the procedure, but can also offer a large variety of solutions and give out-of-the-box and unbiased insights. Based on their value for e from Equation (E.6), the top five solutions are shown in a listbox. The user can now browse through these solutions, where manual tweaking of these variables is also possible.

In order to test RSCMsynth, the values as measured in Appendices A and D are used as input. More precisely, the desired characteristic is set to the silicone glove characteristic, minimum displacement is set to 7.5 mm and the spring's free length, elongation, pretension and stiffness are set to $L_0 = 12.5$ mm, $dL = 10$ mm, $F_0 = 0.63$ N and $k = 1.05\ \mathrm{N\,mm^{-1}}$, respectively. Figure E.8 shows two possible results from RSCMsynth which were optimised to the described situation.

First of all, the results show that the non-circular (cosine) shape of the contour radius R certainly brings the compensation characteristic closer to the glove characteristic. Secondly, it shows that both solutions are feasible options but with distinct downsides,

[2]For example, the free length of the spring should be smaller than the minimum amount of distance between the rollers' centres, in order to maintain tension.

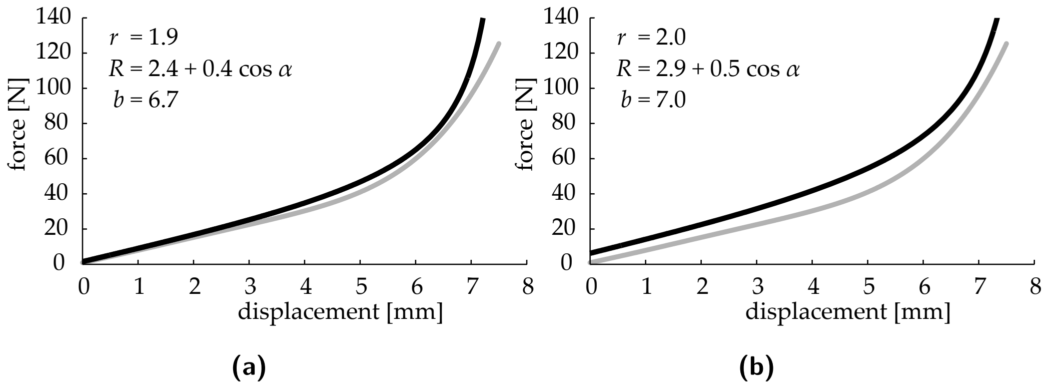

Figure E.8: *Two possible solutions from `RSCMsynth`, showing the predicted absolute compensation characteristic (black) compared to the desired characteristic (grey). Both solutions were optimised for current situation using the same springs (L_0 = 12.5 mm, dL = 10 mm, F_0 = 0.63 N and k = 1.05 N mm^{-1}).*

because E.8a has the risk of undercompensation and E.8b pushes the used spring to its limit (exceeding maximal elongation by 20%). Thirdly, one might see potential in a combination of the two, something which can be easily inserted within `RSCMsynth` by entering the average values. As a result, an interactive process is put in motion which helps in the design process.

E.4 Integration with WILMER WHD-4

The design of a functioning glove stiffness compensation mechanism is only complete when properly integrated with a prosthesis mechanism. In Appendix D, a very simplified wrist unit was manufactured, but was only feasible to work in a controlled measurement setting. For this reason, as closure to this thesis, a proposal for integration with an existing prosthesis (WILMER WHD-4) is made.

E.4.1 The WILMER WHD-4 mechanism

The WILMER WHD-4 is in fact a passive prosthesis, but can be converted into an active prosthesis by using a central pushrod. It becomes a voluntary closing mechanism by directly coupling this pushrod to a Bowden cable, which is then operated by the prosthesis user.

A four-bar linkage connects the fingers with the opposing thumb, but there is an angle of 45° between their axes (see Figure E.9). This officially makes the four-bar linkage impossible to function, but it still works due to the admittance of small amounts of angular play at the pivot points.

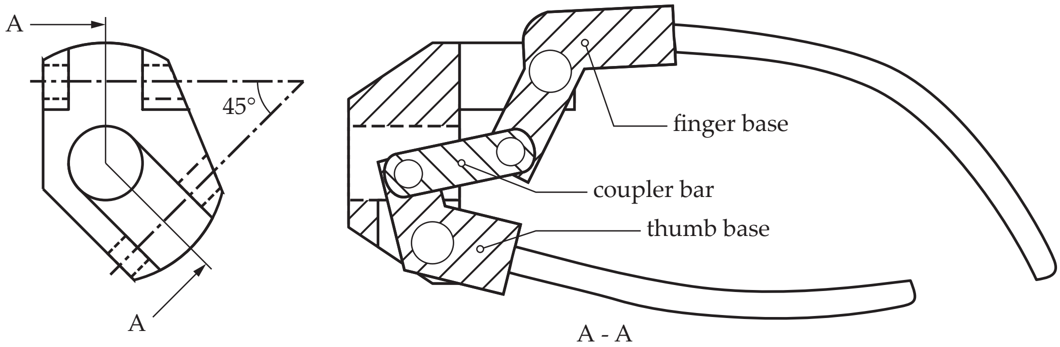

Figure E.9: *Drawing of the WILMER WHD-4 mechanism, showing the different elements in the four-bar mechanism. The angle between the axes of the finger and thumb base adds an additional rotation of the coupler bar.*

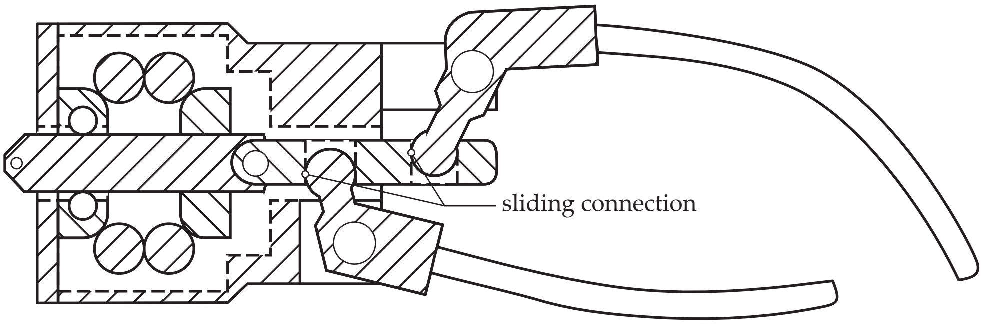

Figure E.10: *Drawing of a WILMER WHD-4 mechanism with integrated compensation mechanism. Bearing points are replaced by slots with sliding contacts, such that a pure linear motion of the coupler bar is possible.*

E.4.2 Connecting the compensation mechanism

The four-bar linkage inside the WILMER WHD-4 poses a problem when trying to connect it with the compensation mechanism. This is because a rigid connection is needed for firmness and the compensation mechanism should only move in a linear path to prevent misalignment. At the same time, however, the coupling bar inside the four-bar linkage rotates along all axes. To solve this, the four-bar linkage needs to be adjusted.

In order for the four-bar linkage to function, while at the same time restricting the coupling bar to a pure linear motion, the bearing points need to be replaced by slots. The arms from the finger and thumb base should then end in a circular shape, such that a sliding connection is established. This is illustrated in Figure E.10.

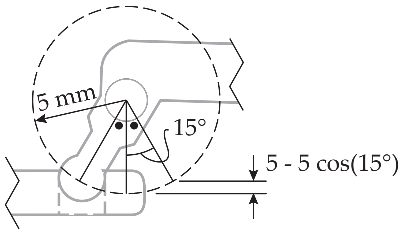

Figure E.11: *Sketch of how the back-and-forth distance of the arms was calculated. It was assumed the total arm rotation of* 30° *resulted from a* 15° *rotation to either side.*

E.4.3 Added energy dissipation

By adding sliding connections in the prosthesis mechanism instead of bearing points, the amount of energy dissipation due to friction increases. A simple prediction for these added losses can be calculated by determining a total slip length and friction coefficient.

In the WILMER WHD-4, the finger and thumb base are connected with the coupler bar with a 10.2 mm arm. They can both rotate approximately 30° ($= \pi/6$ radians) around their own axes. If the circular shapes inside the slots both have a radius of 5 mm, this results in a slip length of ($\pi/6 \cdot 5 =$) 2.6 mm. Additionally, the arms make a back-and-forth motion inside the slots, resulting in an extra ($5 - 5\cos 15 =$) 0.2 mm – Figure E.11 enlightens this last step. As a result, the sliding distance is approximated at 2.8 mm.

The friction coefficient is approximated at $f = 0.2$, a common value for sliding interfaces (Cool, 2006). Because friction occurs at both the finger and thumb base, the total friction force can be calculated according to:

$$F_f(l) = 2fF_{comp}(l) \tag{E.7}$$

$$\text{where:} \quad \begin{aligned} F_f &= \text{ total friction force [N]} \\ f &= \text{ 0.2 = friction coefficient [-]} \\ F_{comp} &= \text{ compensation force [N]} \\ l &= \text{ sliding distance [mm]} \end{aligned}$$

In Equation (E.7), as a matter of simplicity, it is assumed that sliding displacement l is a linear function of vertical displacement y of the compensation mechanism. In this assumption, the approximation of total sliding distance comes in place:

$$l(y) = \frac{l_{tot}}{y_{tot}} y \tag{E.8}$$

$$\text{where:} \quad \begin{aligned} l_{tot} &= \text{ 2.8 = total sliding distance [mm]} \\ y_{tot} &= \text{ 7.5 = total displacement of compensation mechanism [mm]} \end{aligned}$$

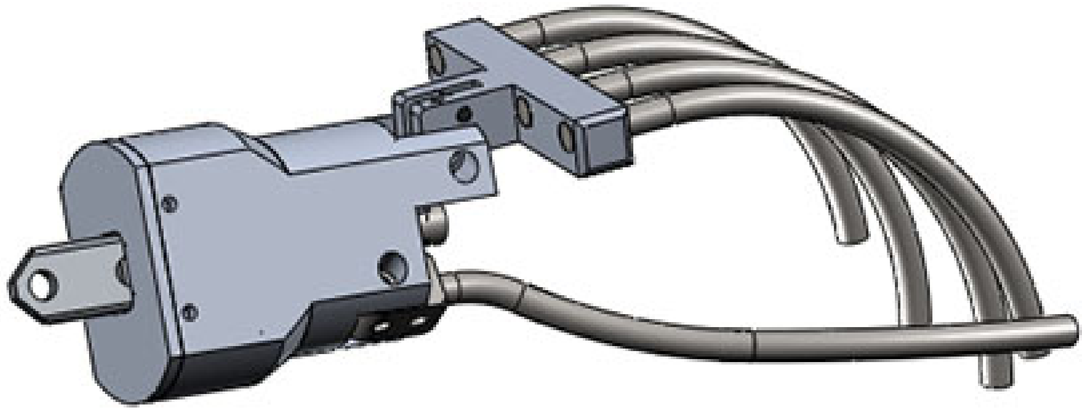

Figure E.12: *3D CAD model of the compensation mechanism integrated with a WILMER WHD-4 prosthesis.*

Using this relation, the friction force can be expressed in terms of y, and an estimation of the amount of energy dissipation can be calculated:

$$E_{diss} = \int_{y=0}^{y=y_{tot}} F_f(y)dy \tag{E.9}$$

The model as described in section B.3.3 is used to calculate compensation force and vertical displacement. Resultingly, the total amount of energy dissipation of the integrated compensation mechanism comes to approximately 2 N mm. This is, however, a rough estimation and does not include additional alignment issues. But it does indicate that this is a feasible concept.

E.4.4 3D CAD model

Finally, a 3D CAD model is created in SolidWorks version 2012 (Dassault Systèmes, Waltham, MA) to better examine the feasibility of current design. The results are shown in Figure E.12 as a general view of the model. An exploded view is shown in Figure E.13, which also indicates the main parts.

The outer dimensions of the wrist were increased to 35 mm, because the compensation mechanism required an inner diameter of at least 33 mm. However, the increased diameter does not dramatically disturb the overall shape of the wrist, as can be seen in Figure E.12. Moreover, improvements to the design of the compensation mechanism may further reduce the overall size. The total mass of the overall mechanism is estimated at 137 g. It is believed, however, that this can further be reduced with a more material-efficient solutions for the hand base.

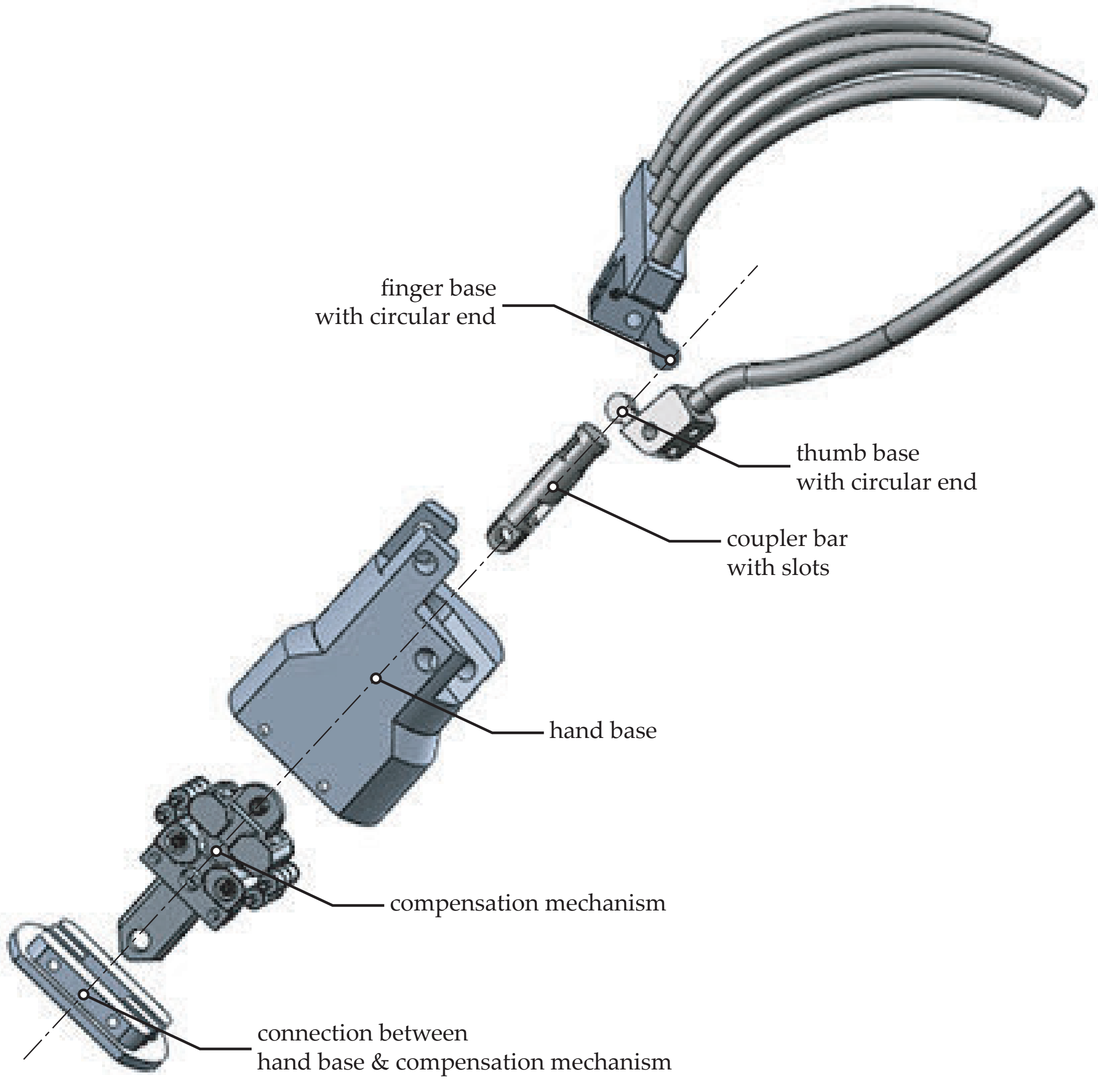

Figure E.13: *Exploded view of the compensation mechanism integrated with a WILMER WHD-4 prosthesis. Bearing points at the coupler bar were replaced by slots and circular ends, such that the coupler bar can move in a linear motion and in line with the compensation mechanism.*

Appendix F

Technical drawings

The following pages show the technical drawings of the first prototype. They represent the exact version that was used during manufacturing and may provide further clarity on the functional design. Suggested improvements are *not* included in these drawings, but are described in detail in Appendix E.

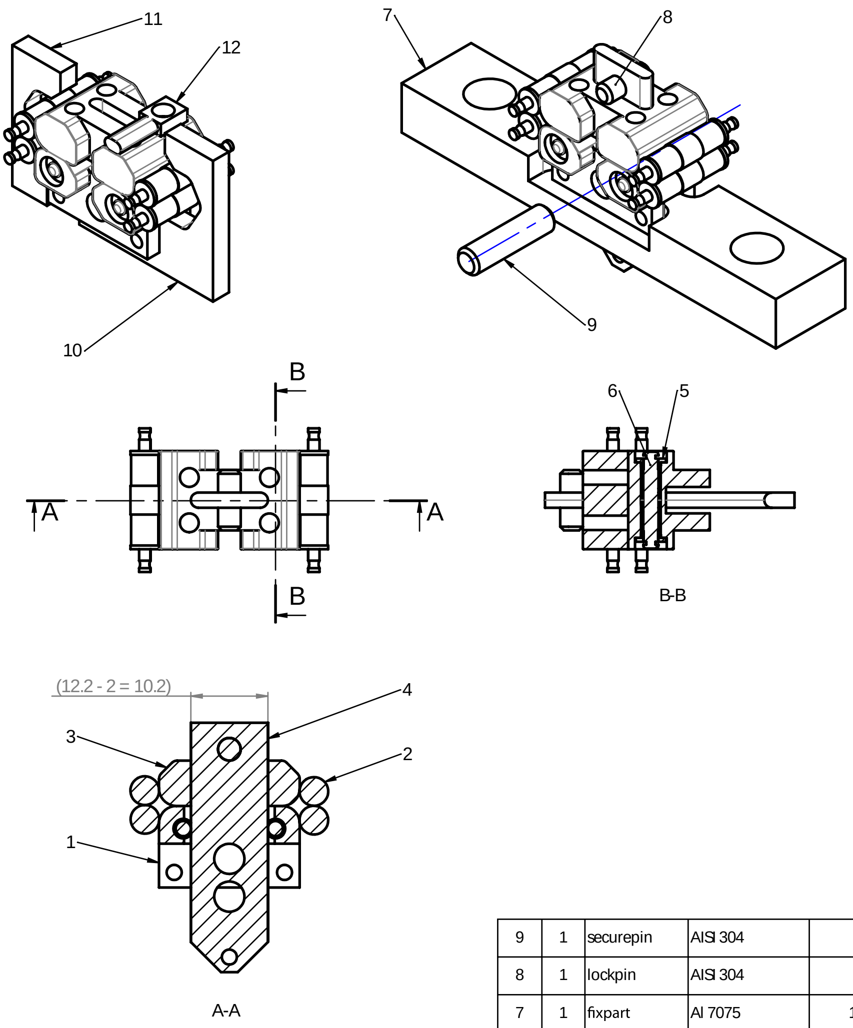

Item No.	Qty.	Name	Material	Weight	Remarks / Draw. No.
12	1	bandclamp	AISI 304	0.49	
11	1	fixbrace_2	Al 7075	0.94	
10	1	fixbrace_1	Al 7075	2.33	

Item No.	Qty.	Name	Material	Weight	Remarks / Draw. No.
9	1	securepin	AISI 304	1.48	
8	1	lockpin	AISI 304	0.44	
7	1	fixpart	Al 7075	14.98	
6	2	rollpin	AISI 304	0.31	
5	4	(28)voering	PCTFE	0.02	
4	1	midpiece	AISI 304	4.36	
3	1	topbase	AISI 314	8.16	
2	4	roller	AISI 314	1.18	
1	1	bottombase	AISI 314	8.78	

TU Delft

scale	1:1	date	12-3-2013
units	mm	remarks	glove compensation-mechanism, upper left with tools for assembly, upper right with tools to fix in null position.
author	Ronald Bos #1518089, r.a.bos@student.tudelft.nl		
group	<<group>>	weight	43.61 grams
name	concept1_glovecomp		

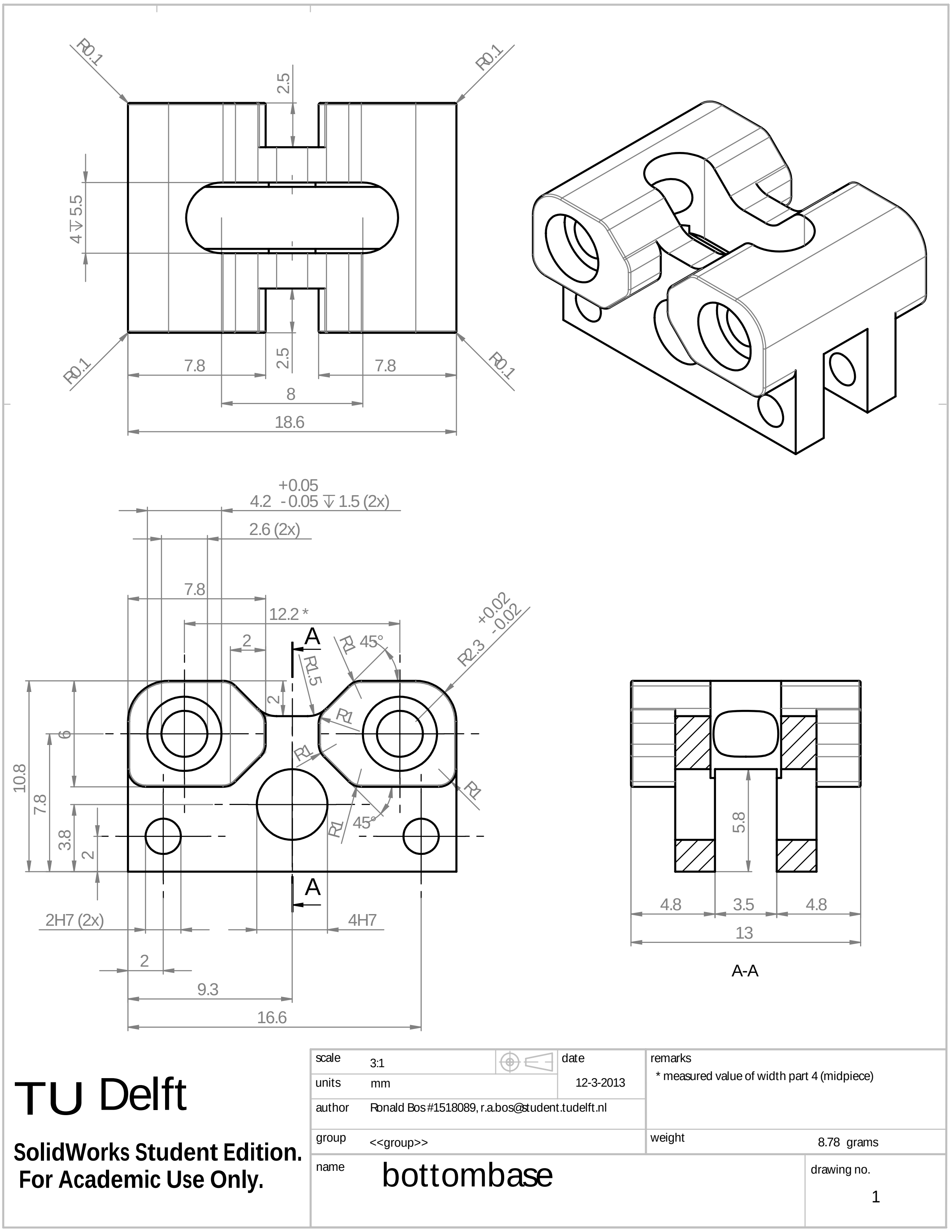
R0.1
R0.1
2.5
4 ↧ 5.5
R0.1
2.5
R0.1
7.8
7.8
8
18.6
+0.05
4.2 -0.05 ↧ 1.5 (2x)
2.6 (2x)
7.8
12.2 *
+0.02
-0.02
R2.3
2
A
R1
45°
R1.5
2
R1
R1
R1
R1
45°
10.8
6
7.8
3.8
2
A
2H7 (2x)
4H7
2
9.3
16.6
5.8
4.8
3.5
4.8
13
A-A
TU Delft
SolidWorks Student Edition.
For Academic Use Only.
scale 3:1
units mm
date 12-3-2013
author Ronald Bos #1518089, r.a.bos@student.tudelft.nl
group <<group>>
remarks
* measured value of width part 4 (midpiece)
weight 8.78 grams
name bottombase
drawing no. 1

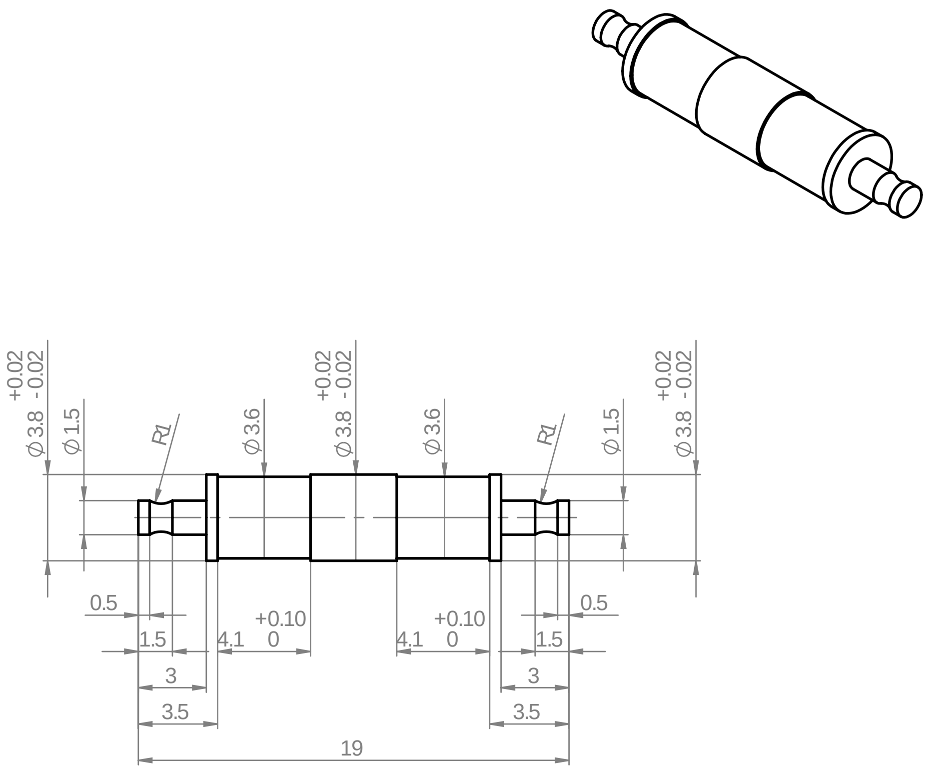

TU Delft

SolidWorks Student Edition.
For Academic Use Only.

scale	3:1	date 12-3-2013	remarks <<remarks>>
units	mm		
author	Ronald Bos #1518089, r.a.bos@student.tudelft.nl		
group	<<group>>	weight	1.18 grams
name	roller	drawing no.	2

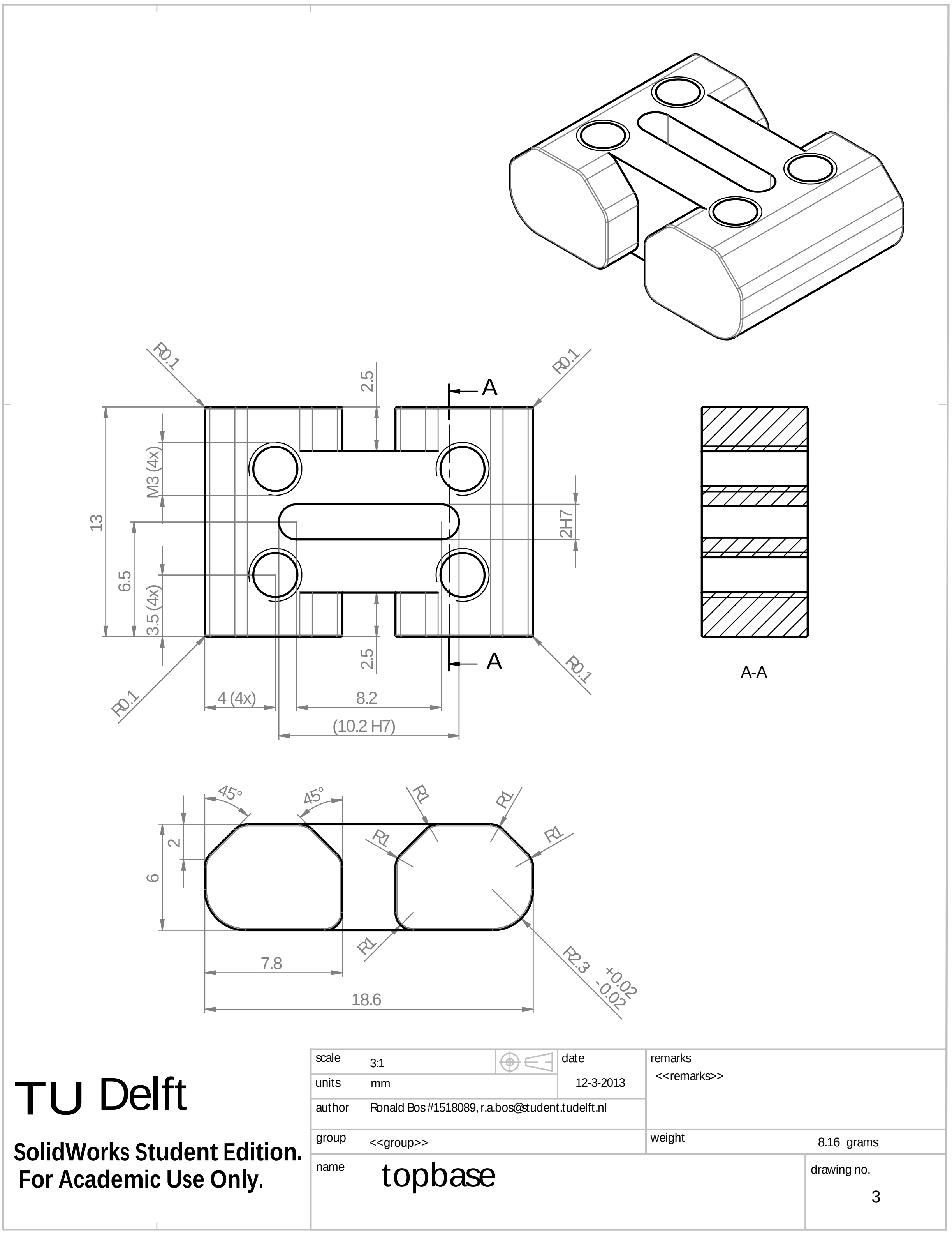
R0.1
2.5
A
13
M3 (4x)
2H7
6.5
3.5 (4x)
4 (4x)
8.2
(10.2 H7)
A-A
45°
R1
2
6
7.8
18.6
R2.3 +0.02 -0.02
TU Delft
SolidWorks Student Edition.
For Academic Use Only.
scale 3:1
date 12-3-2013
units mm
remarks <<remarks>>
author Ronald Bos #1518089, r.a.bos@student.tudelft.nl
group <<group>>
weight 8.16 grams
name topbase
drawing no. 3

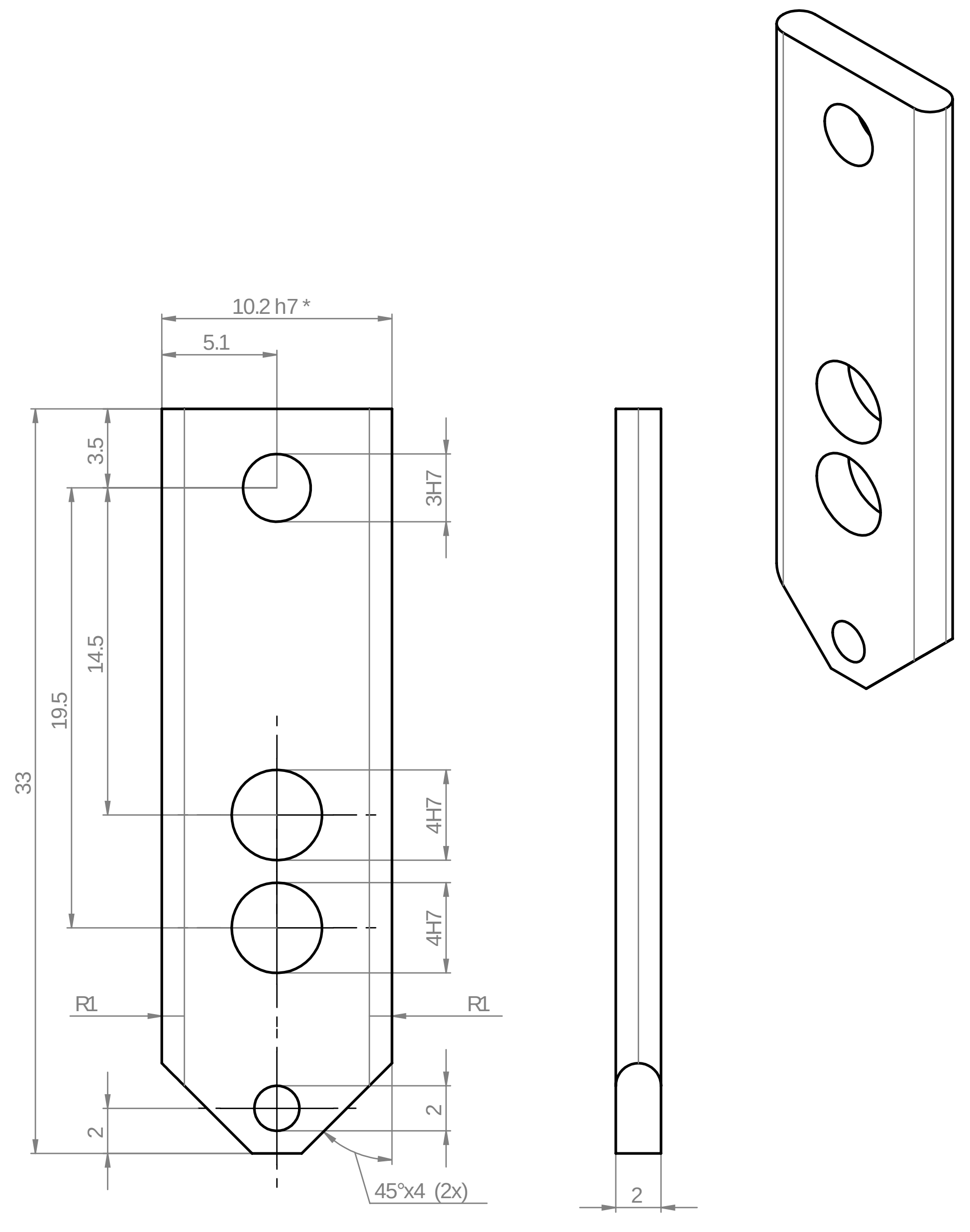

TU Delft

SolidWorks Student Edition.
For Academic Use Only.

scale 3:1	date 12-3-2013	remarks * value to be measured for in part 1 (bottombase)	
units mm			
author Ronald Bos #1518089, r.a.bos@student.tudelft.nl			
group <<group>>		weight 4.36 grams	
name midpiece		drawing no. 4	

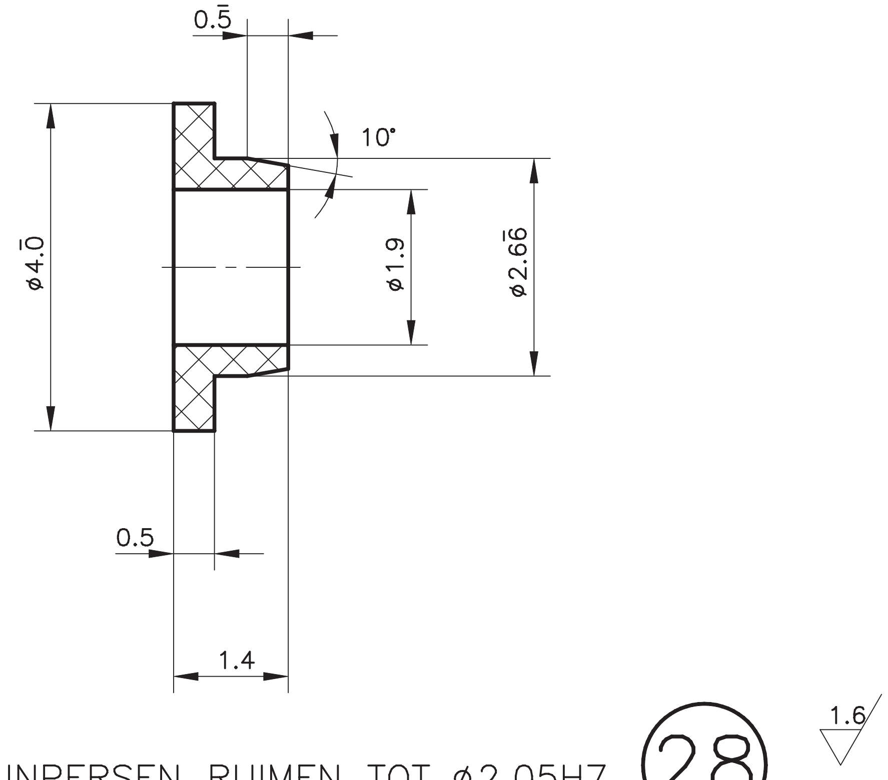

NA INPERSEN RUIMEN TOT ⌀2.05H7

28

TECHNISCHE UNIVERSITEIT DELFT WMR, SECTIE INSTRUMENTEN LANDBERGSTRAAT 3 2628 CE DELFT	VOERING	Get.: SOL Dat.: APR '95 File: WH494_28 Schaal: 10 : 1	Gecont.	Mat.: PCTFE Eriflon Nr.: WHD.4.94.28

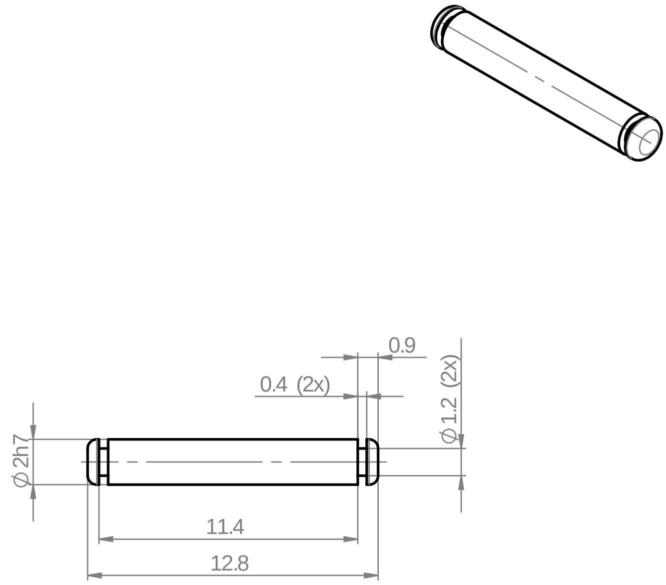

TU Delft

scale	3:1	date 12-3-2013	remarks identical to part 24 of Wilmer WHD-4, only longer
units	mm		
author	Ronald Bos #1518089, r.a.bos@student.tudelft.nl		
group	<<group>>	weight	0.31 grams
name	rollpin	drawing no.	6

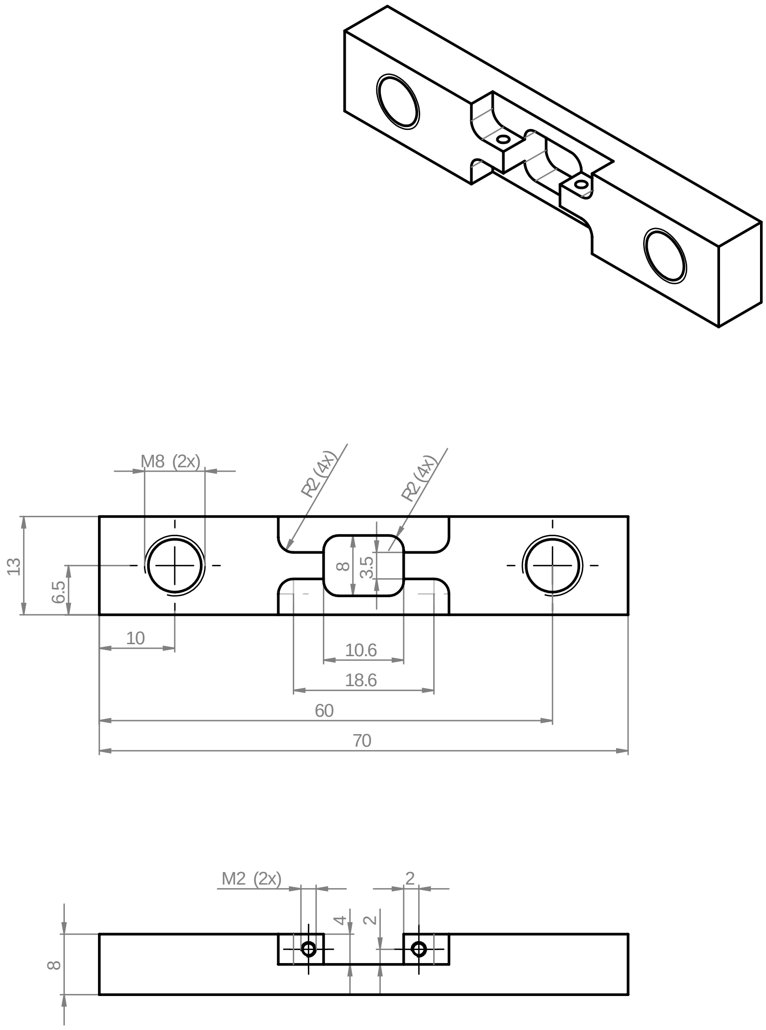

TU Delft

SolidWorks Student Edition.
For Academic Use Only.

scale	1:1	date	remarks
units	mm	12-3-2013	<<remarks>>
author	Ronald Bos #1518089, r.a.bos@student.tudelft.nl		
group	<<group>>	weight	14.98 grams
name	fixpart	drawing no.	7

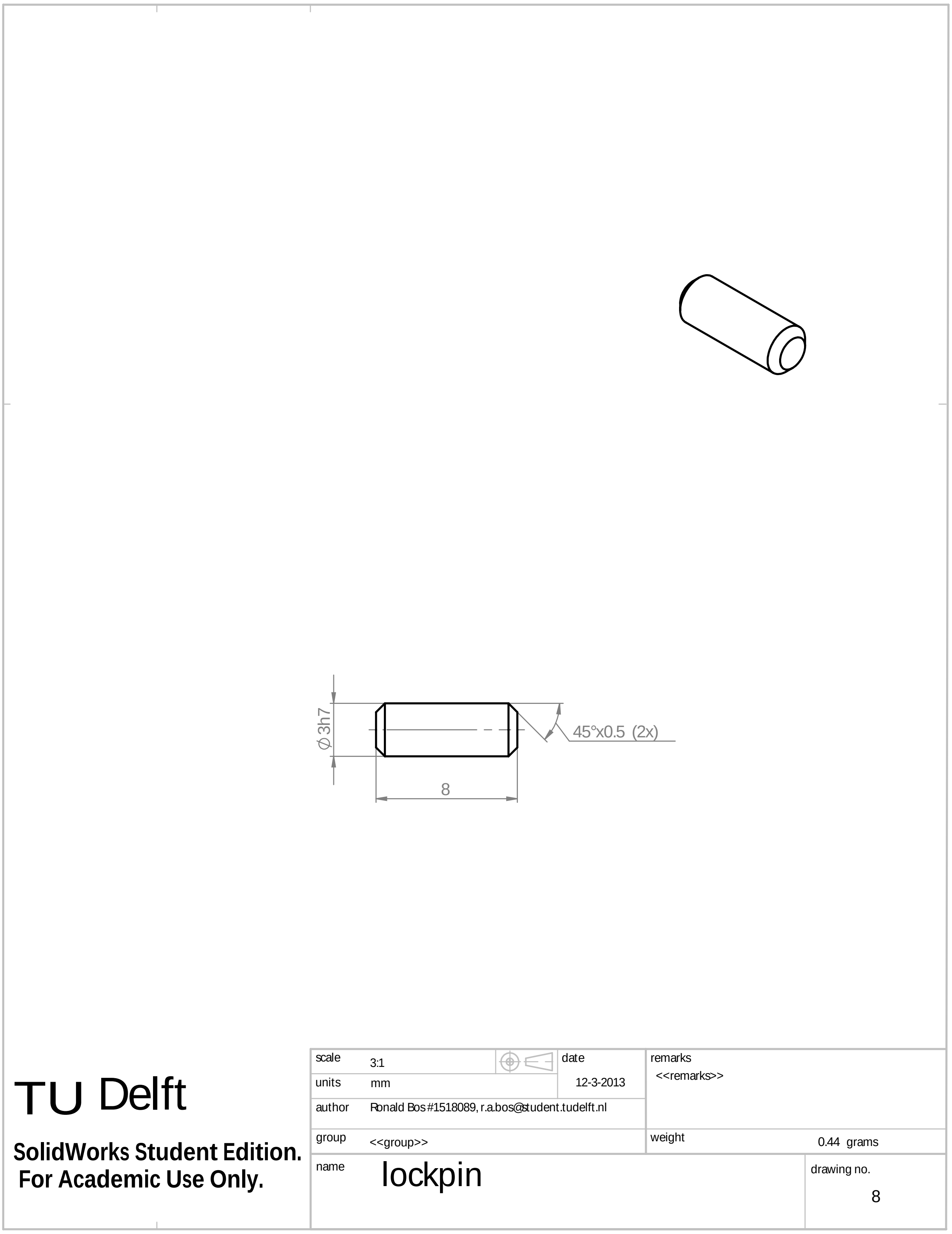
⌀3h7
45°x0.5 (2x)
8
TU Delft
SolidWorks Student Edition.
For Academic Use Only.
scale
3:1
date
12-3-2013
remarks
<<remarks>>
units
mm
author
Ronald Bos #1518089, r.a.bos@student.tudelft.nl
group
<<group>>
weight
0.44 grams
name
lockpin
drawing no.
8

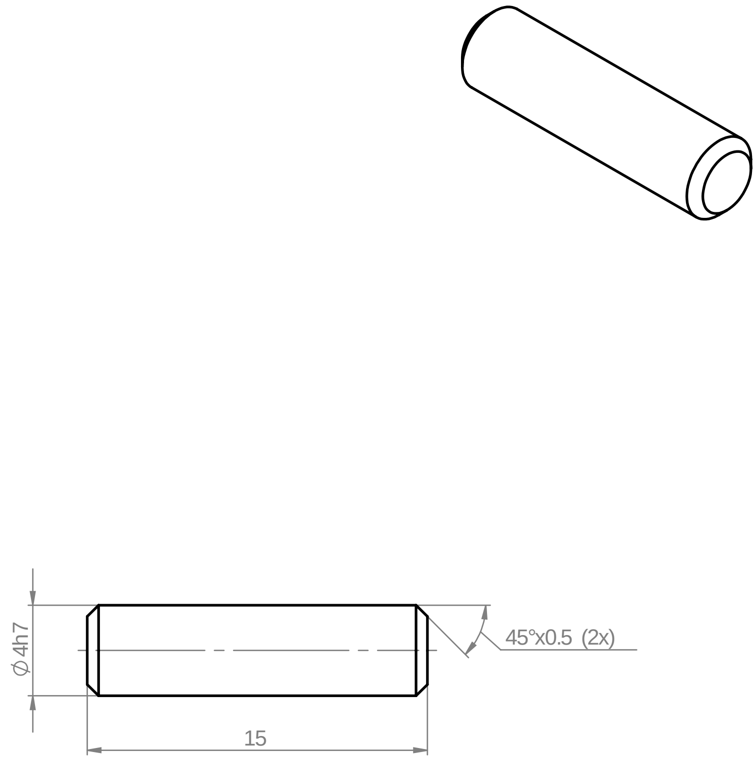

TU Delft

SolidWorks Student Edition.
For Academic Use Only.

scale	3:1	date	remarks
units	mm	12-3-2013	<<remarks>>
author	Ronald Bos #1518089, r.a.bos@student.tudelft.nl		
group	<<group>>	weight	1.48 grams
name	securepin	drawing no.	9

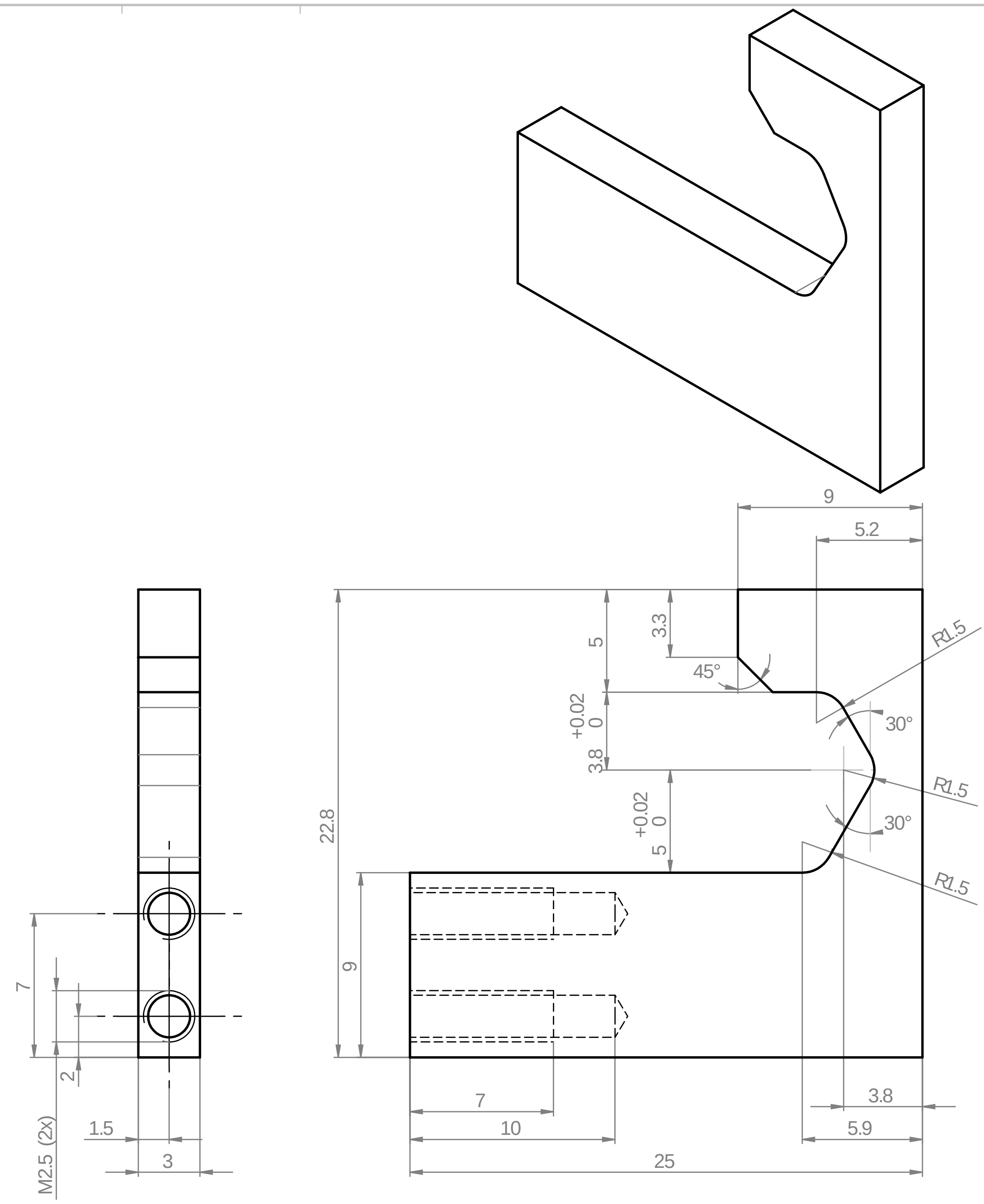

scale	3:1	date	remarks
units	mm	12-3-2013	<<remarks>>
author	Ronald Bos #1518089, r.a.bos@student.tudelft.nl		
group	<<group>>	weight	2.33 grams
name	fixbrace_1	drawing no.	10

TU Delft

SolidWorks Student Edition.
For Academic Use Only.

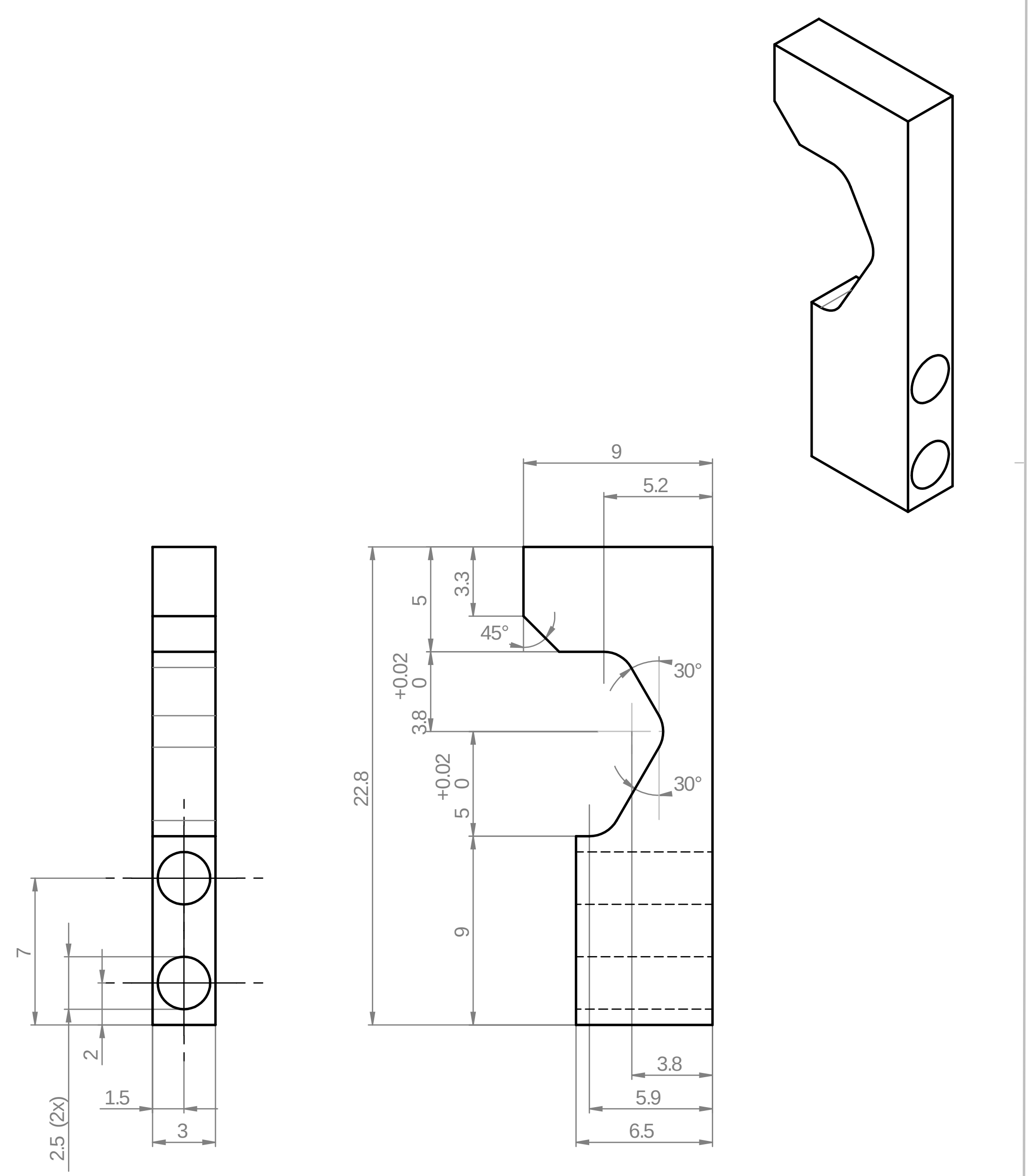

TU Delft

SolidWorks Student Edition.
For Academic Use Only.

scale	3:1	date 12-3-2013	remarks <<remarks>>
units	mm		
author	Ronald Bos #1518089, r.a.bos@student.tudelft.nl		
group	<<group>>		weight 0.94 grams
name	fixbrace_2		drawing no. 11

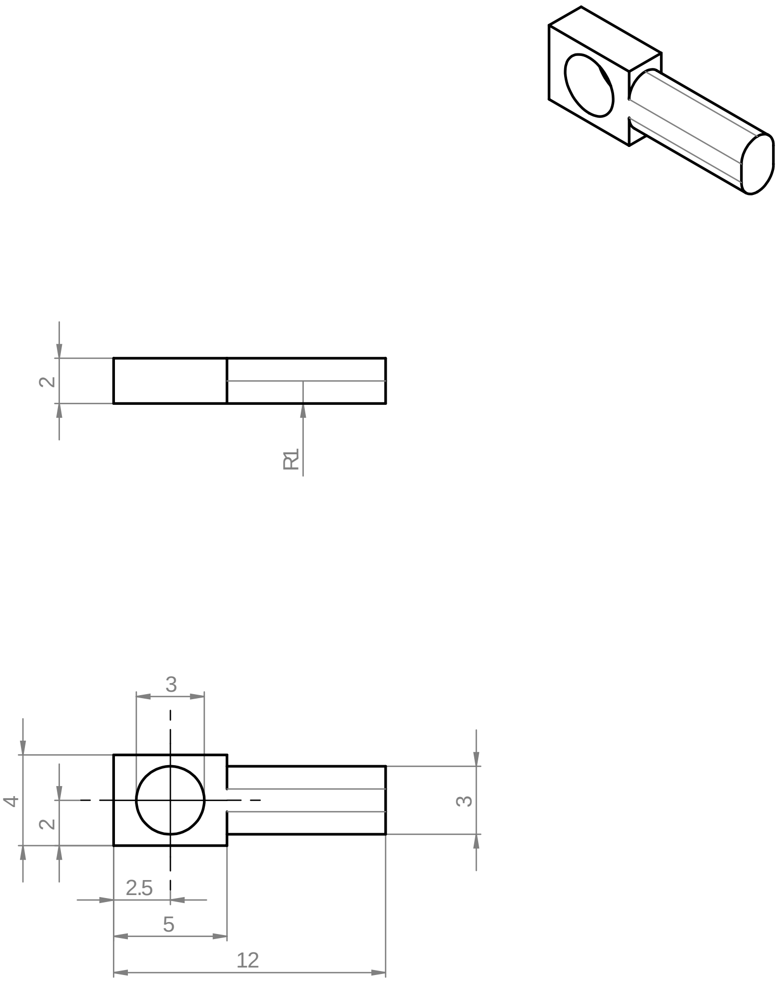

TU Delft

SolidWorks Student Edition.
For Academic Use Only.

scale	3:1	date	12-3-2013
units	mm	remarks	<<remarks>>
author	Ronald Bos #1518089, r.a.bos@student.tudelft.nl		
group	<<group>>	weight	0.49 grams
name	bandclamp	drawing no.	12

Bibliography

Allag, H., J.-P. Yonnet, and M.E.H. Latreche (2009). "3D analytical calculation of forces between linear Halbach-type permanent-magnet arrays." In: *Advanced Electromechanical Motion Systems and Electric Drives Joint Symposium, 2009. ELECTROMOTION 2009. 8th International Symposium on*, pp. 1–6. DOI: 10.1109/ELECTROMOTION.2009.5259084.

Ashby, Mike and David Cebon (2012). *Cambridge Engineering Selector EduPack*.

Barker, C.R. (1985). "A complete classification of planar four-bar linkages." In: *Mechanism and Machine Theory* 20.6, pp. 535–554. DOI: 10.1016/0094-114X(85)90071-0.

van Beek, A. (2009). *Advanced Engineering Design: Lifetime performance and reliability*. TU Delft.

Bellamy, K.E. and M.G.J. Waters (2005). "Designing a prosthesis to simulate the elastic properties of skin." In: *Bio-Medical Materials and Engineering* 15.1, pp. 21–27.

Biddiss, E. and T. Chau (2007). "Upper limb prosthesis use and abandonment: A survey of the last 25 years." In: *Prosthetics and Orthotics International* 31.3, pp. 236–257. DOI: 10.1080/03093640600994581.

Bilotto, S. (1986). "Upper Extremity Cosmetic Gloves." In: *Clinical Prosthetics & Orthotics* 10.2, pp. 87–89.

Bjellerup, M. (2005). "Novel Method for Training Skin Flap Surgery: Polyurethane Foam Dressing Used as a Skin Equivalent." In: *Dermatologic Surgery* 31.9, pp. 1107–1111. DOI: 10.1111/j.1524-4725.2005.31904.

Cabibihan, J.-J., R. Pradipta, and S.S. Ge (2011). "Prosthetic finger phalanges with life-like skin compliance for low-force social touching interactions." In: *Journal of NeuroEngineering and Rehabilitation* 8.1, Article 16. DOI: 10.1186/1743-0003-8-16.

Cabibihan, J.-J. et al. (2009). "Towards Humanlike Social Touch for Sociable Robotics and Prosthetics: Comparisons on the Compliance, Conformance and Hysteresis of Synthetic and Human Fingertip Skins." In: *International Journal of Social Robotics* 1.1, pp. 29–40. DOI: 10.1007/s12369-008-0008-9.

Carey, S.L. et al. (2008). "Compensatory movements of transradial prosthesis users during common tasks." In: *Clinical Biomechanics* 23.9, pp. 1128–1135. DOI: 10.1016/j.clinbiomech.2008.05.008.

Carnelli, W.A., M.G. Defries, and F. Leonard (1955). “Color Realism in the Cosmetic Glove.” In: *Artificial limbs* 2.2, pp. 57–65.

Carrella, A., M.J. Brennan, and T.P. Waters (2007). “Static analysis of a passive vibration isolator with quasi-zero-stiffness characteristic.” In: *Journal of Sound and Vibration* 301.3–5, 678—689. DOI: 10.1016/j.jsv.2006.10.011.

Carwardine, G. (1937). *Equipoising mechanism*. US patent 2,090,439.

Centri AB (2011). *MCV-MSC Gloves*. Accessed at September 14, 2012. URL: http://www.centri.se/mcv_mcs_gloves.html.

Chironis, N.P. (1965). *Mechanisms, linkages, and mechanical controls*. McGraw-Hill, Inc.

Connolly, C. (2008). “Prosthetic hands from Touch Bionics.” In: *Industrial Robot: An International Journal* 35.4, pp. 290–293. DOI: 10.1108/01439910810876364.

Cool, J.C. (2006). *Werktuigkundige systemen*. 3rd ed. VSSD.

Corin, J.D. et al. (1987). “Mechanical Comparison of Terminal Devices.” In: *Clinical Prosthetics & Orthotics* 11.4, pp. 235–244.

Darnall, B.D. et al. (2005). “Depressive symptoms and mental health service utilization among persons with limb loss: Results of a national survey.” In: *Archives of Physical Medicine and Rehabilitation* 86.4, pp. 650–658. DOI: 10.1016/j.apmr.2004.10.028.

Datta, D., K. Selvarajah, and N. Davey (2004). “Functional outcome of patients with proximal upper limb deficiency - acquired and congenital.” In: *Clinical Rehabilitation* 18.2, pp. 172–177. DOI: 10.1191/0269215504cr716oa.

Davies, E.W., W.B. Douglas, and A.D. Small (1977). “A cosmetic functional hand incorporating a silicone rubber cosmetic glove.” In: *Prosthetics and Orthotics Internationa* 1.2, pp. 89–93.

Delft Prosthetics BV (n.d.). *Elleboogbediening*. Accessed at March 13, 2013. URL: http://www.delftprosthetics.nl/body-power/how-it-works#Elleboogbediening.

Dembo, T. and E. Tane-Baskin (1955). “The Noticeability of the Cosmetic Glove.” In: *Artificial Limbs* 2.2, pp. 47–56.

Dempster, W.T. and G.R.L. Gaughran (1967). “Properties of Body Segments Based on Size and Weight.” In: *American Journal of Anatomy* 120.1, pp. 33–54. DOI: 10.1002/aja.1001200104.

Desmond, D.M. (2007). “Coping, affective distress and psychosocial adjustment among people with traumatic upper limb amputations.” In: *Journal of Psychosomatic Research* 62.1, pp. 15–21. DOI: 10.1016/j.jpsychores.2006.07.027.

DINED anthropometric database (1993). *Dutch children, Kima 1993 (12 to 13 years)*. Accessed at January 16, 2013. URL: http://dined.io.tudelft.nl/dined/.

van Eijk, J. and J.F. Dijksman (1979). "Plate Spring Mechanism With Constant Negative Stiffness." In: *Mechanism and Machine Theory* 14, pp. 1–9.

Endo, G. et al. (2010). "A Passive Weight Compensation Mechanism with a Non-Circular Pulley and a Spring." In: *Robotics and Automation (ICRA), 2010 IEEE International Conference on*, pp. 3843–3848. DOI: 10.1109/ROBOT.2010.5509797.

Fillauer, C. and M.J. Quigley (1979). "Clinical Evaluation of an Acrylic Latex Material Used as a Prosthetic Skin on Limb Prostheses." In: *Orthotics and Prosthetics* 33.4, pp. 30–38.

Greenwood, J.A., H. Minshall, and D. Tabor (1961). "Hysteresis Losses in Rolling and Sliding Friction." In: *Proceedings of the Royal Society of London. Series A. Mathematical and Physical Sciences* 259.1299, pp. 480–507. DOI: 10.1098/rspa.1961.0004.

Herder, J.L. (2001). "Energy-free Systems." PhD thesis. Delft University of Technology.

Herder, J.L., J.C. Cool, and D.H. Plettenburg (1998). "Methods for reducing energy dissipation in cosmetic gloves." In: *Journal of Rehabilitation Research and Development* 35.2, pp. 201–209. PMID: 9651892.

Hess, Andrea (n.d.). *Body-powered prostheses*. Accessed at March 13, 2013. URL: http://www.upperlimbprosthetics.info/index.php?p=1_9_Body-Powered.

Hibbeler, R.C. (2007). *Engineering Mechanics: Statics*. 11th ed. Pearson Prentice hall.

Hibbeler, R.C. (2008). *Mechanics of Materials*. 7th ed. Pearson Prentice hall.

Hichert, M. (2010). "Feedback in voluntary closing arm prostheses: Investigation of optimal force feedback in shoulder controlled arm prosthesis operation." Master's thesis. Delft University of Technology.

Hirose, S. et al. (1986). "Internally balanced magnet unit." In: *Advanced Robotics* 1.3, pp. 225–242.

International Magnetics Association (n.d.). *Standard Specifications for Permanent Magnet Materials*. Accessed at October 26, 2012. URL: http://www.intl-magnetics.org/pdfs/0100-00.pdf.

Klopsteg, P.E. and P.D. Wilson (1954). "Human limbs and their substitutes." In: McGraw-Hill Book Company Inc., pp. 239–269.

Krouskop, T.A., P.H. Newell Jr., and L.A. Leavitt (1974). "Cosmetic Covers for Lower-limb Prostheses." In: *Bulletin of prosthetics research*, pp. 411–414.

Kuntz, J.P. (1995). "Rolling Link Mechanisms." PhD thesis. Delft University of Technology.

LeBlanc, M. et al. (1992). "Mechanical Work Efficiencies of Body-Powered Prehensors for Young Children." In: *Journal of the Association of Children's Prosthetic-Orthotic Clinics* 27.3, pp. 70–75.

Lu, Q., C. Ortega, and O. Ma (2011). "Passive Gravity Compensation Mechanisms: Technologies and Applications." In: *Recent Patents on Engineering* 5.1, pp. 32–44.

MatWeb (2012). *Material property data*. Accessed at October 13, 2012. URL: http://www.matweb.com/.

Metzger, A.J. et al. (2012). "Characterization of compensatory trunk movements during prosthetic upper limb reaching tasks." In: *Archives of Physical Medicine and Rehabilitation* 93.11, pp. 2029–2034. DOI: 10.1016/j.apmr.2012.03.011.

Park, S.-T. and T.-T. Luu (2007). "Techniques for optimizing parameters of negative stiffness." In: *Proceedings of the Institution of Mechanical Engineers, Part C: Journal of Mechanical Engineering Science* 221.5, pp. 505–510. DOI: 10.1243/0954406JMES390.

Plettenburg, D.H. (2002). "A sizzling hand prosthesis." PhD thesis. Delft University of Technology.

Plettenburg, D.H. (2006a). "The WILMER Appealing Prehensor." In: *Journal of Prosthetics and Orthotics* 18.2, pp. 43–45.

Plettenburg, D.H. (2006b). *Upper extremity prosthetics: current status & evaluation*. 1st ed. VSSD.

Plettenburg, D.H. (n.d.). *WILMER Friction Wrist*.

Plettenburg, D.H. and J.L. Herder (2003). "Voluntary closing: A promising opening in hand prosthetics." In: *Technology and Disability* 15.2, pp. 85–94.

Plettenburg, D.H., M. Hichert, and G. Smit (2011). "Feedback in voluntary closing arm prostheses." In: *Proceedings of the MEC'11 conference*.

Research Division, College of Engineering, New York University (1949). *Social usefulness of the cosmetic glove: its noticeability and appearance*. College of Engineering, New York University.

Robertson, W.S. et al. (2009). "Theoretical design parameters for a quasi-zero stiffness magnetic spring for vibration isolation." In: *Journal of Sound and Vibration* 326.1–2, pp. 88–103. DOI: 10.1016/j.jsv.2009.04.015.

Schmit, N. and M. Okada (2012). "Design and Realization of a Non-Circular Cable Spool to Synthesize a Nonlinear Rotational Spring." In: *Advanced Robotics* 26.3–4, 235—252. DOI: 10.1163/156855311X614545.

Schnorr Corporation (2003). *Handbook for Disc Springs*. Accessed at October 2, 2012. URL: http://www.schnorr.com/handbook.html.

Schweitzer, Wolf (Mar. 2009). *Technical Below Elbow Amputee Issues - Cosmetic glove for prosthetic mechanical hand*. Accessed at September 12, 2012. URL: http://www.swisswuff.ch/tech/?p=144.

Schweitzer, Wolf (Feb. 2011). *Technical Below Elbow Amputee Issues - The case for a cheap "cosmetic" PVC glove for the prosthetic hand*. Accessed at September 14, 2012. URL: http://www.swisswuff.ch/tech/?p=383.

Shaperman, J. et al. (1995). "Is body powered operation of upper limb prostheses feasible for young limb deficient children?" In: *Prosthetics and Orthotics International* 19.3, pp. 165–175. DOI: 10.3109/03093649509168000.

Smit, G. and D.H. Plettenburg (2010). "Efficiency of voluntary closing hand and hook prostheses." In: *Prosthetics and Orthotics International* 34.4, 411—427. DOI: 10.3109/03093646.2010.486390.

Smit, G. and D.H. Plettenburg (2013). "Comparison of mechanical properties of silicone and PVC (polyvinylchloride) cosmetic gloves for articulating hand prostheses." In: *Journal of Rehabilitation Research & Development* 50.3, pp. 723–732. DOI: 10.1682/JRRD.2011.12.0238.

Smit, G. et al. (2012). "Efficiency of voluntary opening hand and hook prosthetic devices: 24 years of development?" In: *Journal of Rehabilitation Research & Development* 49.4, pp. 523–534. DOI: 10.1682/JRRD.2011.07.0125.

Stevens, P. (Dec. 2011). "Losses Beyond the Limb." In: *The O&P Edge*. URL: http://www.oandp.com/articles/2011-12_01.asp.

Tevema Technical Springs (2008). *Product Module*. Accessed at March 15, 2013. URL: http://www.tevema.com/.

Tolou, N. et al. (2012). "Stiffness Compensation Mechanism for Body Powered Hand Prostheses with Cosmetic Covering." In: *Journal of Medical Devices* 6.1, p. 011004. DOI: 10.1115/1.4005781.

TRS Inc. (2012). *Free-Flex & Super Sport Tds*. Accessed at September 12, 2012. URL: http://www.oandp.com/products/trs/sports-recreation/free_flex-super_sport.asp.

de Visser, H. and J.L. Herder (2000). "Force-directed design of a voluntary closing hand prosthesis." In: *Journal of Rehabilitation Research and Development* 37.3, pp. 261–271. PMID: 10917258.

Vokoun, D. et al. (2009). "Magnetostatic interactions and forces between cylindrical permanent magnets." In: *Journal of Magnetism and Magnetic Materials* 321.22, pp. 3758–3763. DOI: 10.1016/j.jmmm.2009.07.030.

Wang, W. et al. (2006). "Synthesis and Characterization of a Novel Biodegradable, Thermoplastic Polyurethane Elastomer." In: *Journal of Polymer Science Part A: Polymer Chemistry* 44.19, pp. 5505–5512. DOI: 10.1002/pola.21643.

Wijsman, F. (2010). "The Design of a Glove Compensated Hand Prosthesis for Toddlers." Master's thesis. Delft University of Technology.

Yong, Ching Yee et al. (2011). "Prosthetics: Health quality of life effects of limb loss." In: *Biomedical Engineering and Informatics (BMEI), 2011 4th International Conference on*. Vol. 3, pp. 1333–1337. DOI: 10.1109/BMEI.2011.6098617.

Yonnet, J.-P. et al. (1993). “Analytical calculation of permanent magnet couplings.” In: *Magnetics, IEEE Transactions on* 29.6, pp. 2932–2934. DOI: 10.1109/20.280913.